NASA-TM-87651 19860006989

NASA Technical Memorandum 87651

A STUDY OF THE EFFECTS OF INTERFERENCE-REJECTION FILTERS ON FEEDBACK RADIOMETER SENSITIVITY

WILLIAM D. STANLEY AND CHASE P. HEARN

DECEMBER 1985

NASA

National Aeronautics and
Space Administration

Langley Research Center
Hampton, Virginia 23665

INTRODUCTION

A radiometer is a system designed to measure the electromagnetic radiation resulting from thermally-induced molecular motion in matter. Radiometers are basically power-measuring receivers in which the most critical performance parameters are generally held to be sensitivity and linearity. Man-made radio-frequency interference (RFI) constitutes a potential error source for microwave radiometry that is generally underestimated. RFI is an insidious problem in that it may be impossible to know that interference is present until it becomes so large that the radiometer output is grossly erroneous.

RFI may be classified as being either in-band or out-of-band relative to the radiometric channel bandpass. While this paper is concerned with minimizing the deleterious effects of out-of-band RFI on radiometer performance, it is worth noting that it may be possible to establish the presence of RFI, of either category, by observing any characteristics of the interference which differ from the geophysical signal. In this manner, it should be possible to achieve some degree of data correction.

Out-of-band interference can produce radiometric errors through several system imperfections. The first and most obvious is non-ideal, i.e., not rectangular, channel selectivity wherein one or more nearby but still out-of-band interfering signals reach the detector along with the desired signal. This is a linear effect which can, in principle, be reduced to any desired degree by improved selectivity. In practice, sensitivity considerations usually result in the bulk of the selectivity being located well down the signal processing chain (e.g., after the amplifier and mixer stages) where bandpass filter insertion loss does not significantly degrade system sensitivity. However, this arrangement leaves the system elements preceding the primary selectivity susceptible to the nonlinear effects of desensitization and in-band spurious generation from out-of-band RFI. These nonlinear effects are irreversable unless the RFI is clearly identifiable so that it can be "removed" from

the data. Prevention is much preferable to after-the-fact data correction. However, prevention by preceding potentially nonlinear front-end elements, such as amplifiers and mixers, with additional selectivity incurs a cost in sensitivity.

This study examines the trade-offs between sensitivity and interference immunity associated with front-end bandpass filtering. The results are presented in a form that defines the radiometric sensitivity degradation factor, $\Delta T'/\Delta T$, in terms of various filter characteristics. Additionally, the "optimum" filter configuration can be totally defined once the independent (filter) variables of percentage bandwidth, q-factor(s), and desired band-edge rejection are specified.

LIST OF SYMBOLS

A_0	numerator coefficient of $t(s)$
A_p	numerator coefficient of $t_d(s)$ when predistortion is applied
α	magnitude of real part of poles closest to $j\omega$-axis (in main body)
α	attenuation constant (in Appendix A)
B	bandwidth of bandpass filter between attenuation points
B_{no}	radiometer output low-pass noise bandwidth
B_R	arbitrary reference bandwidth
B_s	statistical bandwidth
B_{si}	statistical bandwidth of predetection input filter
β	phase constant
C	constant modifying gain of predistorted filter realization ($C < 1$)
d	dissipation factor
ΔT	unmodified radiometer sensitivity
$\Delta T'$	modified radiometer sensitivity with degradation
f	frequency variable, Hz
f_0	band-pass center frequency
f_1	lower band edge frequency

2

f_2	upper band edge frequency
G	radiometer amplifier power gain
$\gamma_i(j\omega)$	net input reflection function
γ_L	load reflection coefficient
$\gamma_o(j\omega)$	net output reflection function
γ_s	source reflection coefficient
I_L	RMS load current
k	Boltzmann's constant = 1.38×10^{-23} J/K
$|\ell(j\omega)|^2$	power dissipative loss function
L^2	integrated loss factor
ω	frequency variable, rad/sec
ω_k	imaginary part of an arbitrary pole p_k
P_{av}	available source power
p_k	an arbitrary pole of $t(s)$
P_o	filter output power
q	low-pass unload element quality factor
Q	band-pass loaded resonator quality factor
r	passband ripple in dB
R	bandedge attenuation in decibels
R_L	load resistance
R_o	image impedance when it is real
R_s	source resistance
s	Laplace variable
σ_k	real part of an arbitrary pole p_k $(\sigma_k < 0)$
$S_{av}(f)$	available power density of source
$S_i(f)$	incident power density at filter input
$S_o(f)$	output load power density
$S_p(f)$	available internal noise power density

3

$t(s)$	transmission function
$t'(s)$	modified transmission function
$t_d(s)$	transmission function with dissipation
$t_\ell(j\omega)$	predistorted lossless transmission function
τ^2	integrated transmission factor
T_A	antenna brightness temperature
T_{INJ}	injected noise
T'_{INJ}	modified injected noise after filter is added
T_o	filter output noise temperature
T_p	physical temperature of filter
T_R	receiver noise temperature
T_{REF}	reference noise temperature
T_s	equivalent source noise temperature
T_{SYS}	system noise temperature
θ	image propagation constant
V_s	RMS source voltage
Y_{21}	short-circuit filter transfer admittance
$Z_{in}(j\omega)$	input impedance of filter
Z_o	image impedance
$Z_{out}(j\omega)$	output impedance of filter

NOISE MODEL FOR FILTER

The manner in which the noise introduced by the dissipative elements within a filter interacts with the radiometer input signal will be developed in this section. Consider the block diagram of a filter with source and load terminations as shown in figure 1. Assume that all dissipative elements within the filter are at a physical temperature T_p.

The frequency-dependent reflection functions at the input and output are denoted as $\gamma_i(j\omega)$ and $\gamma_o(j\omega)$ respectively. These functions represent the net effect of all multiple reflections and could be expressed in terms of the simpler frequency independent terminal reflection coefficients based on the source and load resistances and the image impedance. However, it is not necessary to express an image impedance explicitly, and this is rarely done with s-plane filter designs, such as were used in this study. A development of the relationship between the terminal reflection coefficients and these net functions is given in Appendix A.

Let $t(j\omega)$ denote the transmission function defined on a magnitude-squared basis as:

$$|t(j\omega)|^2 = \frac{\text{output load power density}}{\text{available source power density}} \tag{1}$$

In the development that follows, it is convenient to define a modified transmission function $|t'(j\omega)|^2$ as

$$|t'(j\omega)|^2 = \frac{\text{output load power density}}{\text{incident power density}} \tag{2}$$

where the incident power density is the fraction of the available power density accepted by the filter.

Let $S_{av}(f)$ represent the source available power density, and assume that it is flat over the frequency range of interest and therefore representable in terms of an effective source temperature T_s. Thus,

$$S_{av}(f) = kT_s \text{ W/Hz} \tag{3}$$

where k = Boltzmann's constant = 1.38×10^{-23} J/K.

Let $S_i(f)$ and $S_o(f)$ represent the incident and output spectral densities respectively. The power density reflected at the filter input is $|\gamma_i(j\omega)|^2 S_{av}$.

5

Thus, the incident power spectral density is related to the available power density by

$$S_i(f) = [1 - |\gamma_i(j\omega)|^2]S_{av}(f) \tag{4}$$

The modified transmission function is

$$|t'(j\omega)|^2 = \frac{S_o(f)}{S_i(f)} = \frac{S_o(f)}{[1 - |\gamma_i(j\omega)|^2]S_{av}(f)} \tag{5}$$

The transmission function is

$$|t(j\omega)|^2 = \frac{S_o(f)}{S_{av}(f)} \tag{6}$$

Comparing (5) and (6), the following relationships between $|t'(j\omega)|^2$ and $|t(j\omega)|^2$ may be deduced:

$$|t'(j\omega)|^2 = \frac{|t(j\omega)|^2}{1 - |\gamma_i(j\omega)|^2} \tag{7}$$

or

$$|t(j\omega)|^2 = [1 - |\gamma_i(j\omega)|^2] \, |t'(j\omega)|^2 \tag{8}$$

The manner in which noise associated with the dissipative elements within the filter interacts with the input noise is illustrated by the block diagram of figure 2. Let $S_p(f)$ represent the available internal noise power density, and assume that

$$S_p(f) = kT_p \text{ W/Hz} \tag{9}$$

6

The noise power propagates in both directions. At the input, the source resistance accepts from the filter a power density $[1 - |\gamma_i(j\omega)|^2]S_p(f)$. For thermal equilibrium, this power must be subtracted from the source power, so the _net_ power accepted by the filter from the source is

$$[1 - |\gamma_i(j\omega)|^2]S_{av}(f) - [1 - |\gamma_i(j\omega)|^2]S_p(f)$$

as shown to the right of the input summing junction. This power density is altered by the modified transmission function. The effect of the output mismatch on this noise has already been considered in the definition of $\gamma_i(j\omega)$.

In addition to internal noise propagating to the left as already considered, internal noise propagates to the right. At the load junction, power density $|\gamma_o(j\omega)|^2 S_p(f)$ is reflected back to the network, so the net contribution of the internal noise to the load is $[1 - |\gamma_o(j\omega)|^2]S_p(f)$.

Combining all the preceding sources, the net output spectral density $S_o(f)$ can be expressed as

$$S_o(f) = \{[1 - |\gamma_i(j\omega)|^2]S_{av}(f) - [1 - |\gamma_i(j\omega)|^2]S_p(f)\}|t'(j\omega)|^2$$

$$+ [1 - |\gamma_o(j\omega)|^2]S_p(f) \tag{10}$$

As shown underneath the block diagram in figure 2, this expression can be simplified to

$$S_o(f) = |t(j\omega)|^2 S_{av}(f) + [1 - |t(j\omega)|^2 - |\gamma_o(j\omega)|^2]S_p(f) \tag{11}$$

A loss function $|\ell(j\omega)|^2$ will now be defined as

$$|\ell(j\omega)|^2 = 1 - |t(j\omega)|^2 - |\gamma_o(j\omega)|^2 \tag{12}$$

7

It is interesting to note that while the focus of analysis is on transmission from source to load, the pertinent reflection function is the _output_ function. However, for networks initially designed on a lossless basis with resistive termination at both ports, it is shown in Appendix B that $\gamma_o(j\omega) = \gamma_i(j\omega)$, so either port could be used to establish the loss function in that case. This situation is not true in general.

Utilizing the preceding definition, the output power density can be expressed as

$$S_o(f) = |t(j\omega)|^2 S_{av}(f) + |\ell(j\omega)|^2 S_p(f) \tag{13}$$

INTEGRATED FILTER FUNCTIONS

Based on the preceding development, assume that the differential output power ΔP_o in a differential bandwidth Δf is to be determined. This quantity is readily expressed as

$$\Delta P_o = |t(j\omega)|^2 S_{av}(f)\Delta f + |\ell(j\omega)|^2 S_p(f)\Delta f$$

$$\tag{14}$$

$$= kT_s |t(j\omega)|^2 \Delta f + kT_p |\ell(j\omega)|^2 \Delta f$$

The total power P_o in a bandwidth $B = f_2 - f_1$ is determined by changing the differential formulation to integral form, and the result is

$$P_o = kT_s \int_{f_1}^{f_2} |t(j\omega)|^2 \, df + kT_p \int_{f_1}^{f_2} |\ell(j\omega)|^2 \, df \tag{15}$$

It is convenient to express the result in terms of an effective temperature T_o, defined over a rectangular bandwidth B according to

$$P_o = kT_o B \tag{16}$$

8

Substitution of (16) in (15) and cancellation of common factors yield

$$T_o = T_s \left[\frac{1}{B} \int_{f_1}^{f_2} |t(j\omega)|^2 \, df \right] + T_p \left[\frac{1}{B} \int_{f_1}^{f_2} |\ell(j\omega)|^2 \, df \right] \qquad (17)$$

The integrated transmission factor τ^2 and the integrated loss factor L^2 will be defined as the symbol τ in the definition of τ^2 should not be confused with the integration time parameter appearing in radiometer sensitivity equations.

$$\tau^2 = \frac{1}{B} \int_{f_1}^{f_2} |t(j\omega)|^2 \, df \qquad (18)$$

$$L^2 = \frac{1}{B} \int_{f_1}^{f_2} |\ell(j\omega)|^2 \, df \qquad (19)$$

With these definitions, T_o can be expressed as

$$T_o = \tau^2 T_s + L^2 T_p \qquad (20)$$

DEGRADATION FACTOR

The preceding definitions will now be used to determine the degree to which the interference-rejection filter degrades the radiometer sensitivity. This development is limited to the closed-loop noise injection feedback radiometer, the configuration of primary interest. The corresponding effect in a total power radiometer is substantially different.

The interference rejection filter is located after the directional coupler and is designed to provide a specified attenuation R (in dB) at two specified band-edges. The basic form of a typical response is shown in figure 3. It is assumed that the primary predetection bandwidth selectivity is obtained after several stages of gain and has a much more ideal, i.e., rectangular, response over $B = f_2 - f_1$.

The attenuation of the interference rejection filter will thus be specified at these frequencies, and the amplitude response will be assumed to be truncated abruptly as shown by the dashed lines. This realistic assumption considerably simplifies the integration process as will be demonstrated later.

The pertinent portion of the system affected by the filter is shown in figure 4. The system without the filter is shown in figure 4(a). Sufficient injected noise temperature T_{INJ} is added to the antenna temperature T_A such that $T_A + T_{INJ} = T_{REF}$, where T_{REF} is the reference temperature. This power balancing condition is maintained by the closed loop.

When the dissipative filter is added as shown in figure 4(b), the resulting integrated transmission function is constrained by the inequality $\tau^2 < 1$. The injection noise T'_{INJ} increases to a level such that the filter output equals T_{REF} as before. Thus, the effective overall noise level at the Dicke switch is not changed. However, the loop gain has been reduced by τ^2. In order to maintain the same loop time response and low-pass output noise bandwidth, a gain of $1/\tau^2$ must be added to the loop as shown. Since $1/\tau^2 > 1$, the fluctuations within the loop are accentuated by this process, and the sensitivity is degraded.

The second effect of the filter is to reduce the statistical bandwidth. The statistical bandwidth B_s in general is defined by

$$B_s = \frac{\left[\int_0^\infty |t(j\omega)|^2 \, df \right]^2}{\left[\int_0^\infty |t(j\omega)|^4 \, df \right]} \tag{21}$$

This quantity is the bandwidth that should be used in the radiometer sensitivity equation. Based on the assumed ideal overall predection filter characteristic, the statistical bandwidth used in this study is therefore:

$$B_s = \frac{\left[\int_{f_1}^{f_2} |t(j\omega)|^2 \, df\right]^2}{\left[\int_{f_1}^{f_2} |t(j\omega)|^4 \, df\right]} \tag{22}$$

Let ΔT represent the idealized sensitivity of the radiometer without regard to the interference filter. This widely used definition is

$$\Delta T = 2T_{SYS} \sqrt{\frac{2B_{no}}{B_{si}}} \tag{23}$$

where the system temperature T_{SYS} is $T_{SYS} = T_R + T_{REF}$ and T_R is the receiver temperature. The quantities B_{si} and B_{no} represent, respectively, the detector input statistical bandwidth and the output noise bandwidth. For the ideal rectangular bandpass $B_{si} = B$. Thus, without the interference filter, the sensitivity is

$$\Delta T = 2 \, T_{SYS} \sqrt{\frac{2B_{no}}{B}} \tag{24}$$

Let $\Delta T'$ represent the sensitivity as degraded by the interference filter. Since the effective statistical bandwidth is now B_s, and the noise fluctuations are accentuated by a factor $1/\tau^2$, equation (23) is modified by

$$\Delta T' = 2 \, \frac{T_{SYS}}{\tau^2} \sqrt{\frac{2B_{no}}{B_s}} \tag{25}$$

Division of (25) by (24) results in

$$\frac{\Delta T'}{\Delta T} = \frac{1}{\tau^2 \sqrt{\frac{B_s}{B}}} \tag{26}$$

11

This ratio will be referred to in all subsequent work as the degradation factor. It is a measure of the degradation in the sensitivity resulting from the loss in gain and the non-rectangular bandshape response of the interference filter.

FILTER FUNCTIONS

The actual interference rejection filter used in a radiometer is normally a band-pass filter. However, the vast majority of band-pass filters are designed from low-pass prototypes using the low-pass to band-pass geometric transformation. Further, the analytical properties of the band-pass response may be mapped to the low-pass region with a resulting one-to-one correspondence between the regions.

The approach used in this study was to perform all the analysis with the low-pass prototype functions. As previously mentioned, the various properties tabulated are invariant with respect to the transformation. The number of poles listed for the low-pass prototypes must be interpreted as the number of resonators (or, equivalently, the number of pole-pairs) when translated to the band-pass case.

The number of low-pass poles was varied from two to seven in the study, thus allowing band-pass filters with from two to seven resonators to be included. Filter types included Butterworth and Chebyshev with ripple ranging from 0.1 dB to 3 dB. The effects of losses were included, and both non-distorted and pre-distorted designs were considered.

Let $t(s)$ represent the s-domain transmission function. For a low-pass filter with all transmission zeros at $s = \infty$, this function for n poles may be expressed as

$$t(s) = \frac{A_o}{(s-p_1)(s-p_2) \ldots (s-p_n)} \tag{27}$$

where A_o is a constant and the various $p_k = \sigma_k + j\omega_k$ represent the poles. The quantities σ_k are the real parts ($\sigma_k < 0$) and ω_k are the imaginary parts. The poles and constants of the filter types considered are tabulated in Appendix C.

Assume that there is uniform dissipation occurring in all the band-pass resonators. In the low-pass prototype, this is accounted for by defining a transmission function $t_d(s)$ with dissipation as

$$t_d(s) = t(s + d) \tag{28}$$

where d is an appropriately defined dissipation factor. With non-predistorted filter designs, the dissipation factor is applied as given in (28).

When predistortion is desired, a modified lossless transmission function $t_\ell(s)$ is first defined as

$$t_\ell(s) = t(s - d) \tag{29}$$

which amounts to shifting all poles of $t(s)$ to the right. The maximum value of d is limited to the smallest real part of any of the poles. This function is then realized as a lossless network. Because of maximum power constraints, the practical realization of the associated peaked response results in $Ct(s - d)$, where $C < 1$. When dissipation is subsequently applied, the function $t_d(s)$ now becomes

$$t_d(s) = Ct_\ell(s + d) = Ct(s + d - d) = Ct(s) \tag{30}$$

The effect, the desired passband response shape is preserved through the process. Unfortunately, predistorted designs suffer more midband loss as a result of the pole shifting, with possible deleterious consequences in radiometer applications.

The magnitude-squared transmission function for any $t(s)$ may be expressed as

$$\left| t(j\omega) \right|^2 = t(s)\ t(-s) \Big|_{s=j\omega} \tag{31}$$

13

The resulting function is a rational function of ω^2 and may be easily formulated on a geometrical basis in terms of the pole locations, the frequency ω, and the dissipation factor d.

For predistorted designs, a significant loss occurs because the initial shift of the poles to the right creates a more underdamped response with significant peaking. Let A_0 represent the numerator constant of $\tau(s)$. It can be shown that a very good approximation to the corresponding constant A_p for the predistorted filter is

$$A_p = \left(\frac{\alpha - d}{\alpha}\right)A_0 \tag{32}$$

where α is the magnitude of the real part of the pair of poles closest to the $j\omega$-axis.

COMPUTATION OF DEGRADATION FACTORS

Several computer programs were developed for evaluating the degradation factor as a function of the number of poles, the pole values, dissipation losses, and band-edge attenuation. The various programs evolved over a period of time as data were plotted and evaluated.

The two major programs used in the final tabulation of data are defined as "FILTER1" and "FILTER2", and they are written in BASIC. Listings of these programs are provided in Appendix D.

Both programs perform a numerical integration of the transmission function magnitude-squared and magnitude to the fourth power so that statistical bandwidth and degradation factor may be computed.

PRESENTATION OF GENERAL RESPONSE CURVES

The program "FILTER1" was used to generate a large quantity of data for various filter types, order, attenuation, and dissipation factor d. The results are shown graphically in Appendix E. Each figure represents a different filter order and type.

14

Let q represent the unloaded "Q-factor" for the normalized low-pass prototype design. Since $\omega = 1$ rad/s was assumed as the normalized reference,

$$q = \frac{1}{d} \tag{33}$$

The dissipation factor was used as the parameter in generating the curves, but was converted to the equivalent q value for plotting.

The band-pass filter Q is related to the low-pass prototype q by

$$Q = \frac{f_o}{B_R} q \tag{34}$$

where f_o is the band-pass center frequency and B_R is the low-pass reference bandwidth.

Although the data of Appendix E are useful and display some interesting trends, there is a subtle point that must be considered in interpreting the results. The value of d (and subsequently of q) is based on the bandwidth of the reference definition of the particular filter type. For example, assume that a 0.5-dB Chebyshev filter is to be modified with a dissipation $d = 0.1$. This means that $q = 10$ at a frequency $\omega = 1$ rad/s in the low-pass prototype. Unless the design is predistorted, however, there is no simple way of predicting the exact shape of the response after dissipation is added. This poses some difficulty in making a "fine" interpretation of the results of Appendix E.

A somewhat different approach was used in the development of the program "FILTER2", and these results are tabulated in Appendix F. All of the curves obtained in these presentations were based on a specified attenuation of either 10 dB or 20 dB. The two frequencies producing these values of attenuation with dissipation added are determined numerically. The value of q is adjusted so that the value plotted corresponds to the exact q at the bandedge where the desired attenuation is

achieved. For example, with $R = 20$ dB and $q = 30$, the low-pass prototype filter has $q = 30$ at the exact frequency where $R = 20$ dB.

For Appendix F, therefore, the relationship between low-pass prototype q and band-pass Q is

$$Q = \frac{f_o}{B} q \qquad\qquad (35)$$

where B is either the 10-dB or 20-dB bandwidth.

Some summary results are provided in the three figures of Appendix G. Figures G1 and G2 provide some curves of degradation factor versus the number of poles with q as a parameter for 10 dB and 20 dB respectively. Although the independent variable is obviously restricted to integer values, the curves are enhanced by extrapolating between points.

Figure G3 provides a macroscopic range of operating conditions between three poles and seven poles with low-pass q between 30 and ∞. The lowest order (two poles) was not used because it is felt that three poles would represent the lowest order of practical interest.

SUMMARY AND CONCLUSIONS

This paper quantifies the sensitivity loss which results from the presence of interference-rejection bandpass filters in the front-end of noise injection feedback radiometers. This sensitivity loss was expressed in terms of a "radiometric sensitivity degradation factor", which is the ratio of the actual sensitivity $\Delta T'$ to the theoretical sensitivity ΔT. Sensitivity degradation results from the combined effects of changes in the input statistical bandwidth and changes in the transmission function resulting from the filter. Both of these changes are determined from integration of the appropriate frequency-dependent functions.

In the course of the investigation, various models concerning noise and dissipative effects were developed. Some of these models show promise for additional investigations on radiometer sensitivity. Computer programs employing numerical techniques were developed for processing the data. Numerous data were generated and plotted. Several common filter types were employed and various unloaded resonator quality factors were assumed. This resulted in a comprehensive compilation of data having potential use in radiometer system design and analysis. The results of this paper allow the radiometer system designer (a) to make an intelligent choice with regard to the number of poles, and passband ripple in the front-end filter, given the inherent Q of the filter elements, and (b) to recognize the radiometric penalty incurred by the interference immunity gained with the input filter.

$t(j\omega)$ $t'(j\omega)$

R_s

$\gamma_i(j\omega)$ T_P $\gamma_o(j\omega)$ R_L
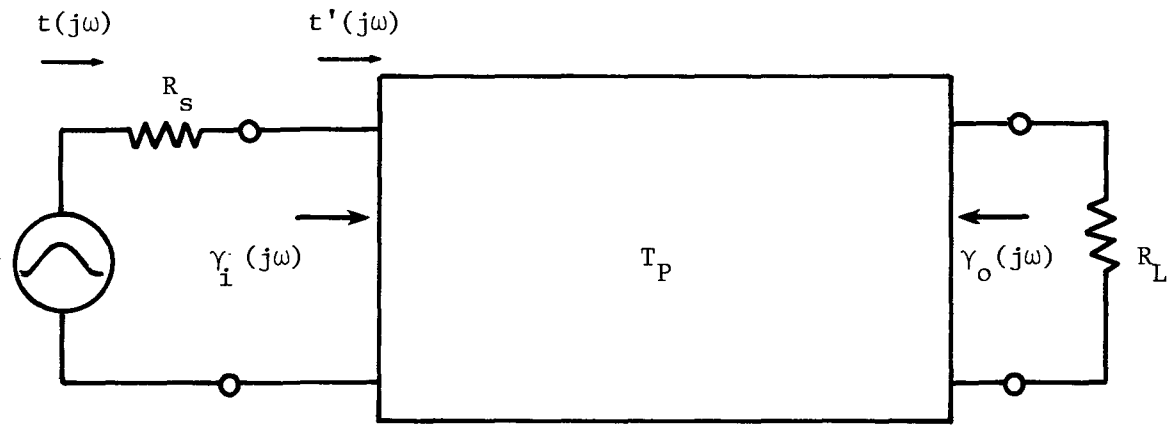
Fig. 1. Block diagram of filter with source and load terminations.
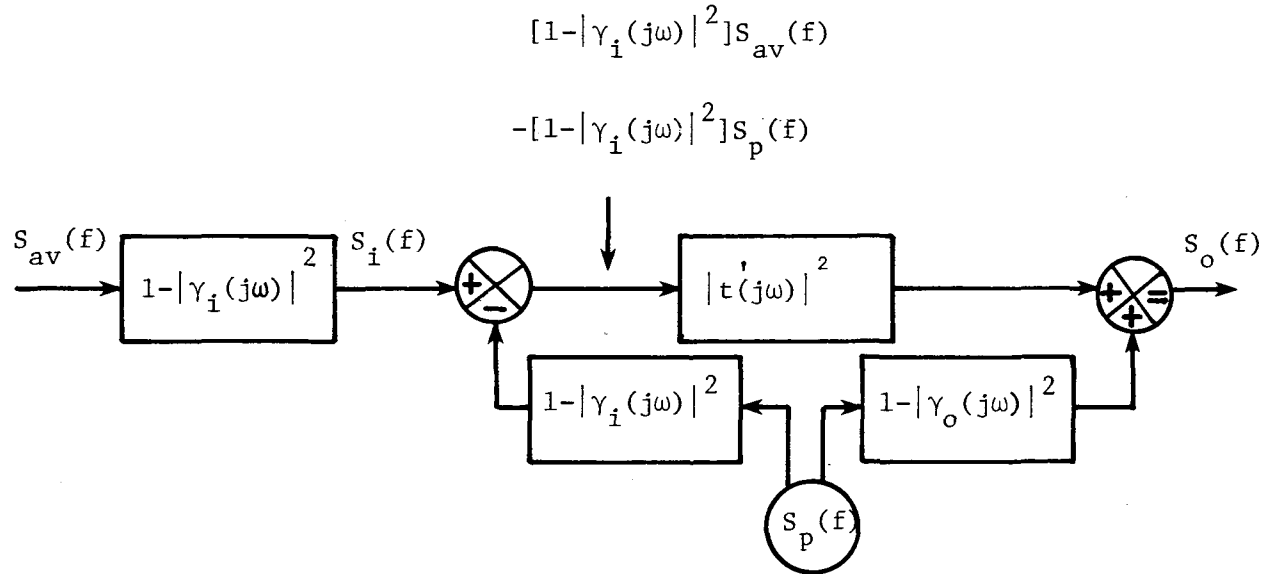
$$[1-|\gamma_i(j\omega)|^2]S_{av}(f)$$

$$-[1-|\gamma_i(j\omega)|^2]S_p(f)$$

$$S_o(f) = \left\{ [1-|\gamma_i(j\omega)|^2]S_{av}(f) - [1-|\gamma_i(j\omega)|^2]S_p(f) \right\} |t'(j\omega)|^2 + [1-|\gamma_o(j\omega)|^2]S_p(f)$$

$$= [1-|\gamma_i(j\omega)|^2] |t'(j\omega)|^2 [S_{av}(f)-S_p(f)] + [1-|\gamma_o(j\omega)|^2]S_p(f)$$

$$= |t(j\omega)|^2[S_{av}(f)-S_p(f)] + [1-|\gamma_o(j\omega)|^2]S_p(f)$$

$$= |t(j\omega)|^2 S_{av}(f) + [1-|t(j\omega)|^2-|\gamma_o(j\omega)|^2]S_p(f)$$

$$= |t(j\omega)|^2 S_{av}(f) + |\ell(j\omega)|^2 S_p(f)$$

Fig. 2. Block diagram of filter showing interaction
of dissipative losses and input noise.

$$|t(j\omega)|^2$$
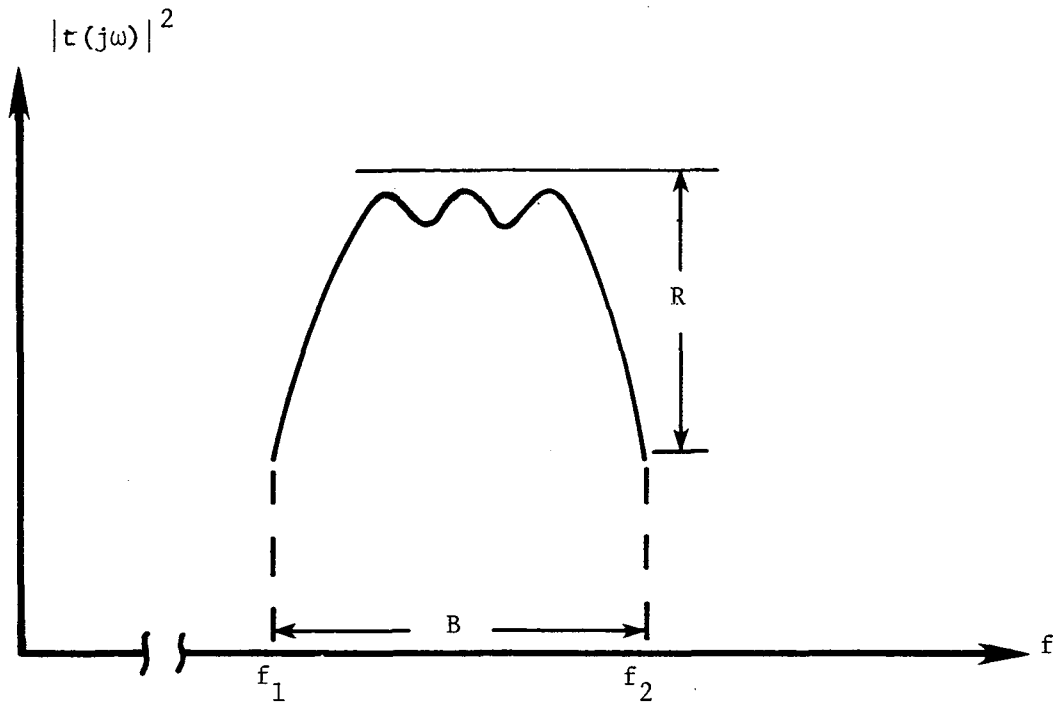
Fig. 3. Typical response of interference filter coupled with more ideal detector input response.

(a)

$T_A + T_{INJ} = T_{REF}$

DICKE SWITCH

T_A → DIRECTIONAL COUPLER

T_{INJ}

T_{REF}

G

(b)

T_{REF}

$T_A + T'_{INJ}$

DICKE SWITCH

GAIN MULTIPLIER $= \dfrac{1}{\tau^2}$

T_A → DIRECTIONAL COUPLER

FILTER τ^2, B_S

$\dfrac{1}{\tau^2}$

G

T'_{INJ}

T_{REF}
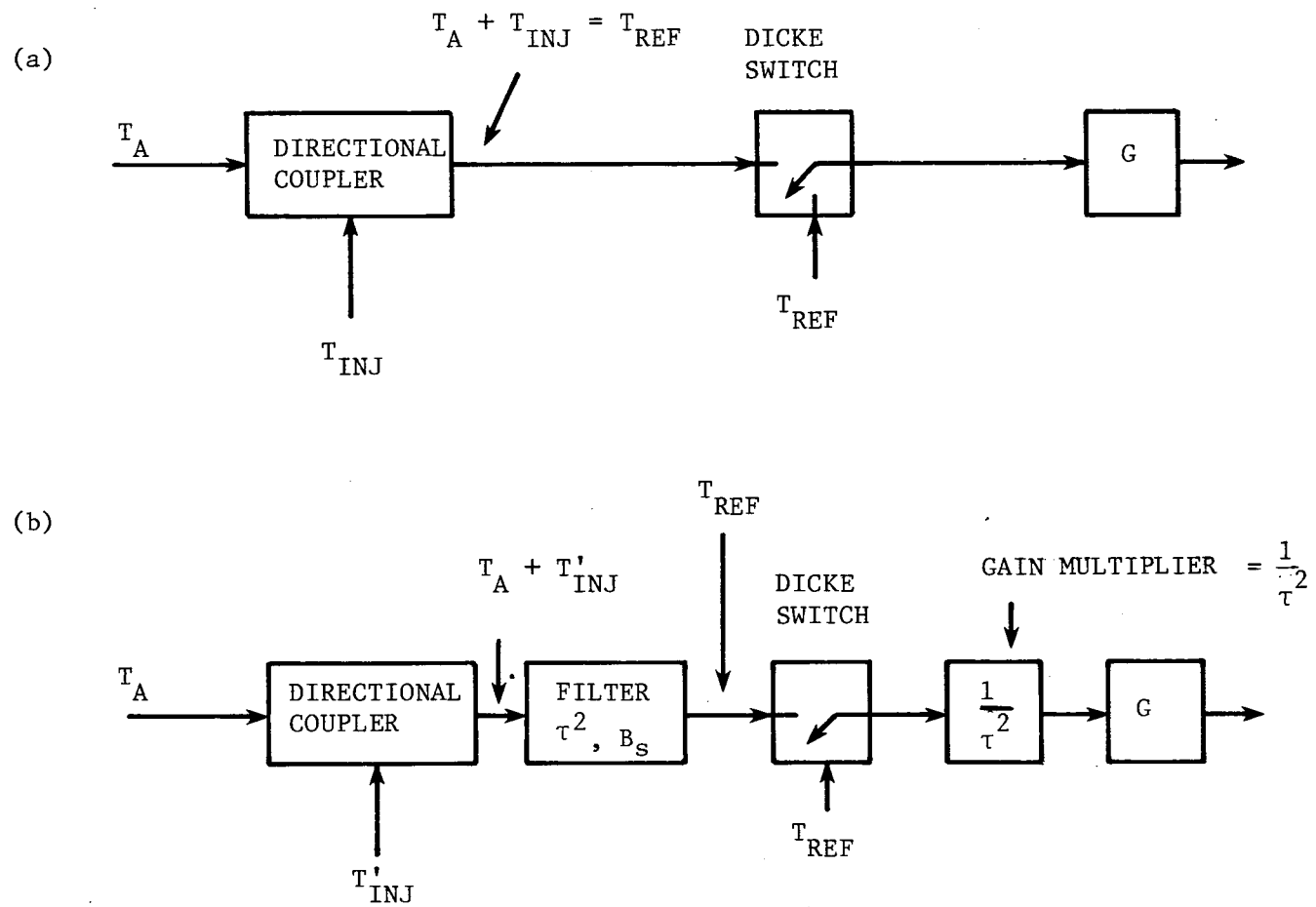
Fig. 4. Block diagram of portion of radiometer showing
addition of filter and compensation.

APPENDIX A

INTERACTION OF REFLECTIONS

Consider the transmission system shown in figure A1 with a source resistance R_s and a load resistance R_L. Using image parameter network theory, the image propagation constant is $\theta = \alpha + j\beta$, where α is the attenuation constant and β is the phase constant. The image impedance is assumed to be Z_0. The source reflection coefficient γ_s is defined as

$$\gamma_s = \frac{R_s - Z_0}{R_s + Z_0} \tag{A-1}$$

The load reflection coefficient γ_L is defined as

$$\gamma_L = \frac{R_L - Z_0}{R_L + Z_0} \tag{A-2}$$

Let $Z_{in}(j\omega)$ represent the complex impedance reflected to the input. This function can be shown to be

$$Z_{in}(j\omega) = Z_0 \left[\frac{1 + \gamma_L \varepsilon^{-2\theta}}{1 - \gamma_L \varepsilon^{-2\theta}} \right] \tag{A-3}$$

Let $Z_{out}(j\omega)$ represent the complex impendance reflected to the output. This function is

$$Z_{out}(j\omega) = Z_0 \left[\frac{1 + \gamma_s \varepsilon^{-2\theta}}{1 - \gamma_s \varepsilon^{-2\theta}} \right] \tag{A-4}$$

22

An effective frequency-dependent input reflection function $\gamma_i(j\omega)$ can be defined as

$$\gamma_i(j\omega) = \frac{R_s - Z_{in}(j\omega)}{R_s + Z_{in}(j\omega)} \tag{A-5}$$

Substitution of (A-3) in (A-5) and subsequent simplification yield

$$\gamma_i(j\omega) = \frac{\gamma_s - \gamma_L \varepsilon^{-2\theta}}{1 - \gamma_s \gamma_L \varepsilon^{-2\theta}} \tag{A-6}$$

An effective complex output reflection function $\gamma_o(j\omega)$ can be defined as

$$\gamma_o(j\omega) = \frac{R_L - Z_{out}(j\omega)}{R_L + Z_{out}(j\omega)} \tag{A-7}$$

Substitution of (A-4) in (A-7) and subsequent simplification yield

$$\gamma_o(j\omega) = \frac{\gamma_L - \gamma_s \varepsilon^{-2\theta}}{1 - \gamma_L \gamma_s \varepsilon^{-2\theta}} \tag{A-8}$$

The quantities γ_s and γ_L relate to reflections of a single wave incident on the particular boundry. However, $\gamma_i(j\omega)$ and $\gamma_o(j\omega)$ are effective reflection functions that take into consideration the effects of multiple reflections.

Several special cases should be noted.

(a) $\underline{Z_o = R_o = R_L}$

In this case $\gamma_L = 0$, and when this value is substituted in (A-3), (A-6), and (A-8), there results

$$Z_{in}(j\omega) = R_o \tag{A-9}$$

23

$$\gamma_i(j\omega) = \gamma_s \tag{A-10}$$

$$\gamma_o(j\omega) = -\gamma_s \epsilon^{-2\theta} \tag{A-11}$$

Thus, when the image impedance is real and the load end is matched, the input impedance is simply the image impedance, and the effective input reflection coefficient is simply the source reflection coefficient.

(b) $\underline{Z_o = R_o = R_s}$

In this case $\gamma_s = 0$, and when this value is substituted in (A-4), (A-6), and (A-8)

$$Z_{out}(j\omega) = R_o \tag{A-11}$$

$$\gamma_o(j\omega) = \gamma_L \tag{A-12}$$

$$\gamma_i(j\omega) = -\gamma_L \epsilon^{-2\theta} \tag{A-13}$$

Thus, when the image impedance is real and the source end is matched, the output impedance is simply the image impedance, and the effective output reflection coefficient is simply the load reflection coefficient.

(c) $\underline{R_L = R_s}$

In this case, $\gamma_s = \gamma_L$. It can then be shown from (A-6) and (A-8) that

$$\gamma_i(j\omega) = \gamma_o(j\omega) = \frac{\gamma_L (1 - \epsilon^{-2\theta})}{1 - \gamma_L^2 \epsilon^{-2\theta}} = \frac{\gamma_s(1 - \epsilon^{-2\theta})}{1 - \gamma_s^2 \epsilon^{-2\theta}} \tag{A-14}$$

24
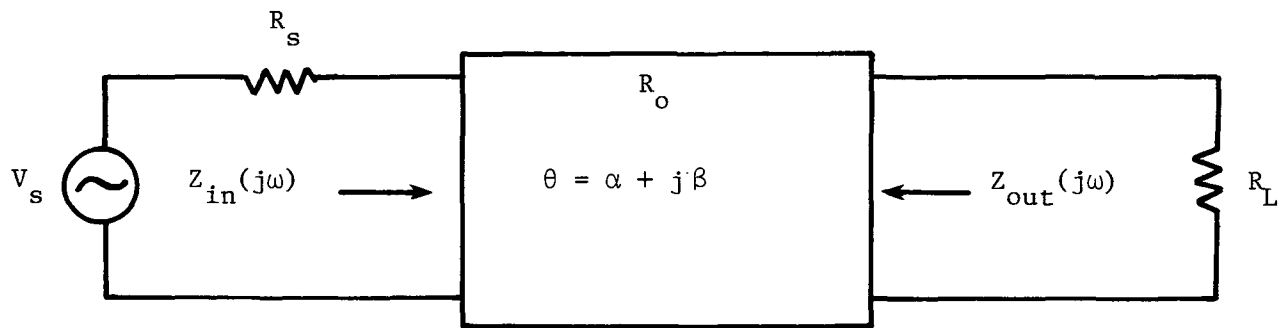
Fig. Al.. Model used in formulating reflection functions.

APPENDIX B

RECIPROCITY OF TRANSMISSION FUNCTION

Consider the passive bilateral circuit model shown in figure B1(a). A source with RMS voltage V_s and internal resistance R_s excites the circuit, and the output is connected to a load R_L. The output power P_o expressed in terms of the RMS load current I_L is

$$P_o = I_L^2 R_L \tag{B-1}$$

The maximum available source power P_{av} is

$$P_{av} = \frac{V_s^2}{4R_s} \tag{B-2}$$

The transmission function $|\tau|^2$ is defined as

$$|\tau|^2 = \frac{P_o}{P_{av}} = \frac{I_2^2 R_L}{V_s^2/4R_s} = 4R_s R_L \left(\frac{I_2}{V_s}\right)^2 = 4R_s R_L Y_{21}^2 \tag{B-3}$$

where Y_{21} is the transfer admittance.

Assume now that the network is turned around as shown in figure B1(b). The output power P_o' is now

$$P_o' = (I_L')^2 R_s \tag{B-4}$$

The available source power is now

$$P_{av}' = \frac{V_s^2}{4R_L} \tag{B-5}$$

26

The new transmission function $|\tau'|^2$ is

$$|\tau'|^2 = \frac{P'_o}{P'_{av}} = 4R_sR_L\left(\frac{I'_2}{V_s}\right)^2 = 4R_sR_L(Y'_{21})^2 \tag{B-6}$$

By reciprocity, however, $Y'_{21} = Y_{21}$. Comparing (B-6) and (B-3), it can be concluded that the transmission function obeys reciprocity for a linear bilateral circuit.

If, in <u>addition</u>, the network is lossless, the reflection functions $|\gamma_i(j\omega)|^2$ and $|\gamma_o(j\omega)|^2$ are expressible as

$$|\gamma_i(j\omega)|^2 = 1 - |\tau|^2 = |\gamma_o(j\omega)|^2 \tag{B-7}$$

since $|\tau|^2$ is the same in both directions. Thus, for a linear, bilateral lossless network, the reflection functions at both ports are identical.

(a)

(b)
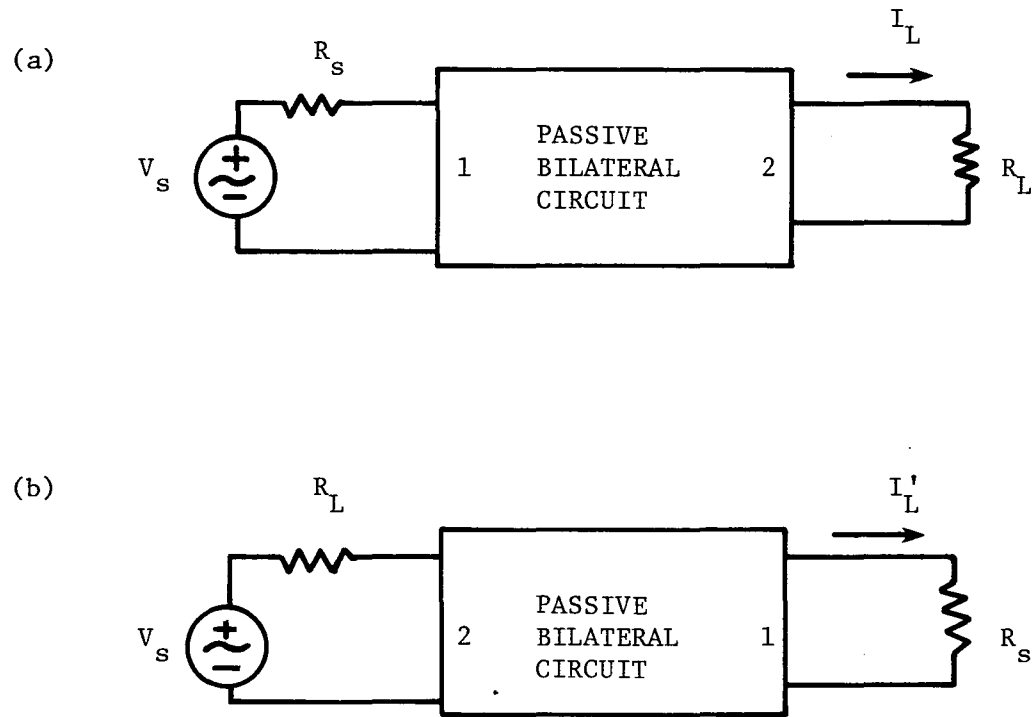
Fig. B1. Network models used in reciprocity development.

APPENDIX C

POLES FOR LOW-PASS PROTOTYPE FILTERS

The following definitions are used in the tables that follow:

    r = pass band ripple in decibels. Table C-1 (r = 0) corresponds to the Butterworth case, and all other cases correspond to Chebyshev types.

    n = number of poles in low-pass prototype filter.

       = number of resonators in band-pass filter.

Transmission Constant = numerator of $|\tau(j\omega)|^2$ when denominator coefficient of s^{2n} term is unity.

The value $\omega = 1$ rad/s on a normalized basis is the frequency corresponding to the band-edge last ripple bound point.

29

Table C-1. Poles for r = 0 (Butterworth case)

r = 0

n	Poles	Transmission Constant
2	$-0.7071068 \pm j0.7071068$	1
3	$-0.5000000 \pm j0.8660254$ -1.0000000	1
4	$-0.3826834 \pm j0.9238795$ $-0.9238795 \pm j0.3826834$	1
5	$-0.3090170 \pm j0.9510565$ $-0.8090170 \pm j0.5877852$ -1.0000000	1
6	$-0.2588190 \pm j0.9659258$ $-0.7071068 \pm j0.7071068$ $-0.9659258 \pm j0.2588190$	1
7	$-0.2225209 \pm j0.9749279$ $-0.6234898 \pm j0.7818315$ $-0.9009689 \pm j0.4338837$ -1.0000000	1

Table C-2.   Poles for r = 0.1 dB

r = 0.1 dB

n	Poles	Transmission Constant
2	$-1.1861781 \pm j1.3809484$	10.7328410
3	$-0.4847029 \pm j1.2061553$ -0.9694057	2.6832106
4	$-0.2641564 \pm j1.1226098$ $-0.6377299 \pm j0.4650002$	0.6708026
5	$-0.1665337 \pm j1.0803720$ $-0.4359908 \pm j0.6677066$ -0.5389143	0.1677006
6	$-0.1146934 \pm j1.0565189$ $-0.3133481 \pm j0.7734255$ $-0.4280415 \pm j0.2830934$	0.04192516
7	$-0.08384097 \pm j1.0418333$ $-0.2349172 \pm j0.8354855$ $-0.3394651 \pm j0.4636595$ -0.3767779	0.01048129

Table C-3. Poles for r = 0.5 dB

r = 0.5 dB

n	Poles	Transmission Constant
2	$-0.7128122 \pm j1.0040425$	2.0488703
3	$-0.3132282 \pm j1.0219275$ -0.6264565	0.5122176
4	$-0.1753531 \pm j1.0162529$ $-0.4233398 \pm j0.4209457$	0.1280542
5	$-0.1119629 \pm j1.0115574$ $-0.2931227 \pm j0.6251768$ -0.3623196	0.03201359
6	$-0.0776501 \pm j1.0084608$ $-0.2121440 \pm j0.7382446$ $-0.2897940 \pm j0.2702162$	0.008003395
7	$-0.0570032 \pm j1.0064085$ $-0.1597194 \pm j0.8070770$ $-0.2308012 \pm j0.4478939$ -0.2561700	0.002000849

Table C-4. Poles for r = 1 dB

r = 1 dB

n	Poles	Transmission Constant
2	−0.5488672 ± j0.8951286	0.9655292
3	−0.2470853 ± j0.9659987 −0.4941706	0.2413823
4	−0.1395360 ± j0.9833792 −0.3368697 ± j0.4073290	0.06034558
5	−0.0894584 ± j0.9901071 −0.2342050 ± j0.6119198 −0.2894933	0.01508638
6	−0.0621810 ± j0.9934115 −0.1698817 ± j0.7272275 −0.2320627 ± j0.2661837	0.003771601
7	−0.0457089 ± j0.9952839 −0.1280736 ± j0.7981557 −0.1850717 ± j0.4429430 −0.2054141	0.0009428962

Table C-5.   Poles for r = 2 dB

r = 2 dB

n	Poles	Transmission Constant
2	−0.4019082 ± j0.8133451	0.4274285
3	−0.1844554 ± j0.9230771 −0.3689108	0.1068571
4	−0.1048872 ± j0.9579530 −0.2532202 ± j0.3967971	0.02671428
5	−0.0674610 ± j0.9734557 −0.1766151 ± j0.6016287 −0.2183083	0.006678567
6	−0.0469732 ± j0.9817052 −0.1283332 ± j0.7186581 −0.1753064 ± j0.2630471	0.001669642
7	−0.0345566 ± j0.9866139 −0.0968253 ± j0.7912029 −0.1399167 ± j0.4390845 −0.1552958	0.0004170907

Table C-6. Poles for r = 3 dB

r = 3 dB

n	Poles	Transmission Constant
2	$-0.3224498 \pm j0.7771576$	0.251190075
3	$-0.1493101 \pm j0.9038144$ -0.2986202	0.06279750
4	$-0.0851704 \pm j0.9464844$ $-0.2056195 \pm j0.3920467$	0.01569938
5	$-0.0548531 \pm j0.9659238$ $-0.1436074 \pm j0.5969738$ -0.1775085	0.003923656
6	$-0.0382295 \pm j0.9764060$ $-0.1044450 \pm j0.7147788$ $-0.1426745 \pm j0.2616272$	0.0009812111
7	$-0.0281456 \pm j0.9826957$ $-0.0788623 \pm j0.7880608$ $-0.1139594 \pm j0.4373407$ -0.1264854	0.0002453029

PROGRAM LISTINGS

FILTER1

```
10    INPUT "NUMBER OF POLES";NP
15    DSHIFT=0
20    FOR N=1 TO NP STEP 2
30    INPUT "TRANS DENOM:SIGMA,OMEGA(+VALUES)";SIGMAD(N),OMEGAD(N)
40    SIGMAD(N)=-SIGMAD(N)
50    NEXT N
55    T2MULT=1
60    FOR N=2 TO NP STEP 2
70    SIGMAD(N)=SIGMAD(N-1)
80    OMEGAD(N)=-OMEGAD(N-1)
90    NEXT N
100   INPUT "TRANS CONSTANT";T2CON
110   INPUT "VALUE OF D";D
120   INPUT "FREQ INCREM";DELW
130   INPUT "INTEGER OF HIGHEST FREQ";KMAX
132   FOR N=1 TO NP
134   SIGMAD(N)=SIGMAD(N)+DSHIFT
136   NEXT N
138   T2CON=T2CON*T2MULT
140   LPRINT "POLES"
150   FOR N=1 TO NP
160   LPRINT SIGMAD(N),OMEGAD(N)
170   NEXT N
180   LPRINT
190   LPRINT "NUMBER OF POLES =";NP,"D =";D,"NUM CON =";  T2CON
200   LPRINT
210   LPRINT "FREQUENCY","TRANS SQ","ACCUM TRANS","ACCUM 4"
220   LPRINT,"DB RESPONSE","ACCUM NOR TRAN","STAT NOR BW","DEGRAD"
230   W=0
240   INTTSQ=0
250   INTT4=0
260   A2=0
270   A4=0
280   TRANS=0
290   BSTATN=0
300   DEGRAD=0
310   FOR K=0 TO KMAX
320   DF1=1
330   FOR N=1 TO NP
340   DF2=(SIGMAD(N)-D)^2+(W-OMEGAD(N))^2
350   DF1=DF1*DF2
360   NEXT N
370   TSQ=T2CON/DF1
380   TDB=4.34294*LOG(TSQ)
390   T4=TSQ^2
400   IF K=0 THEN 460
410   INTTSQ=INTTSQ+.5*(TSQ+A2)*DELW
```

```
420 INTT4=INTT4+.5*(T4+A4)*DELW
430 TRANS=INTTSQ/W
440 BSTATN=INTTSQ^2/(INTT4*W)
450 DEGRAD=1/(TRANS*SQR(BSTATN))
460 LPRINT W,TSQ,INTTSQ,INTT4
470 LPRINT,TDB,TRANS,BSTATN, DEGRAD
480 W=W+DELW
490 A2=TSQ
500 A4=T4
510 NEXT K
520 LPRINT
530 LPRINT
540 INPUT "ANOTHER RUN (Y OR N)";B$
550 IF B$="N" THEN 630
551 FOR N=1 TO NP
552 SIGMAD(N)=SIGMAD(N)-DSHIFT
553 NEXT N
554 T2CON=T2CON/T2MULT
555 DSHIFT=0
556 T2MULT=1
560 INPUT "DO YOU WANT TO PREDISTORT (Y OR N)";C$
570 IF C$="N" THEN 110
580 INPUT "VALUE OF D SHIFT";DSHIFT
590 C1=SIGMAD(1)^2
600 C2=(SIGMAD(1)+DSHIFT)^2
610 T2MULT=C2/C1
620 GOTO 110
630 END
```

```
10    INPUT "NUMBER OF POLES";NP
15    DSHIFT=0
20    FOR N=1 TO NP STEP 2
30    INPUT "TRANS DENOM:SIGMA,OMEGA(+VALUES)";SIGMAD(N),OMEGAD(N)
40    SIGMAD(N)=-SIGMAD(N)
50    NEXT N
55    T2MULT=1
60    FOR N=2 TO NP STEP 2
70    SIGMAD(N)=SIGMAD(N-1)
80    OMEGAD(N)=-OMEGAD(N-1)
90    NEXT N
100   INPUT "TRANS CONSTANT";T2CON
110   INPUT "VALUE OF Q";Q
115   D=1/Q
120   DELW=.01
132   FOR N=1 TO NP
134   SIGMAD(N)=SIGMAD(N)+DSHIFT
136   NEXT N
138   T2CON=T2CON*T2MULT
140   LPRINT "POLES"
150   FOR N=1 TO NP
160   LPRINT SIGMAD(N),OMEGAD(N)
170   NEXT N
180   LPRINT
190   LPRINT "NUMBER OF POLES =";NP,"Q=";Q,"NUM CON =";T2CON
200   LPRINT
210   LPRINT "FREQUENCY","MODIFIED Q","DEGRAD"
220   RCOMP=-10
230   W=0
235   TDB=0
240   INTTSQ=0
250   INTT4=0
260   A2=0
270   A4=0
275   ADEG=0
280   TRANS=0
290   BSTATN=0
300   DEGRAD=0
310   FOR K=1 TO 2
320   DF1=1
330   FOR N=1 TO NP
340   DF2=(SIGMAD(N)-D)^2+(W-OMEGAD(N))^2
350   DF1=DF1*DF2
360   NEXT N
370   TSQ=T2CON/DF1
380   TDB=4.34294*LOG(TSQ)
390   T4=TSQ^2
410   INTTSQ=INTTSQ+.5*(TSQ+A2)*DELW
420   INTT4=INTT4+.5*(T4+A4)*DELW
430   TRANS=INTTSQ/W
440   BSTATN=INTTSQ^2/(INTT4*W)
450   DEGRAD=1/(TRANS*SQR(BSTATN))
460   IF TDB<=RCOMP THEN 504
```

```
470 ADB=TDB
480 W=W+DELW
490 A2=TSQ
500 A4=T4
501 ADEG=DEGRAD
502 GOTO 320
504 ADJ=(RCOMP-ADB)/(TDB-ADB)
506 WMOD=W-DELW+ADJ*DELW
508 DMOD=D/WMOD
509 QMOD=1/DMOD
510 LPRINT WMOD,QMOD,DEGRAD
512 RCOMP=RCOMP-10
514 ADB=TDB
516 W=W+DELW
518 A2=TSQ
520 A4=T4
521 ADEG=DEGRAD
522 NEXT K
525 LPRINT
530 LPRINT
540 INPUT "ANOTHER RUN (Y OR N)";B$
550 IF B$="N" THEN 630
551 FOR N=1 TO NP
552 SIGMAD(N)=SIGMAD(N)-DSHIFT
553 NEXT N
554 T2CON=T2CON/T2MULT
555 DSHIFT=0
556 T2MULT=1
560 INPUT "DO YOU WANT TO PREDISTORT (Y OR N)";C$
570 IF C$="N" THEN 110
580 INPUT "VALUE OF D SHIFT";DSHIFT
590 C1=SIGMAD(1)^2
600 C2=(SIGMAD(1)+DSHIFT)^2
610 T2MULT=C2/C1
620 GOTO 110
630 END
```

CURVES OF DEGRADATION FACTOR VS BAND—EDGE ATTENUATION WITH q AS A PARAMETER

All curves contained in Appendix E are plots of the degradation factor vs band-edge attenuation. To simplify the presentation, each caption provides only the pass-band ripple and the number of poles for the particular set of curves.

In general, the following low-pass reference q values were considered: ∞, 100, 30, and 10. The values of q were established at the lossless low-pass proto-type "cutoff" frequency corresponding to the filter type. For Butterworth filters (r = 0 dB) and 3-dB Chebyshev filters (r = 3 dB), this corresponds to the frequency at which the response is down 3 dB. For other ripple levels, it is the highest frequency at which the response crosses the ripple bound.

For the three lossy q values, both standard and predistorted designs were con-sidered. For lower order filters and higher values of q, the standard and pre-distorted cases essentially coincided. For higher order filters and lower values of q, the curves were off the scales and are not shown.

The low-pass reference q values are denoted in a row above, and in the same sense as, the curves.

The pole values in Appendix E were <u>not</u> adjusted to compensate for shifts in reference frequencies as the dissipation increased.

NOTE: In all cases, solid curves represent standard designs, and broken lines represent predistorted designs.

q = 10, 10, 30, 30, 100, ∞
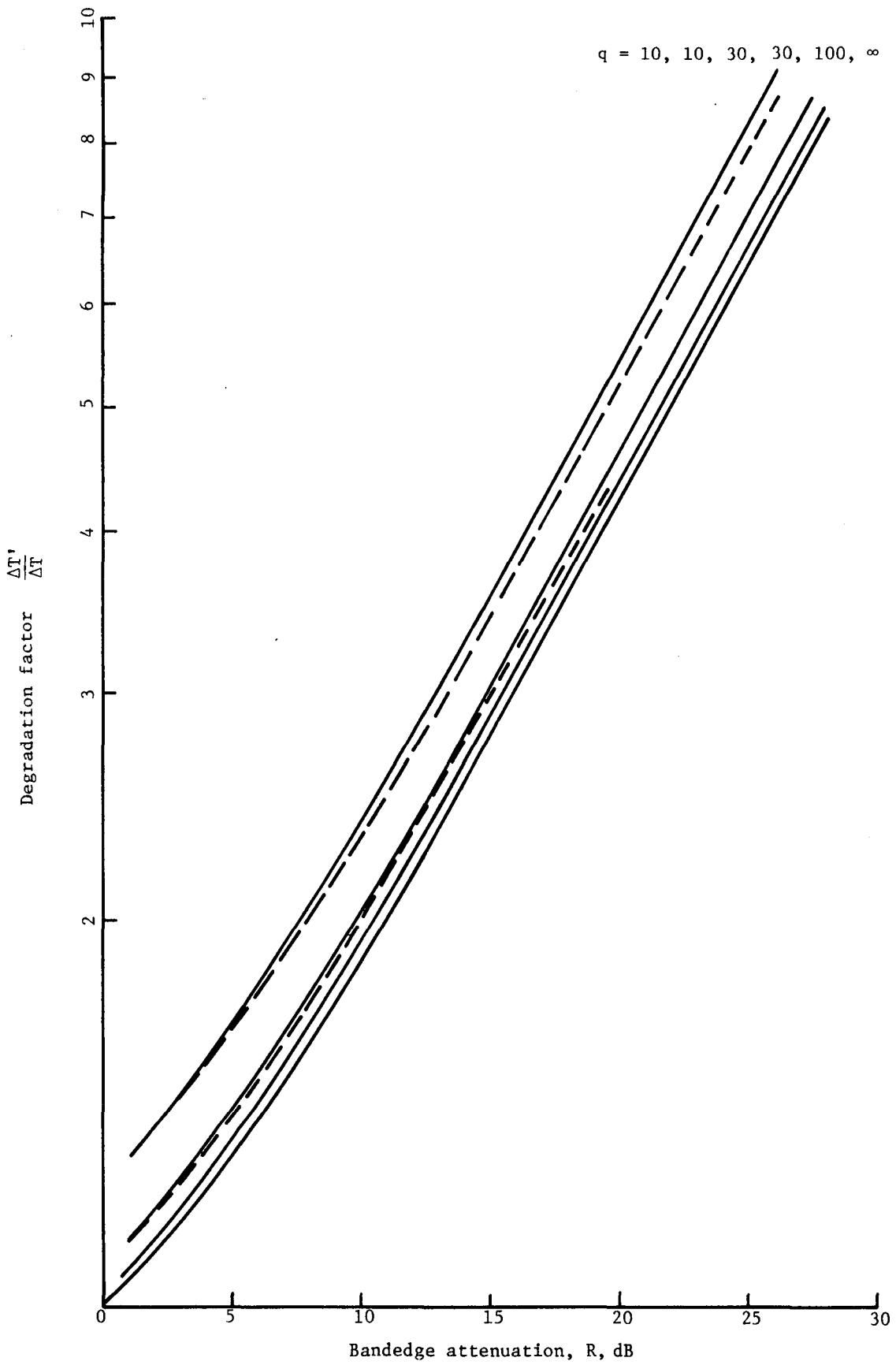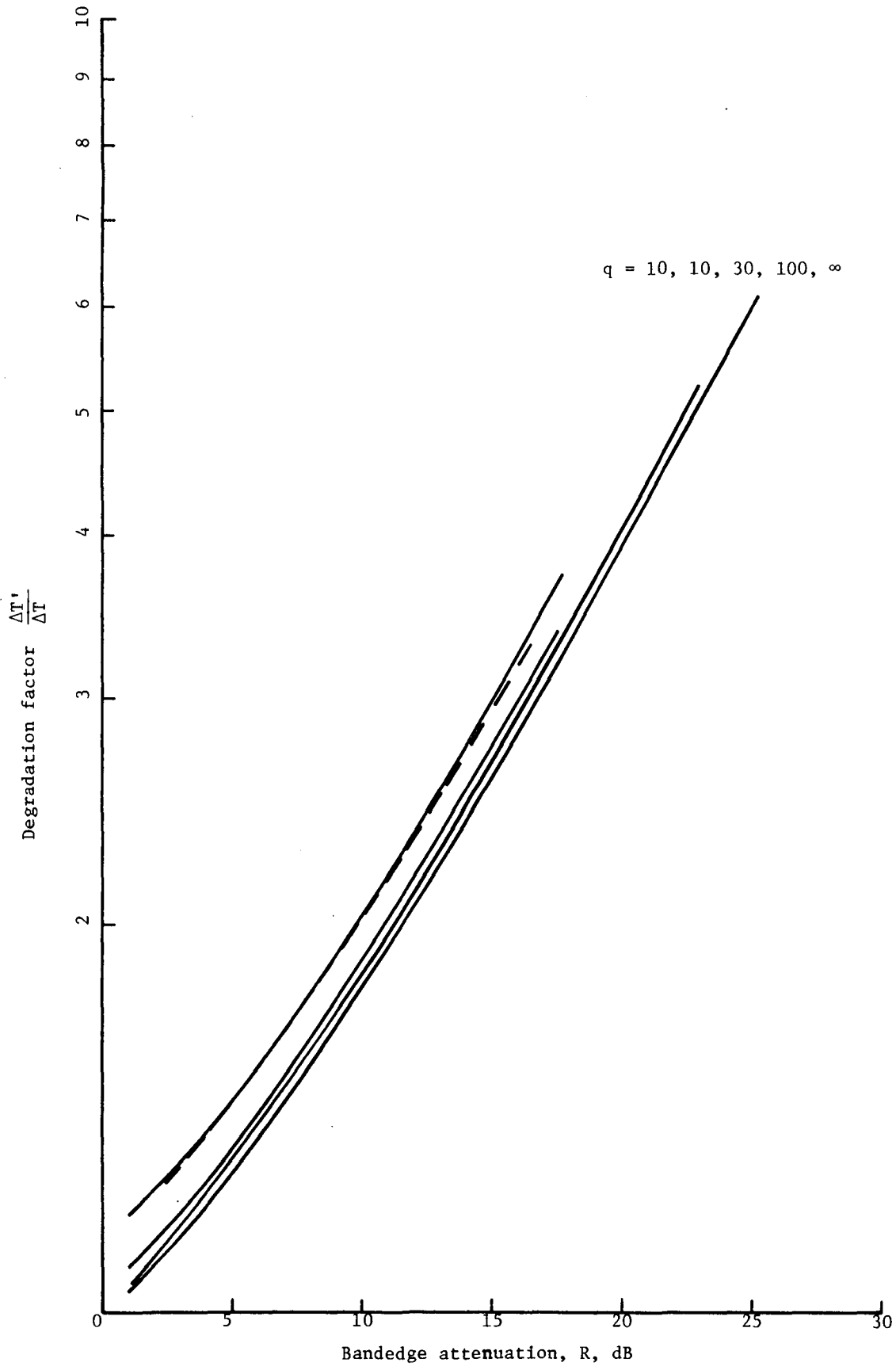
Fig. E1.   r = 0 dB, 2 poles.
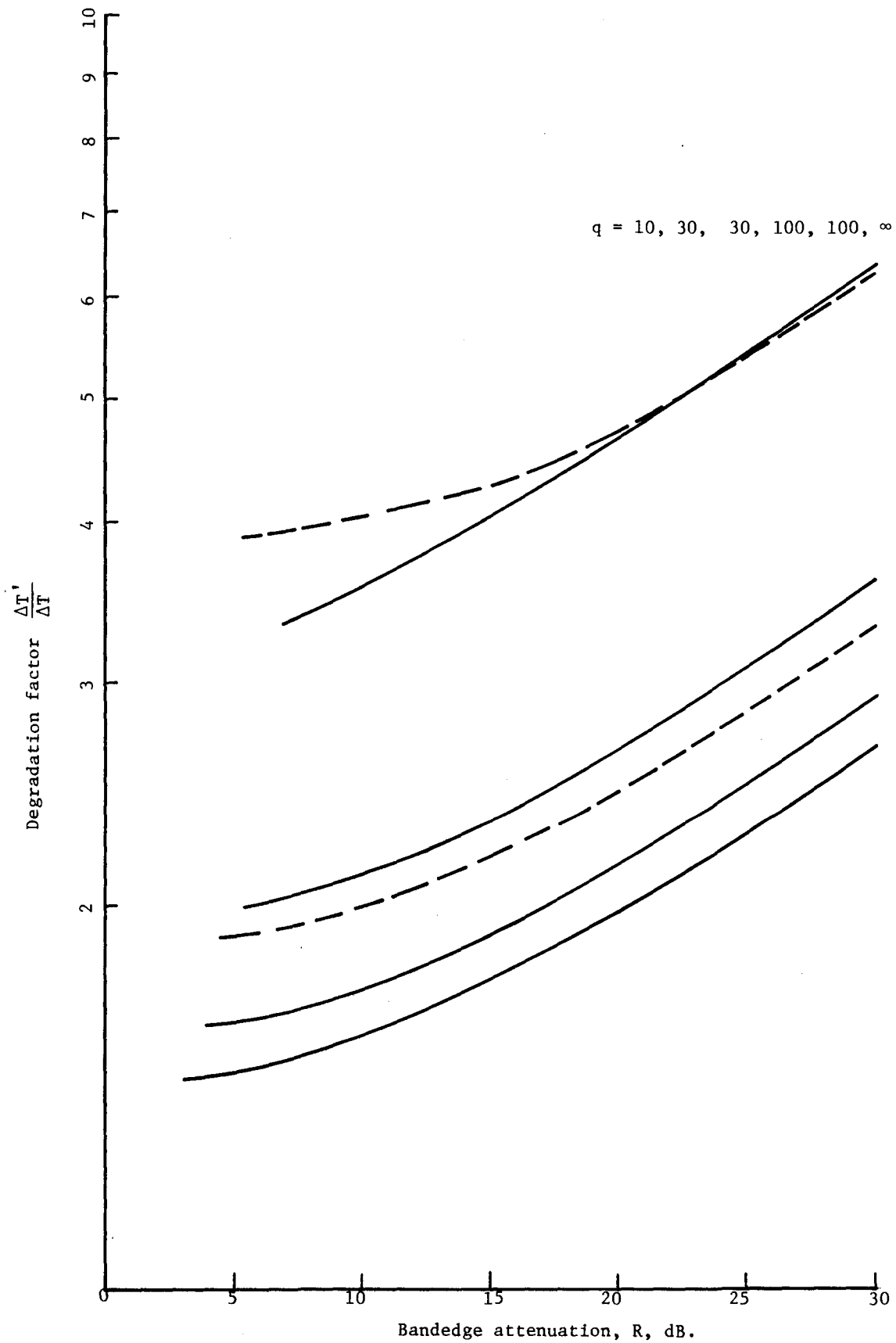
Fig. E2.   r = 0.1 dB, 2 poles
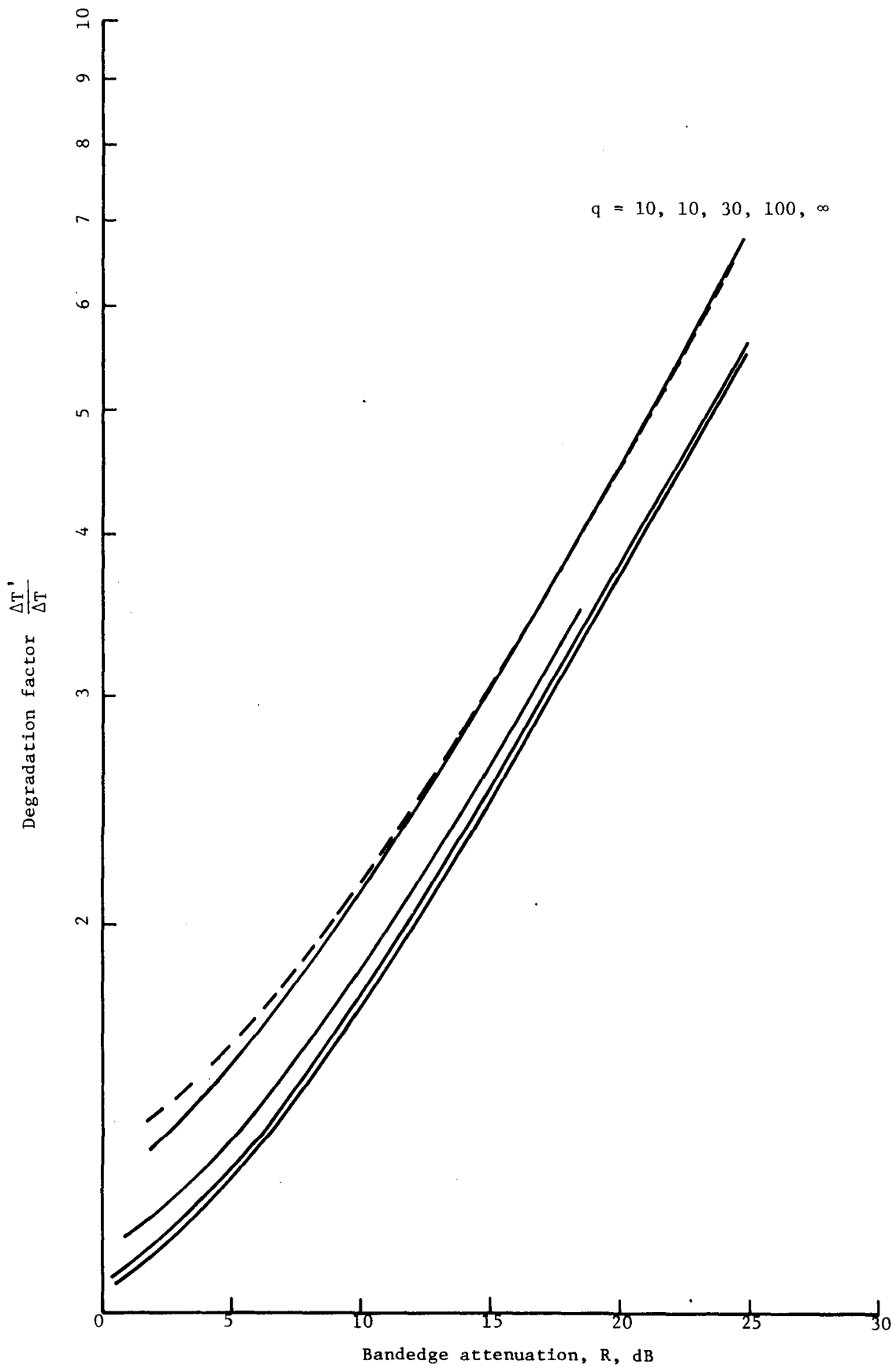
Fig. E3. r = 0.5 dB, 2 poles.

q = 10, 10, 30, 100, ∞

Degradation factor $\frac{\Delta T'}{\Delta T}$

Bandedge attenuation, R, dB

Fig. E4.   r = 1 dB, 2 poles.

q = 10, 10, 30, 30, 100, ∞

Degradation factor $\frac{\Delta T'}{\Delta T}$

Bandedge attenuation, R, dB

Fig. E5. r = 2 dB, 2 poles.

q = 10, 10, 30, 30, 100, ∞

Degradation factor $\frac{\Delta T'}{\Delta T}$

Bandedge attenuation, R, dB

Fig. E6.   r = 3 dB, 2 poles.

q = 10, 10, 30, 30, 100, ∞

Degradation factor $\frac{\Delta T'}{\Delta T}$

Bandedge attenuation, R, dB

Fig. E7. r = 0 dB, 3 poles.

Degradation factor $\frac{\Delta T'}{\Delta T}$
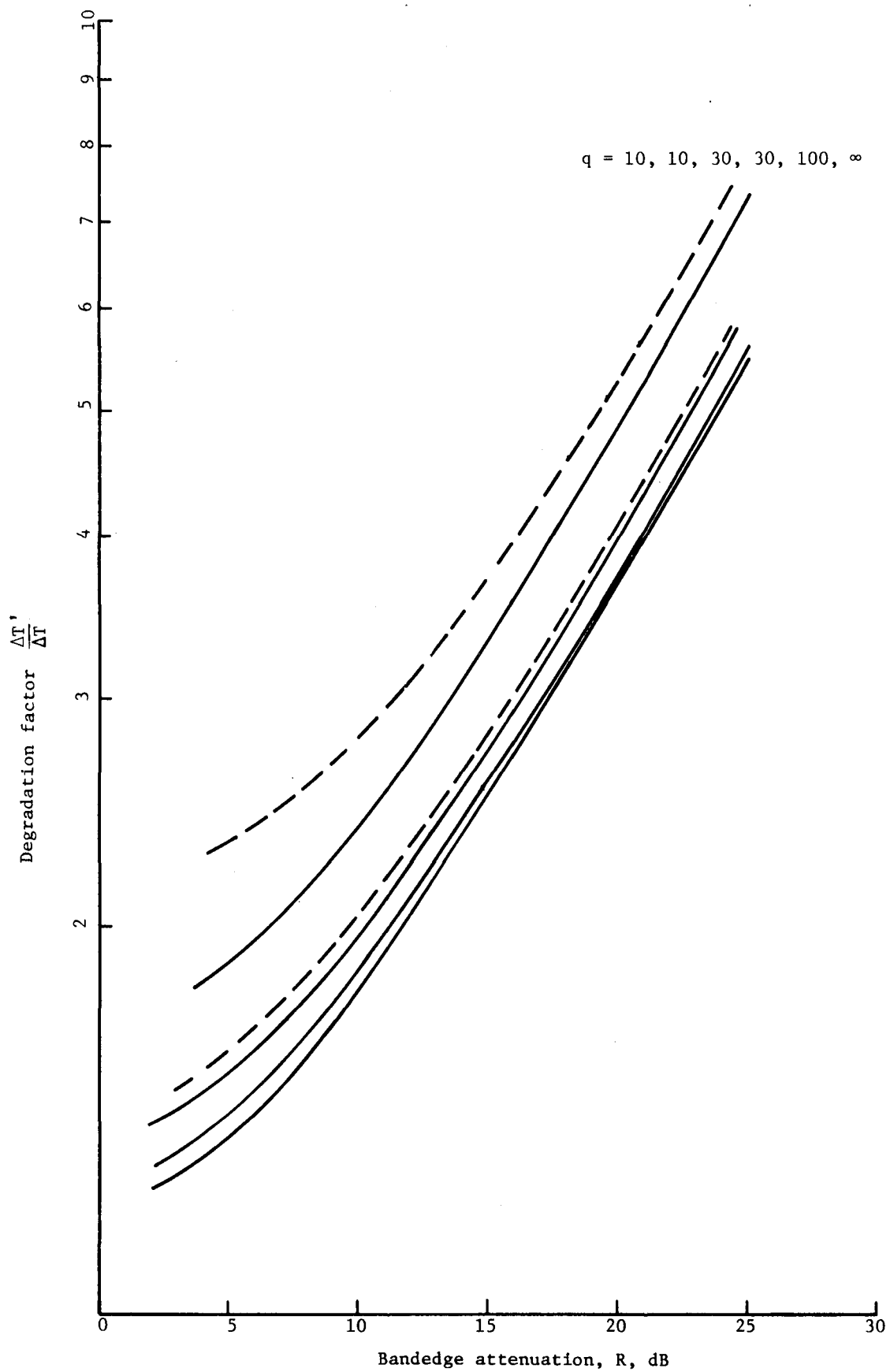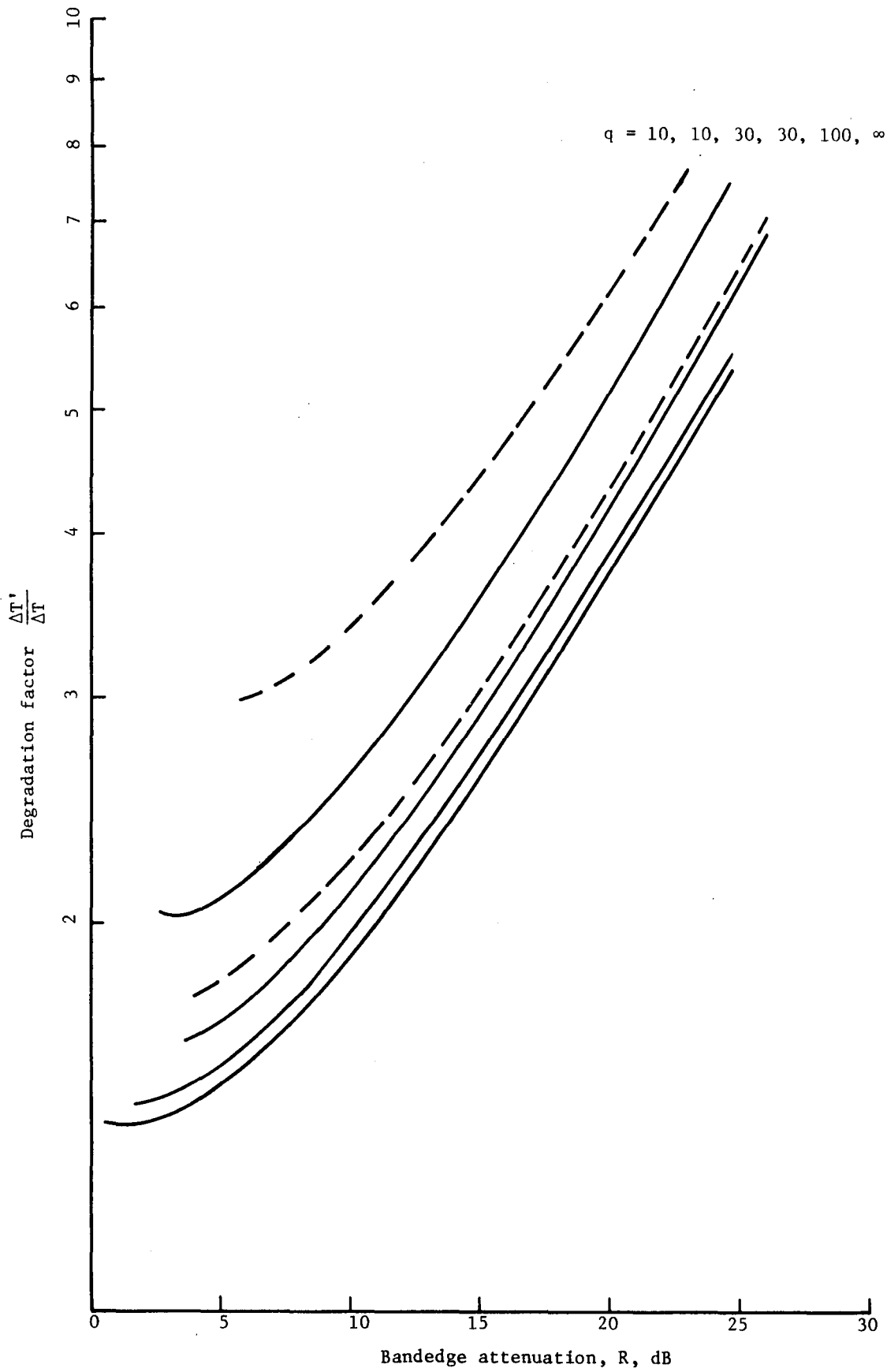
Bandedge attenuation, R, dB
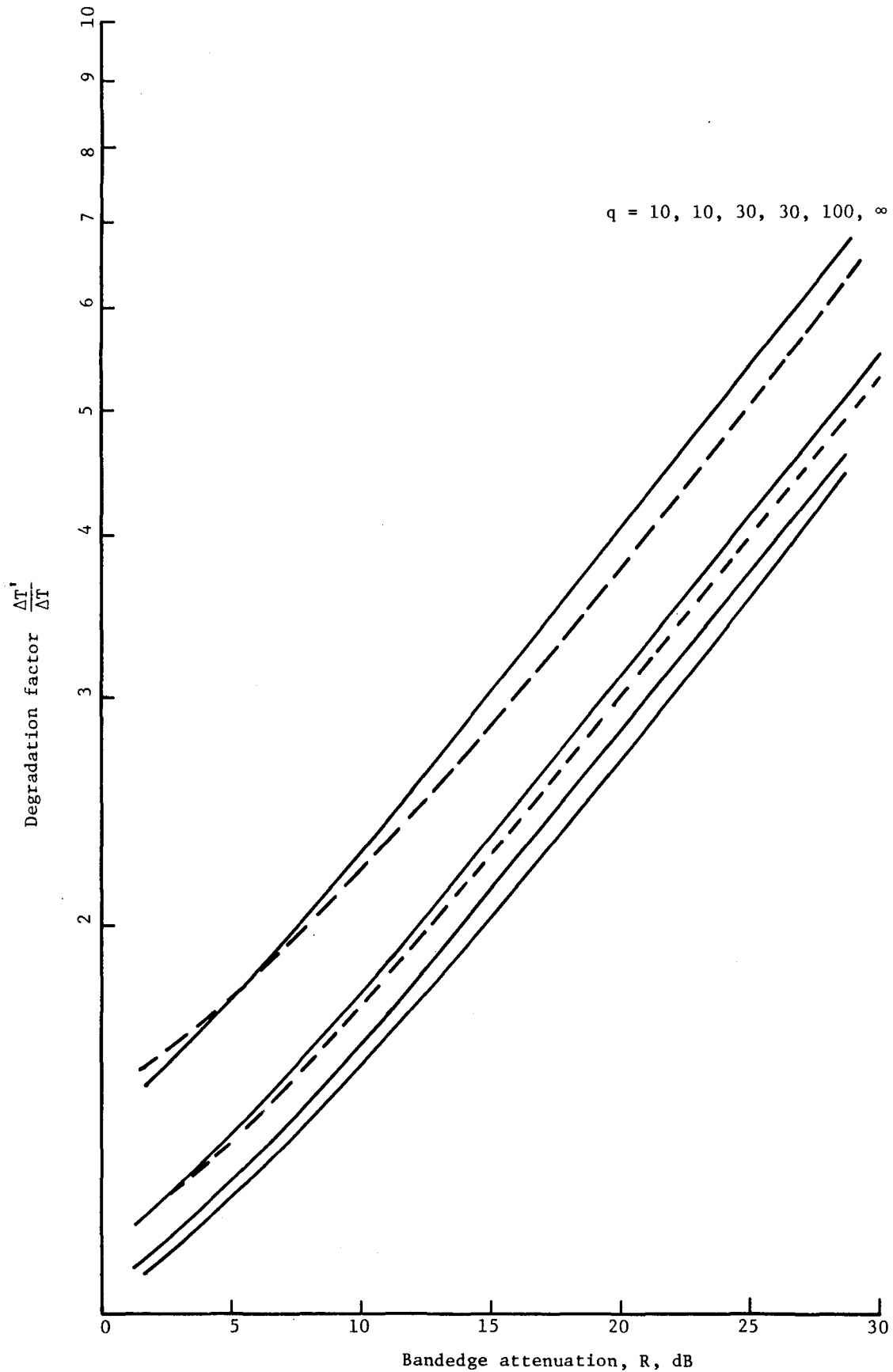
q = 10, 10, 30, 30, 100, ∞
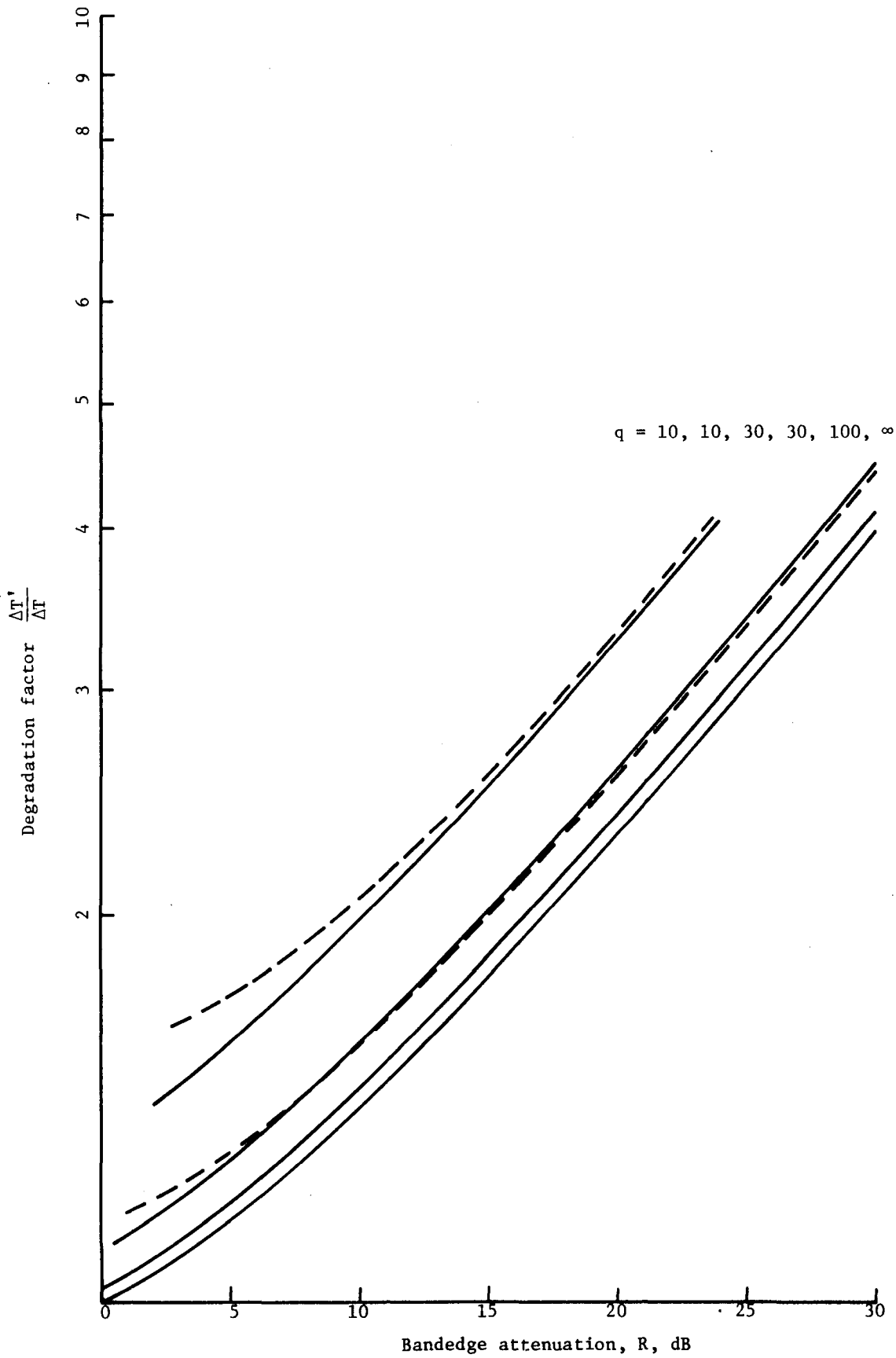
q = 10, 10, 30, 30, 100, ∞

Fig. E8. r = 0.1 dB, 3 poles.

Fig. E9. r = 0.5 dB, 3 poles.
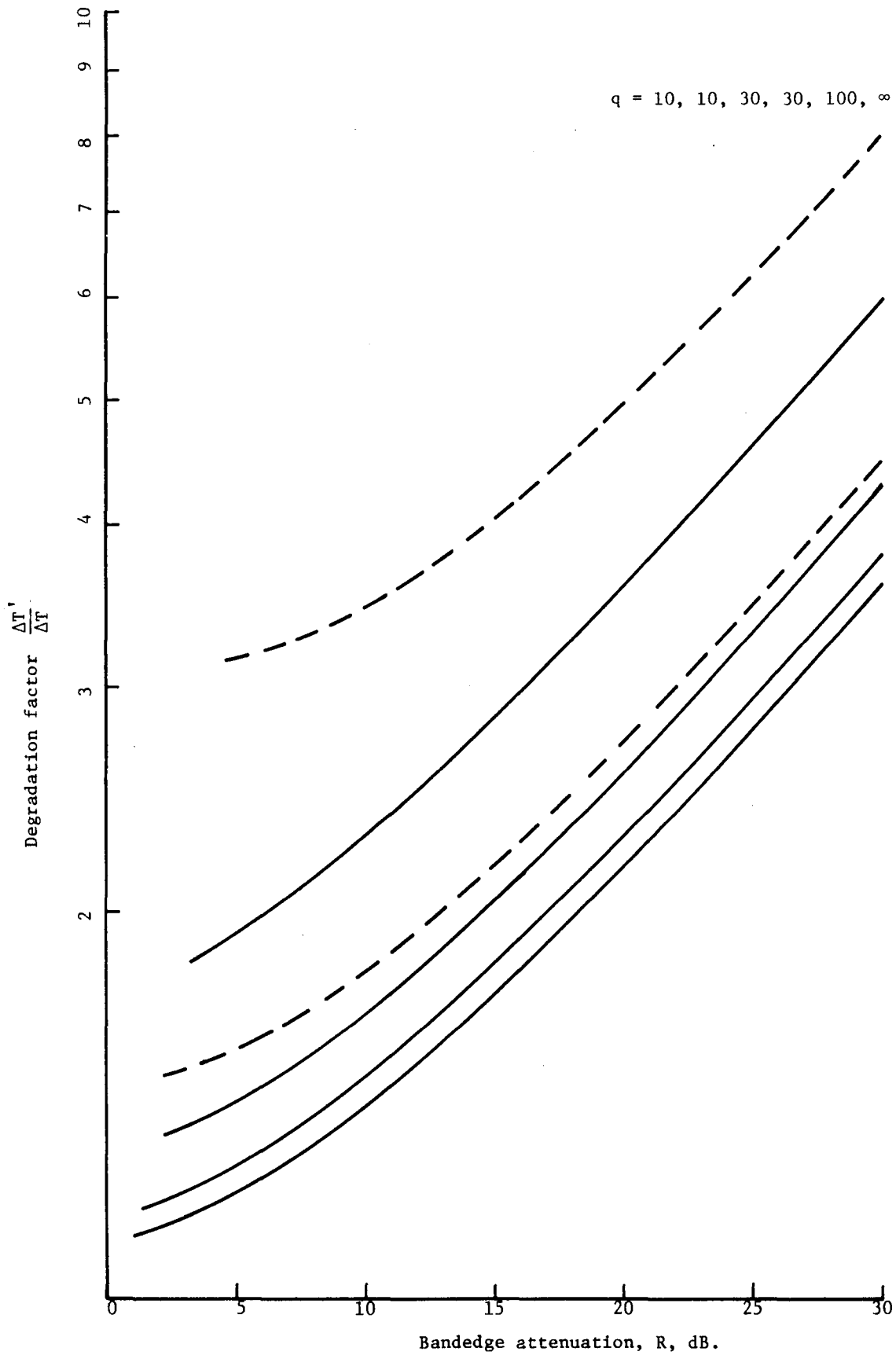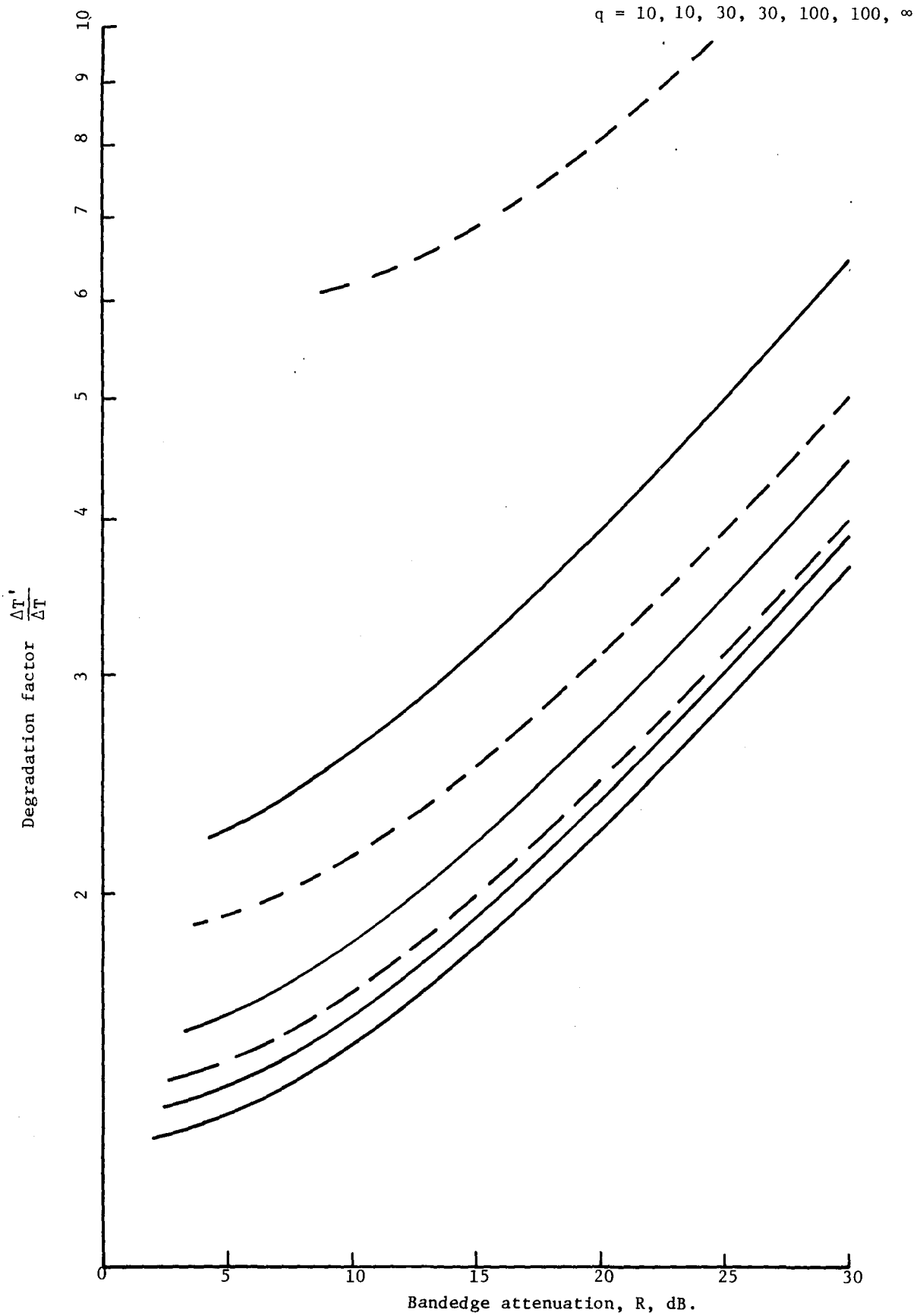
q = 10, 10, 30, 30, 100, ∞

Degradation factor $\frac{\Delta T'}{\Delta T}$

Bandedge attenuation, R, dB.

q = 10, 10, 30, 30, 100, ∞

Degradation factor $\frac{\Delta T'}{\Delta T}$

Bandedge attenuation, R, dB.

Fig. E10. r = 1 dB, 3 poles.

q = 10, 10, 30, 30, 100, 100, ∞

Fig. E11.   r = 2 dB, 3 poles.

q = 10, 30, 30, 100, 100, ∞

Bandedge attenuation, R, dB.

Fig. E12.   r = 3 dB, 3 poles.

52

Fig. E13. r = 0 dB, 4 poles.

q = 10, 10, 30, 30, 100, ∞

Degradation factor $\frac{\Delta T'}{\Delta T}$
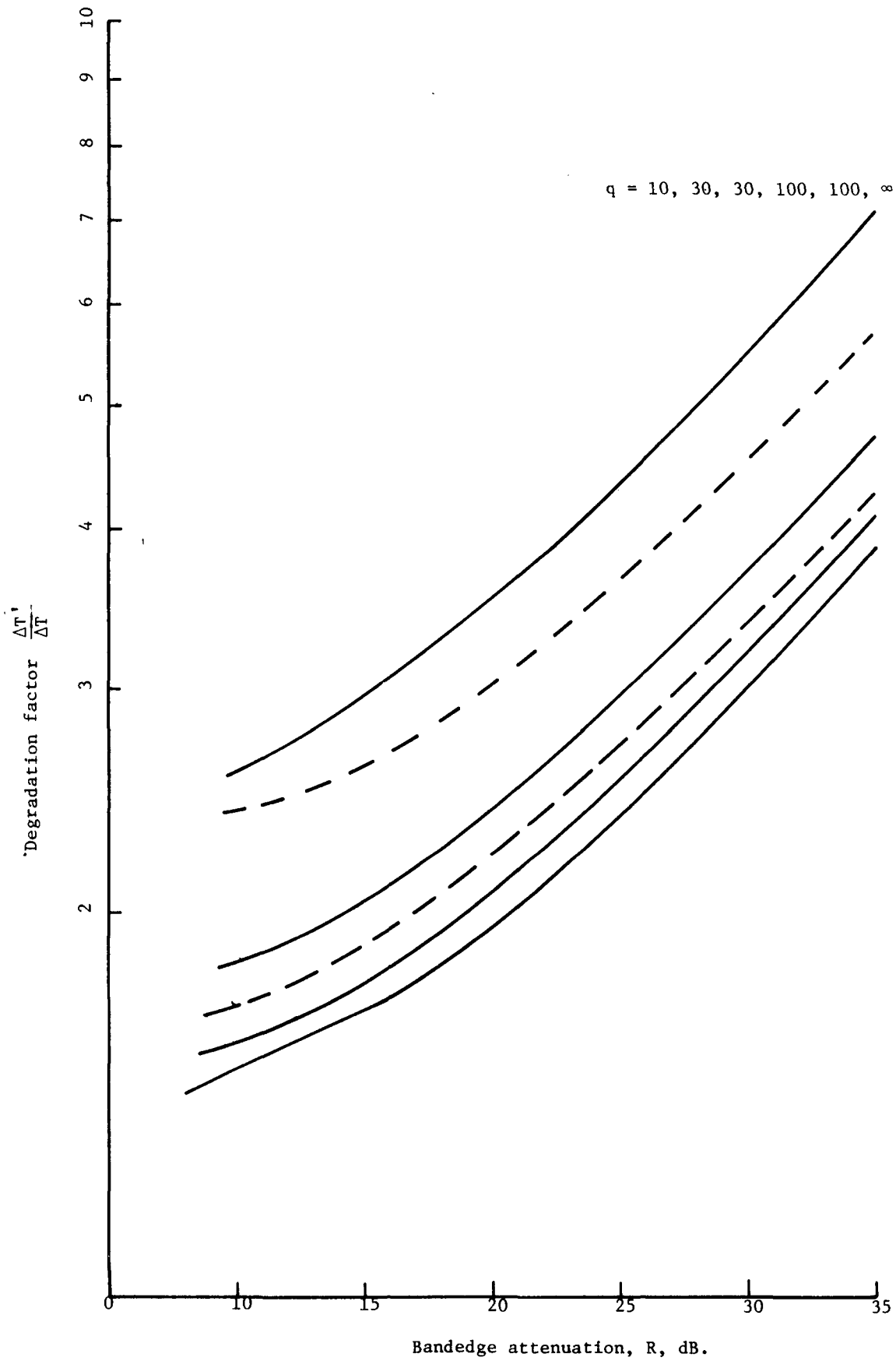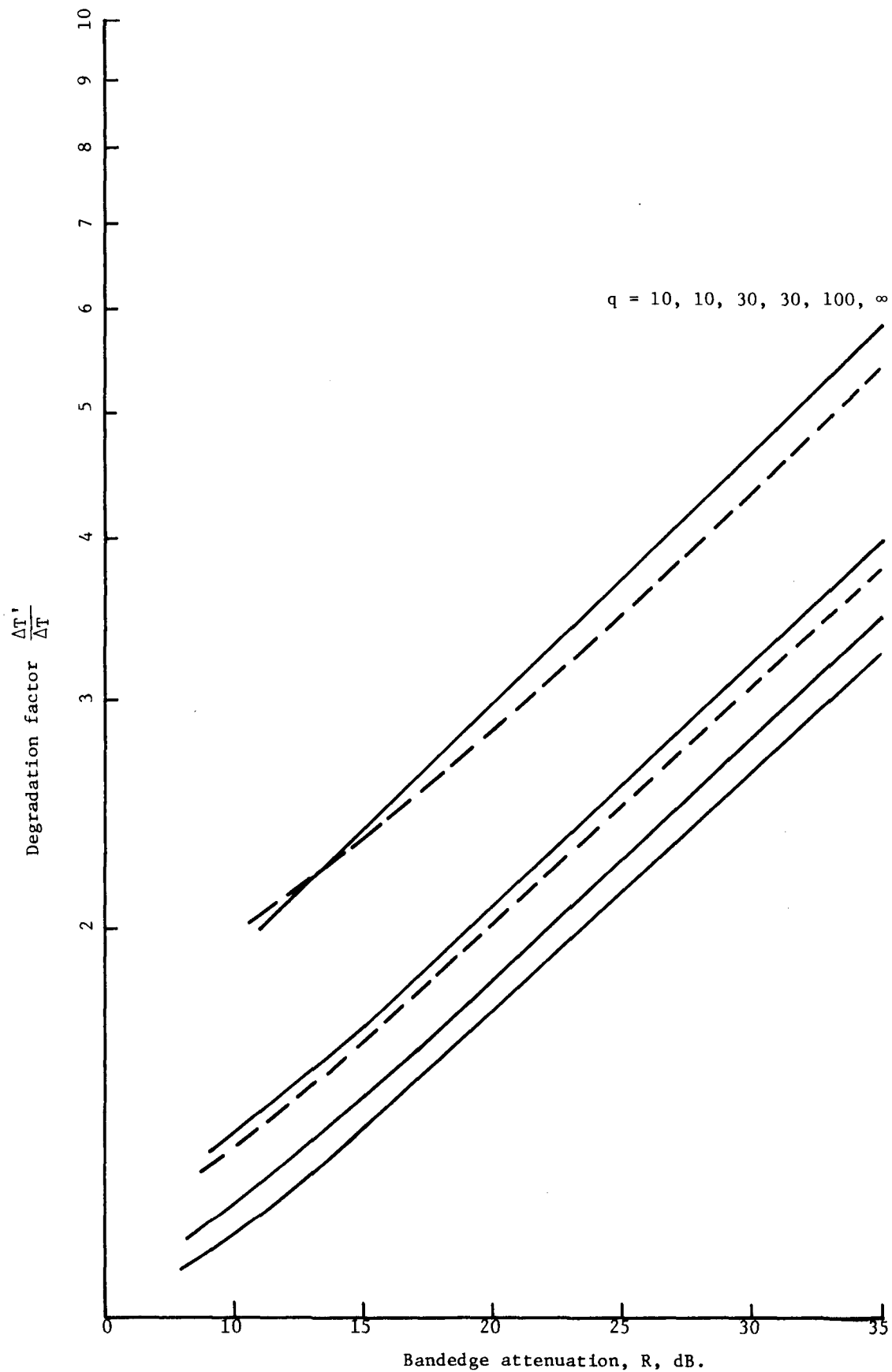
Bandedge attenuation, R, dB.
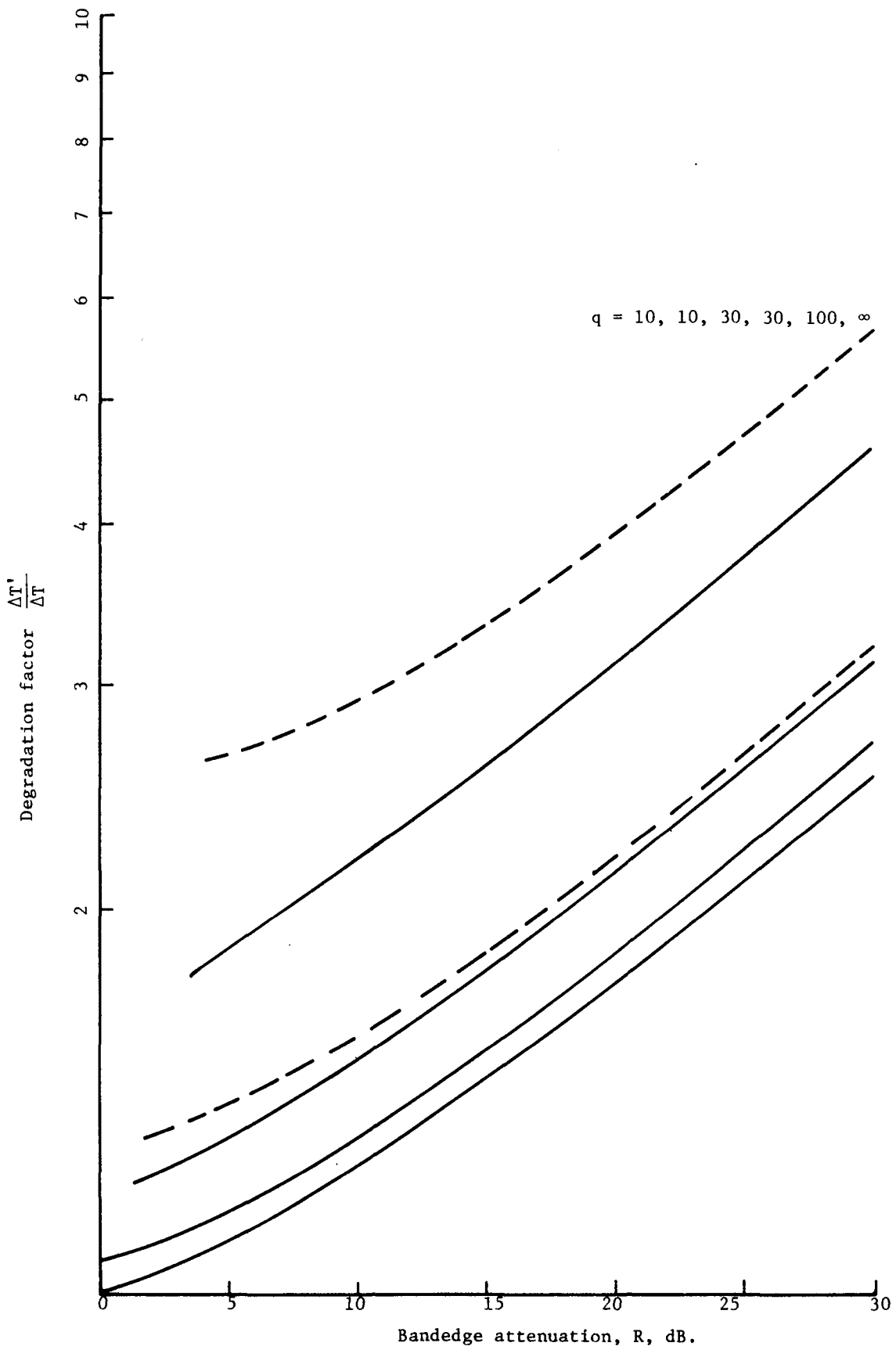
Fig. E14. r = 0.1 dB, 4 poles.

q = 10, 10, 30, 30, 100, 100, ∞

Bandedge attenuation, R, dB.

Fig. E15. r = 0.5 dB, 4 poles.

q = 10, 30, 30, 100, 100, ∞

Bandedge attenuation, R, dB.

Fig. E16.   r = 1 dB, 4 poles.

56

q = 10, 30, 30, 100, 100, ∞

Fig. E17. r = 2 dB, 4 poles.

Bandedge attenuation, R, dB.

Degradation factor $\frac{\Delta T'}{\Delta T}$

Fig. E18. r = 3 dB, 4 poles.

q = 10, 30, 30, 100, 100, ∞

Degradation factor $\frac{\Delta T'}{\Delta T}$

Bandedge attenuation, R, dB.

q = 10, 10, 30, 30, 100, 100, ∞

Degradation factor $\frac{\Delta T'}{\Delta T}$

Bandedge attenuation, R, dB.

Fig. E19.   r = 0 dB, 5 poles.

q = 10, 10, 30, 30, 100, 100, ∞

Fig. E20.   r = 0.1 dB, 5 poles.

Fig. E21.   r = 0.5 dB, 5 poles.

q = 10, 30, 30, 100, 100, ∞

Degredation factor $\frac{\Delta T'}{\Delta T}$
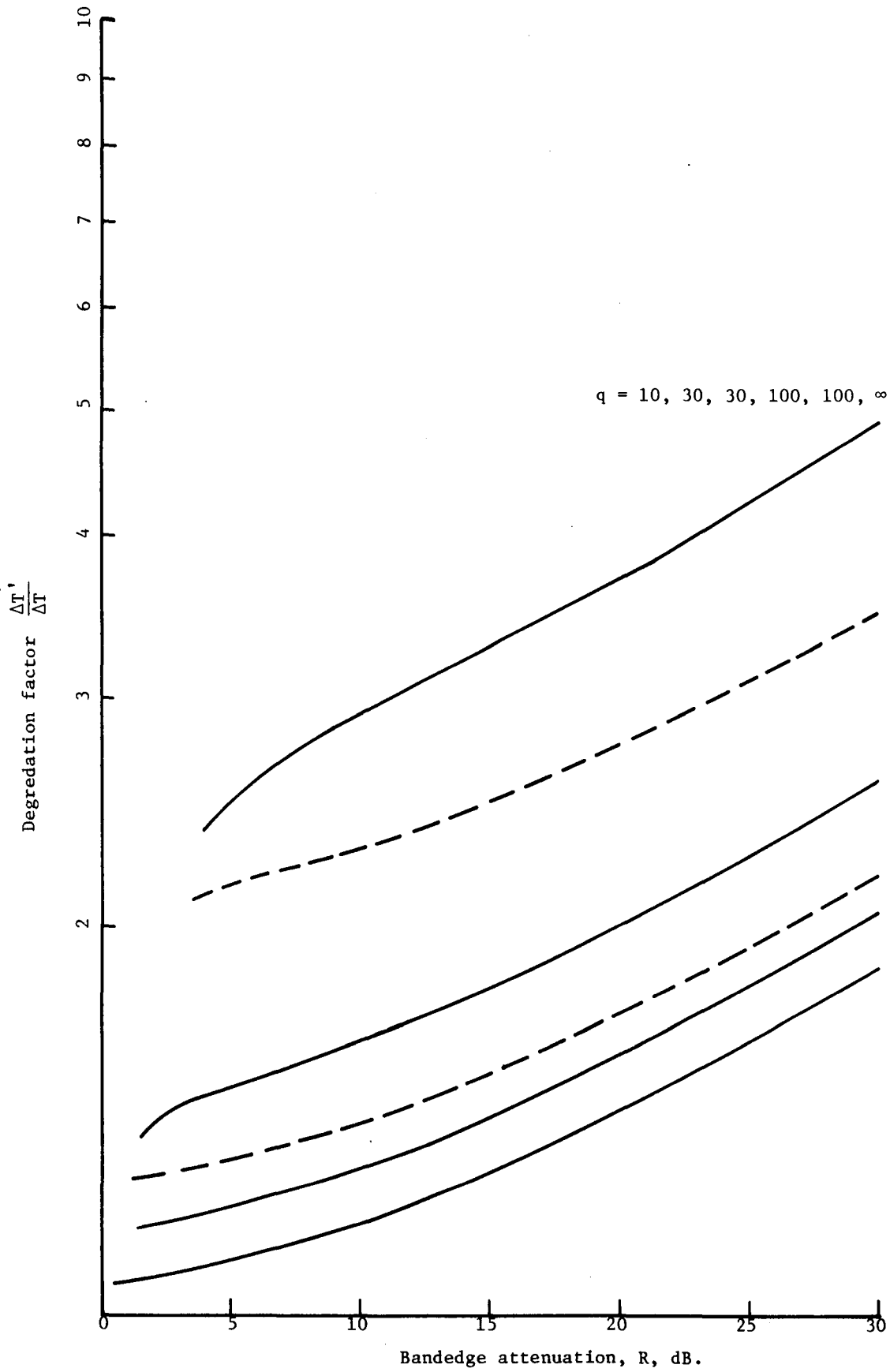
Bandedge attenuation, R, dB.
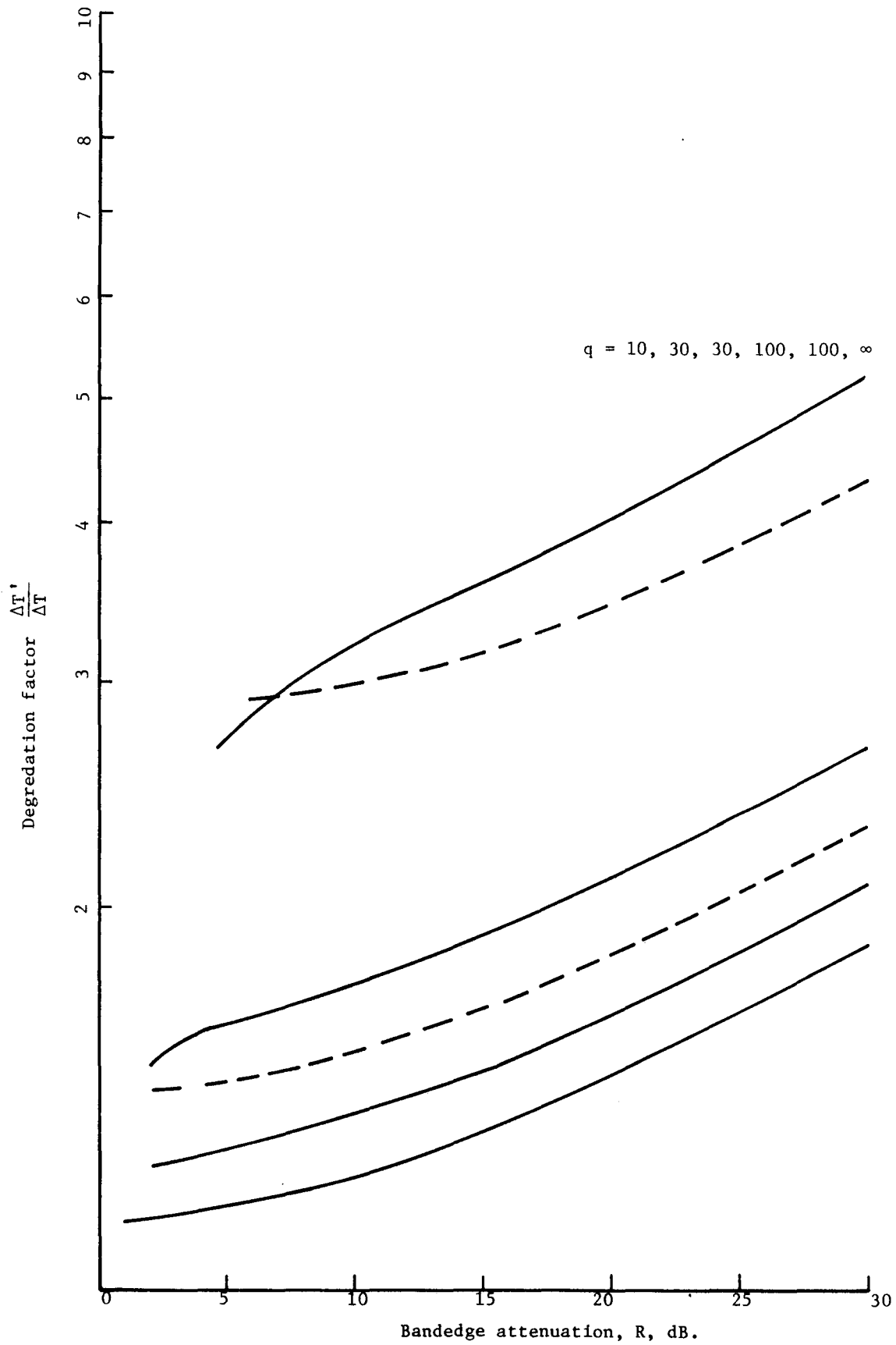
Fig. E22. r = 1 dB, 5 poles.

Fig. E23.   r = 2 dB, 5 poles.

q = 30, 10, 30, 100, 100, ∞

Degredation factor $\frac{\Delta T'}{\Delta T}$

Bandedge attenuation, R, dB.

q = 30, 10, 30, 100, 100, ∞

Fig. E24. r = 3 dB, 5 poles.

Bandedge attenuation, R, dB.

Degredation factor $\frac{\Delta T'}{\Delta T}$

64

q = 10, 10, 30, 30, 100, 100, ∞

Degredation factor $\frac{\Delta T'}{\Delta T}$
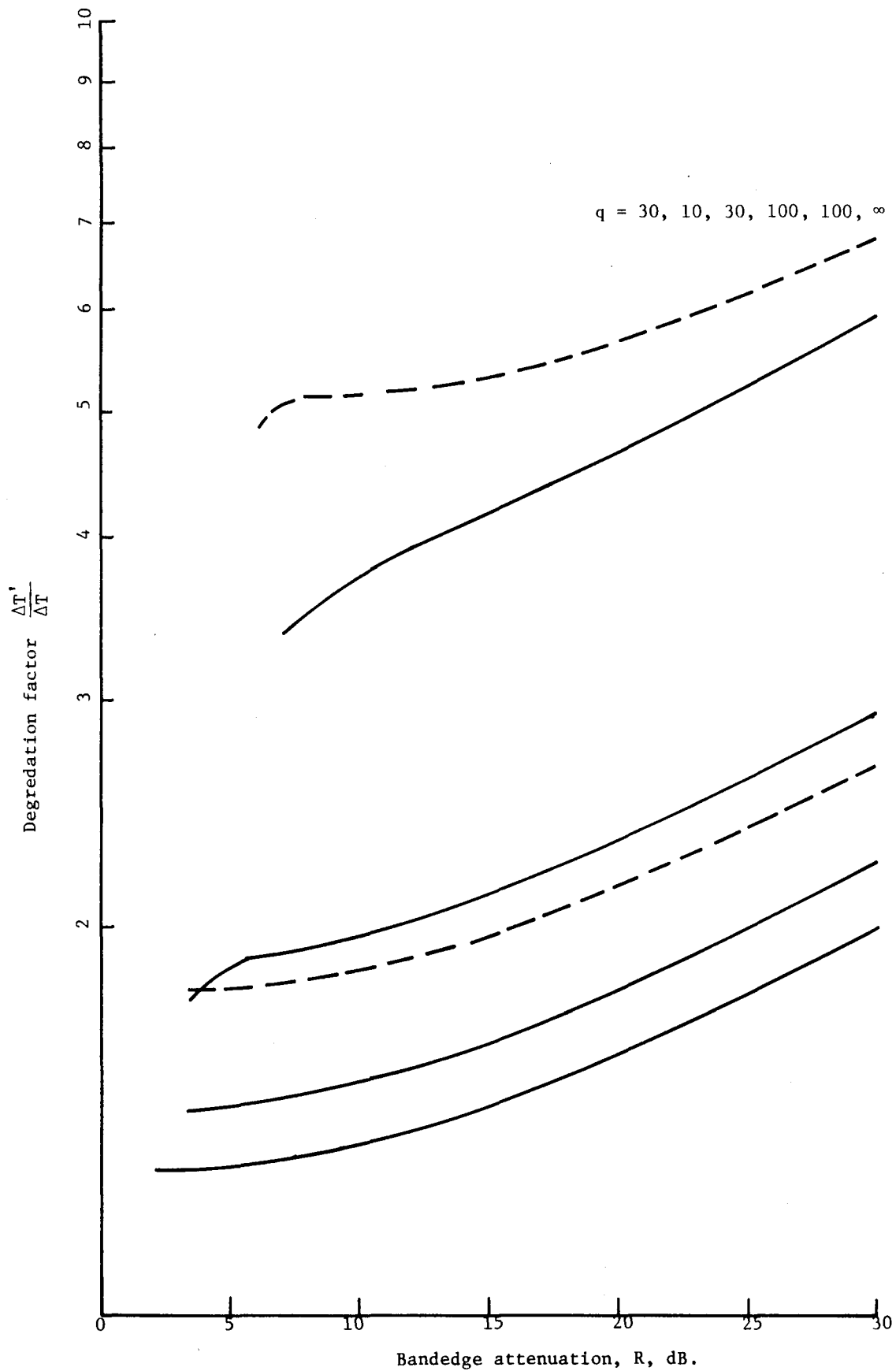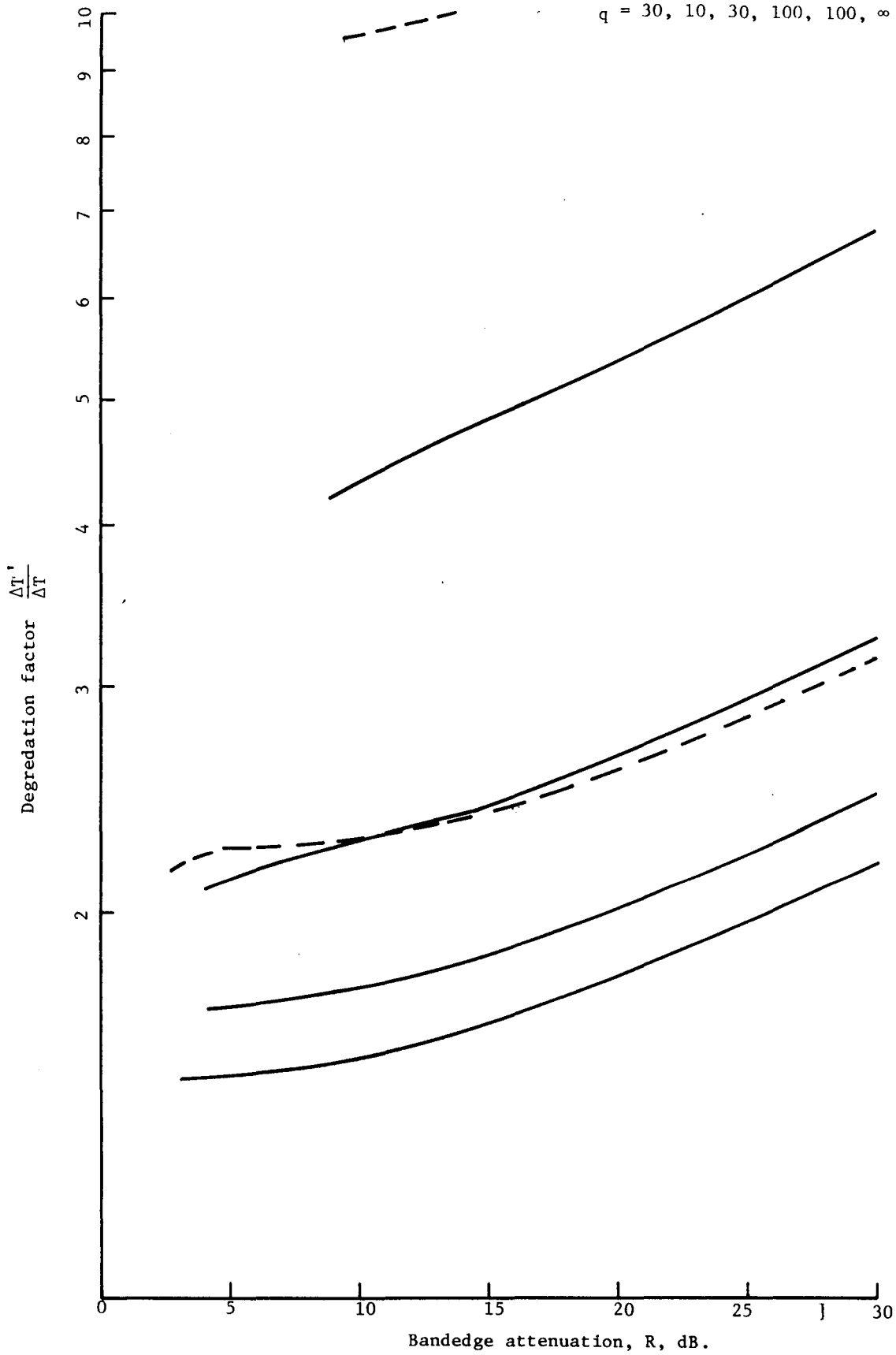
Bandedge attenuation, R, dB.
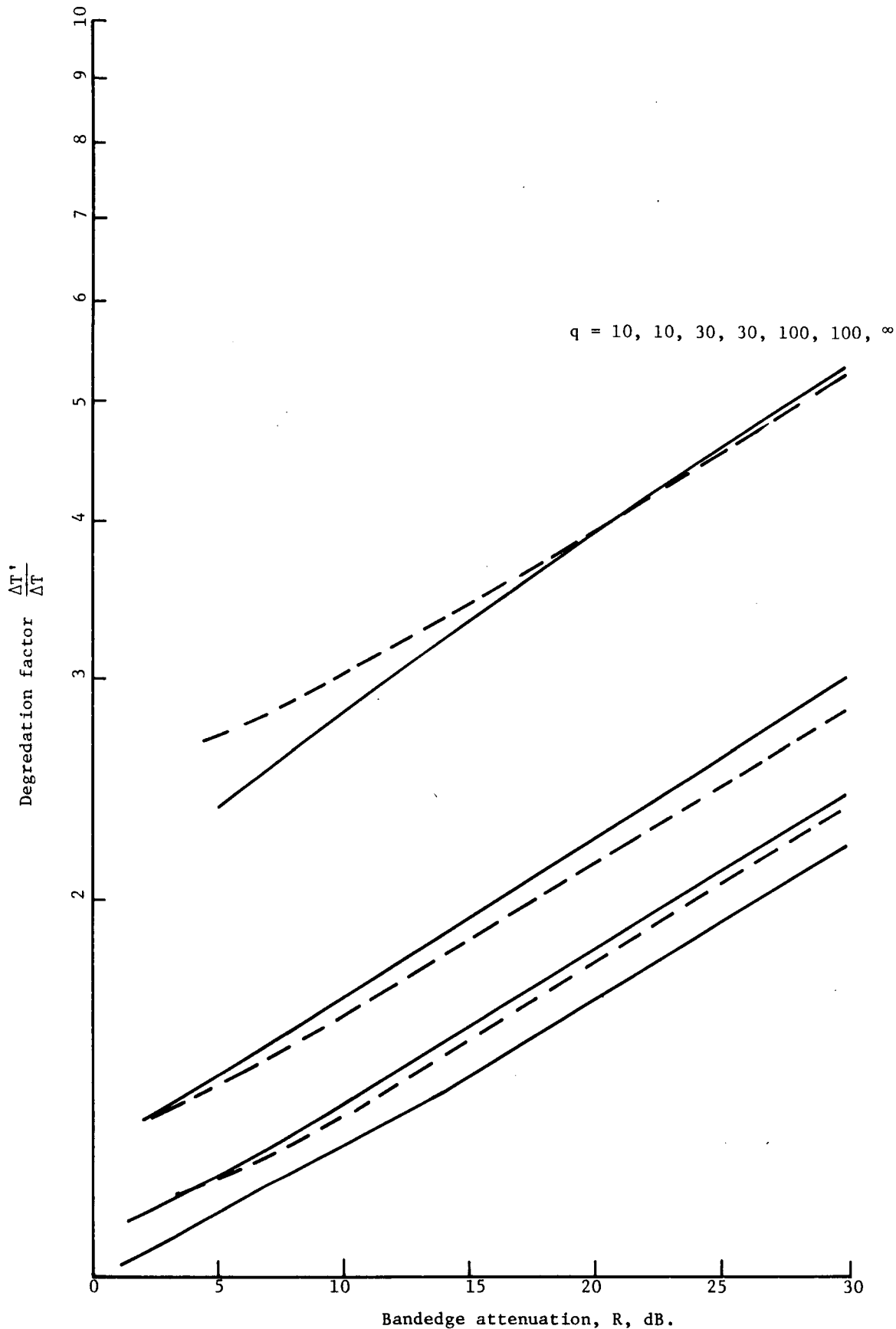
Fig. E25.   r = 0, 6 poles.

Fig. E26. r = 0.1 dB, 6 poles.
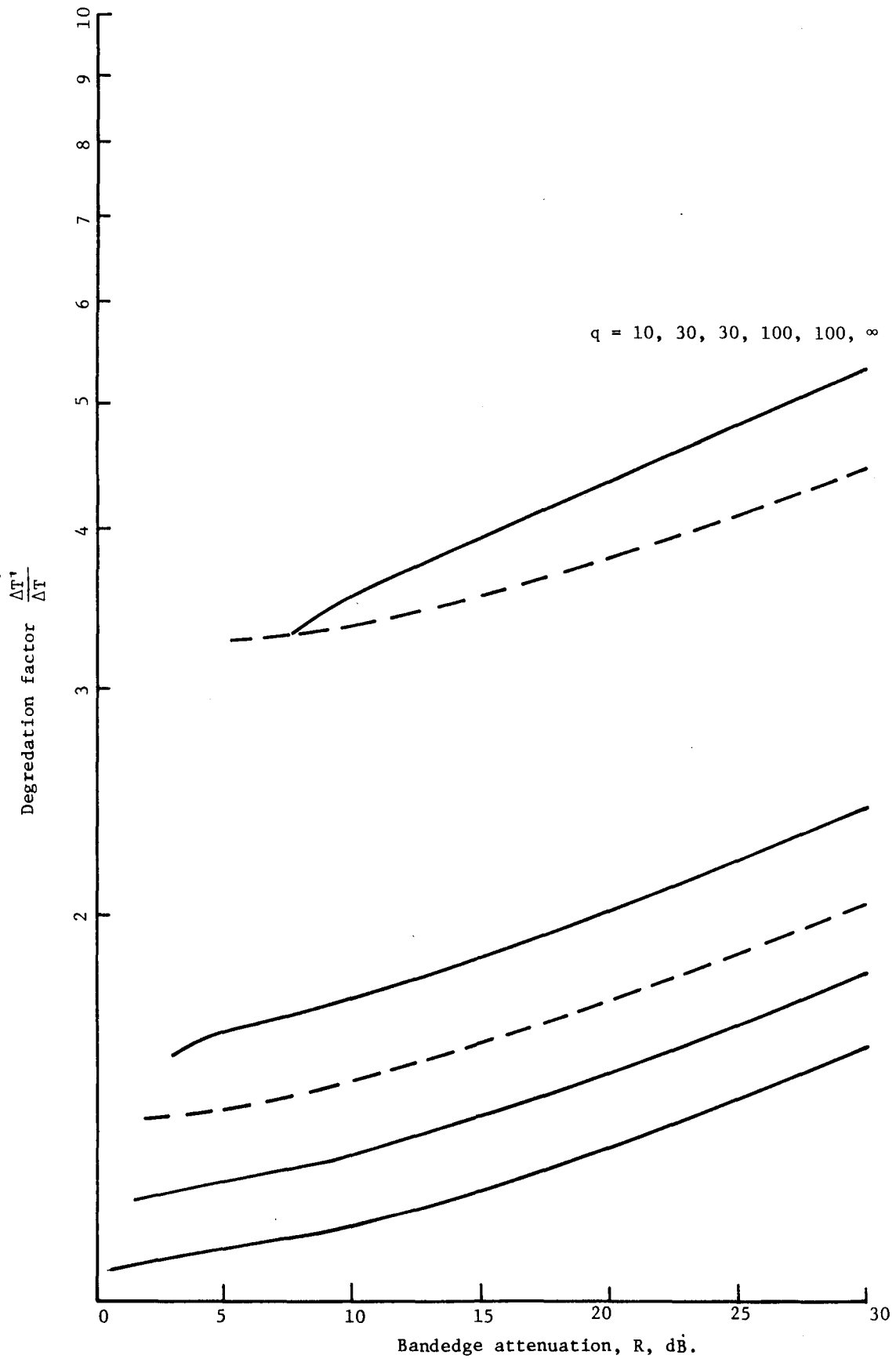
q = 10, 30, 30, 100, 100, ∞

Degredation factor $\frac{\Delta T'}{\Delta T}$

Bandedge attenuation, R, dB.

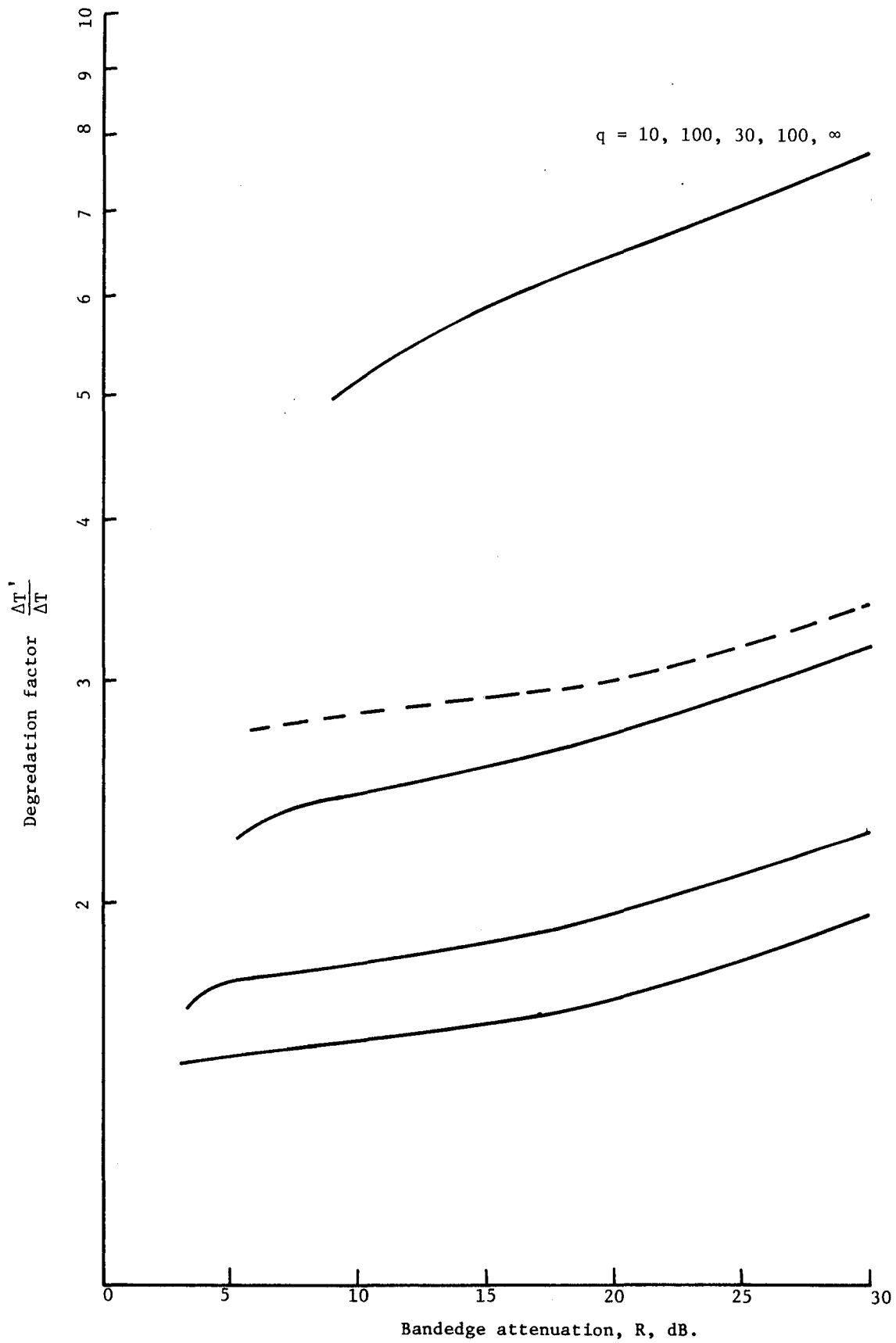Fig. E27.   r = 0.5 dB, 6 poles.

67

Fig. E28. r = 1 dB, 6 poles.

q = 30, 10, 30, 100, 100, ∞

Degredation factor $\frac{\Delta T'}{\Delta T}$

Bandedge attenuation, R, dB.

Fig. E29. r = 2 dB, 6 poles.

q = 10, 30, 100, 100, ∞

Degredation factor $\frac{\Delta T'}{\Delta T}$

Bandedge attenuation, R, dB.

q = 10, 100, 30, 100, ∞

Degredation factor $\frac{\Delta T'}{\Delta T}$
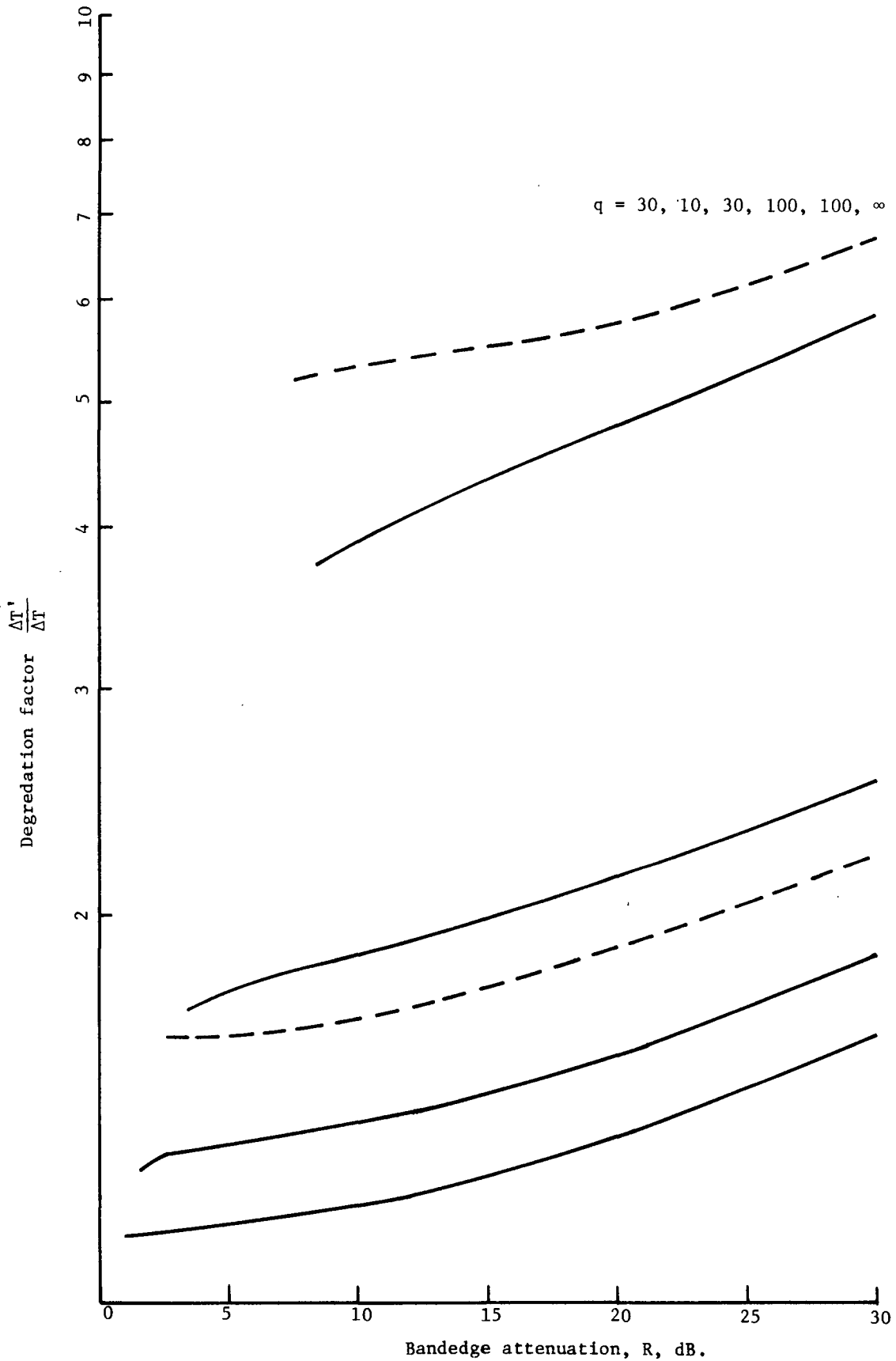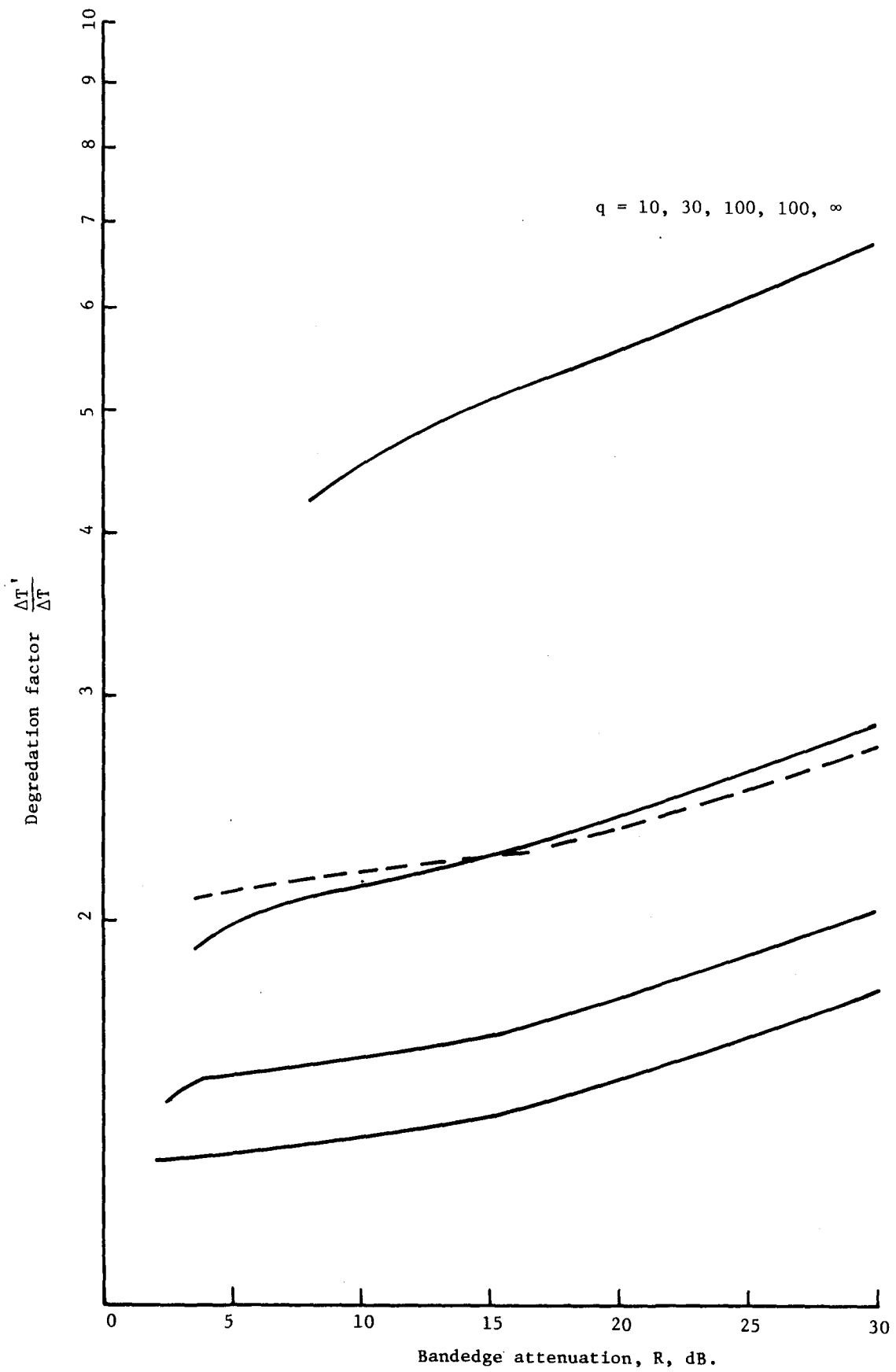
Bandedge attenuation, R, dB.

Fig. E30.   r = 3 dB, 6 poles.
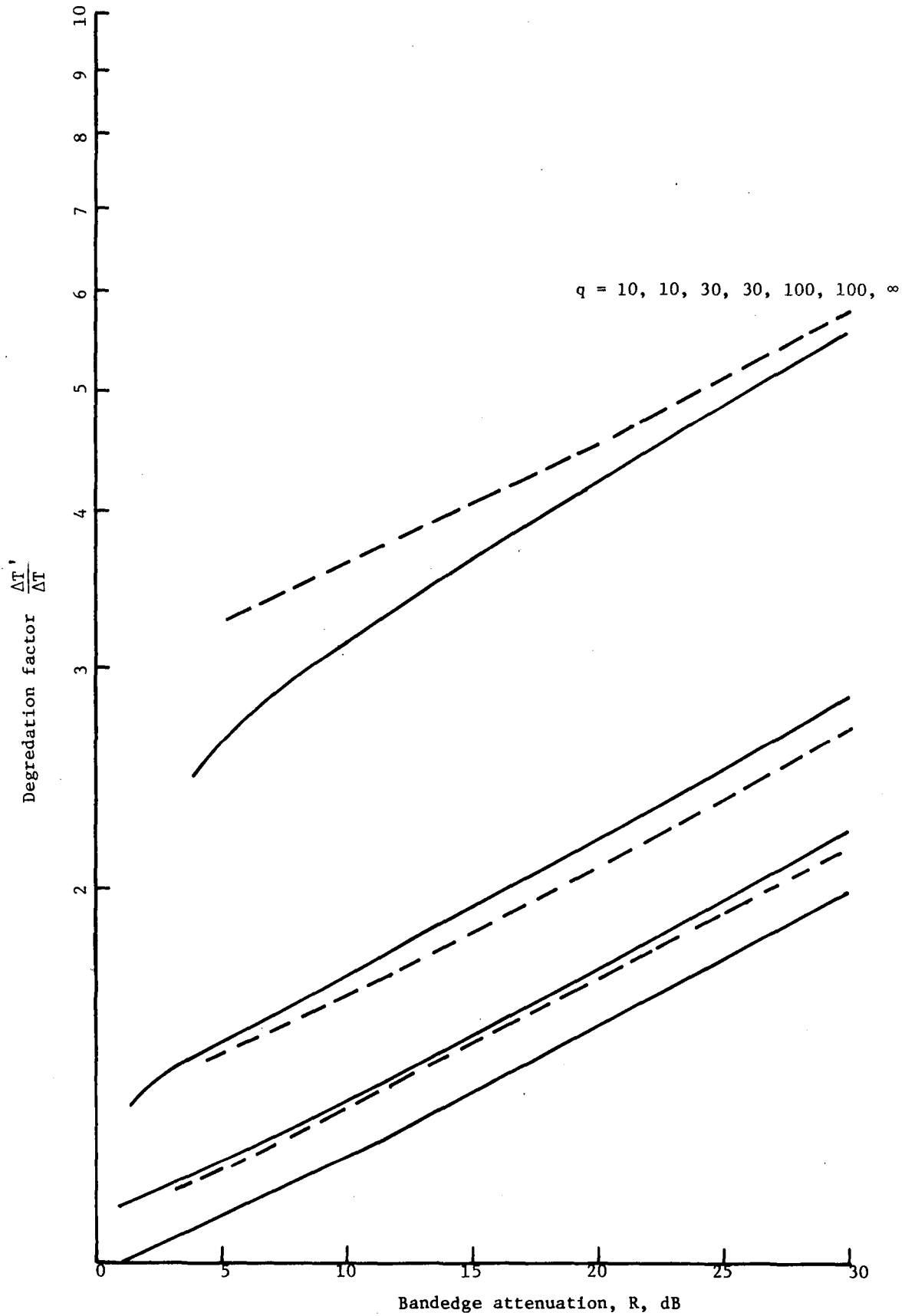
Fig. E31. r = 0 dB, 7 poles.

Fig. E32.   r = 0.1 dB, 7 poles.

Fig. E33. r = 0.5 dB, 7 poles.

q = 30, 10, 30, 100, 100, ∞

Degredation factor $\frac{\Delta T'}{\Delta T}$

Bandedge attenuation, R, dB.

73

q = 10, 30, 100, 100, ∞
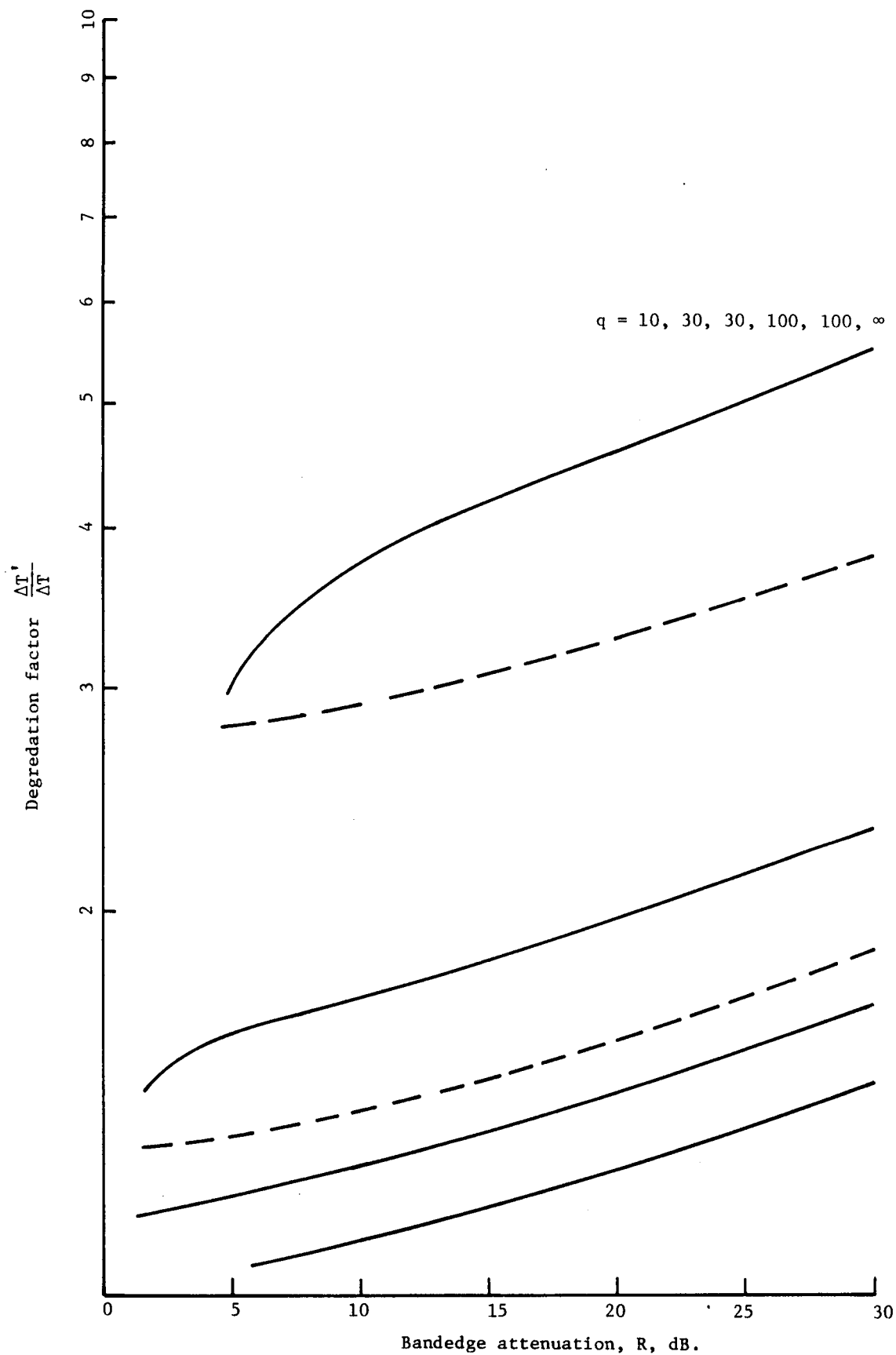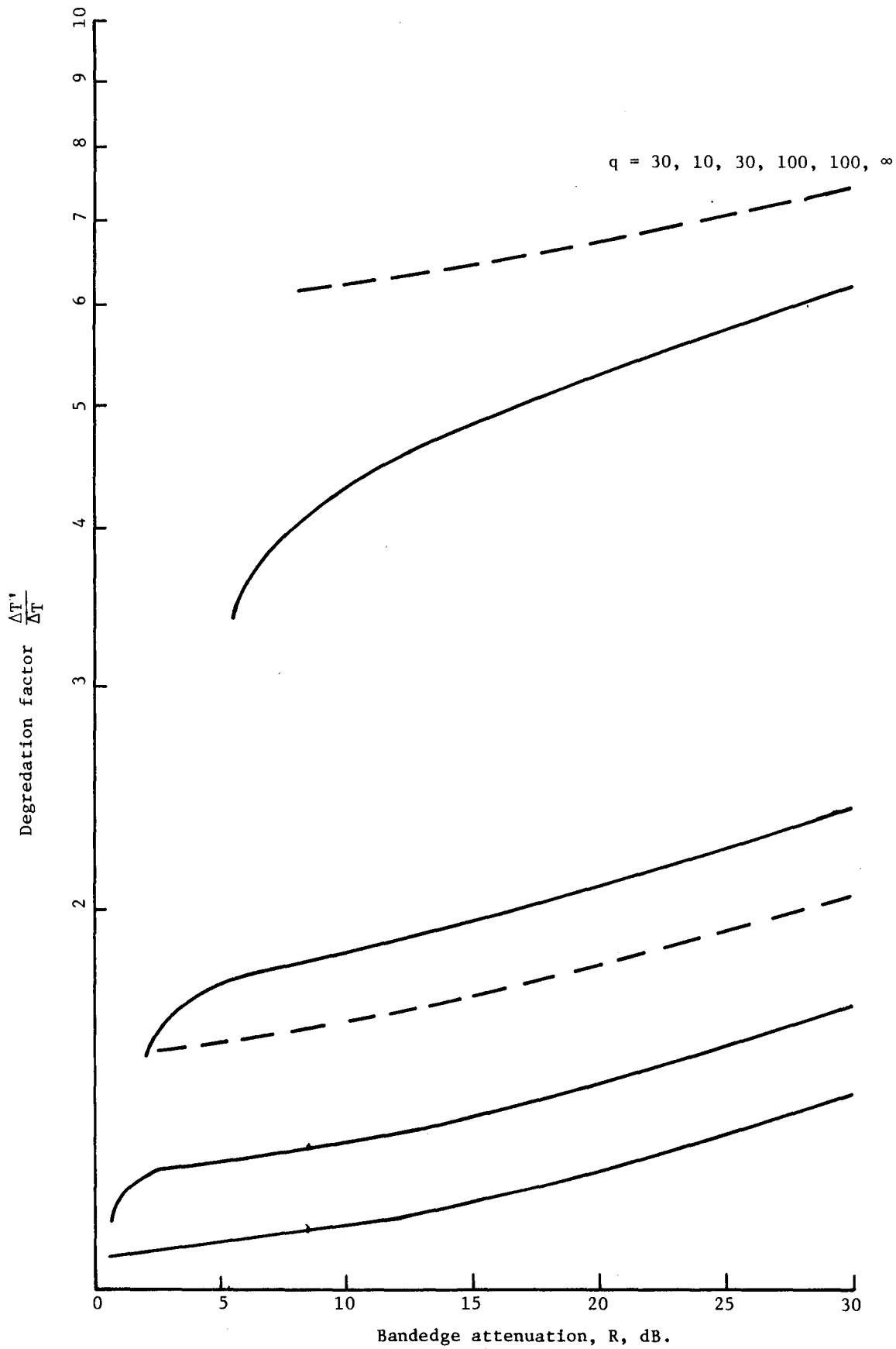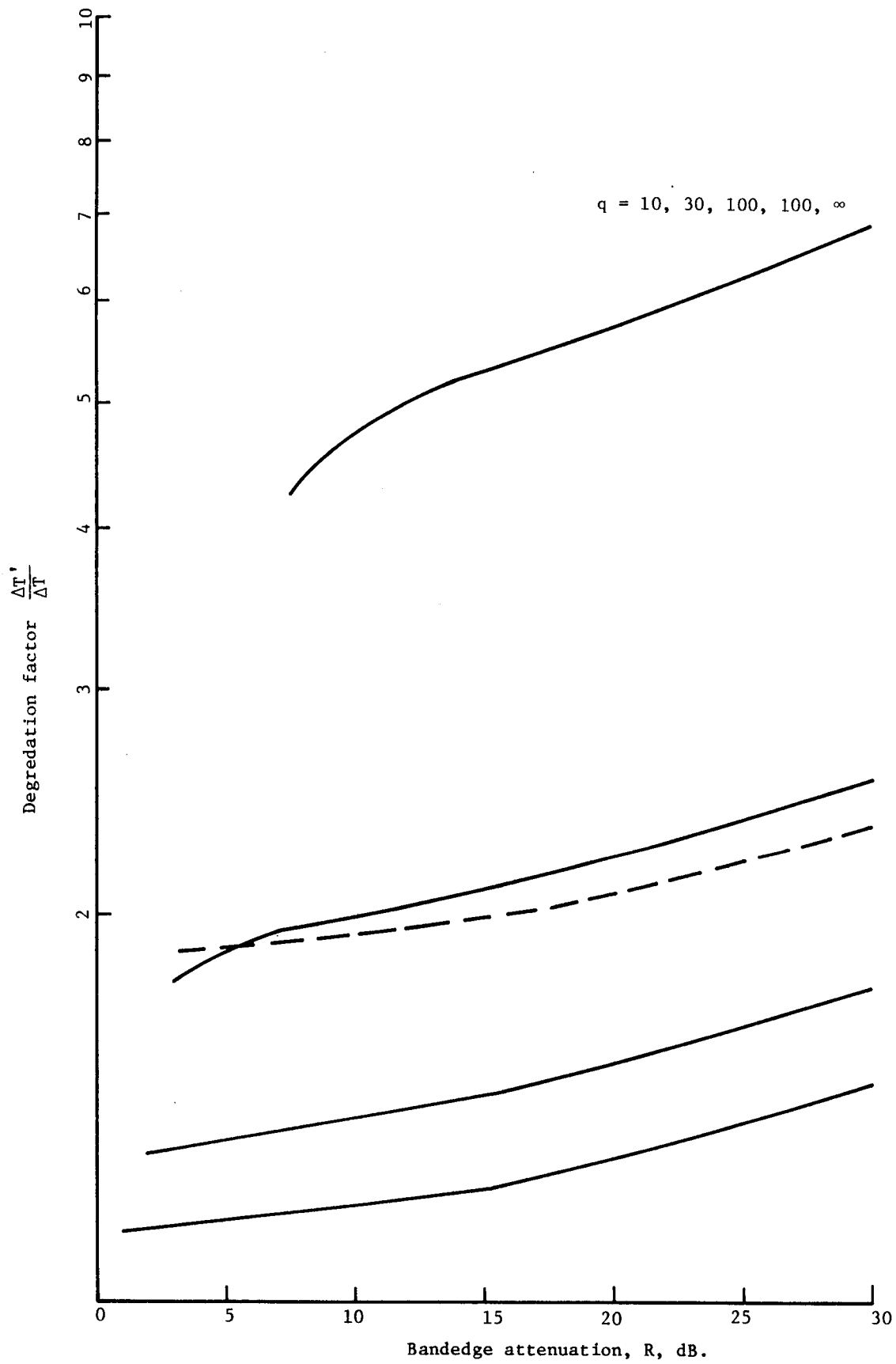
Fig. E34.   r = 1 dB, 7 poles.

74

Fig. E35. r = 2 dB, 7 poles.

q = 10, 100, 30, 100, ∞
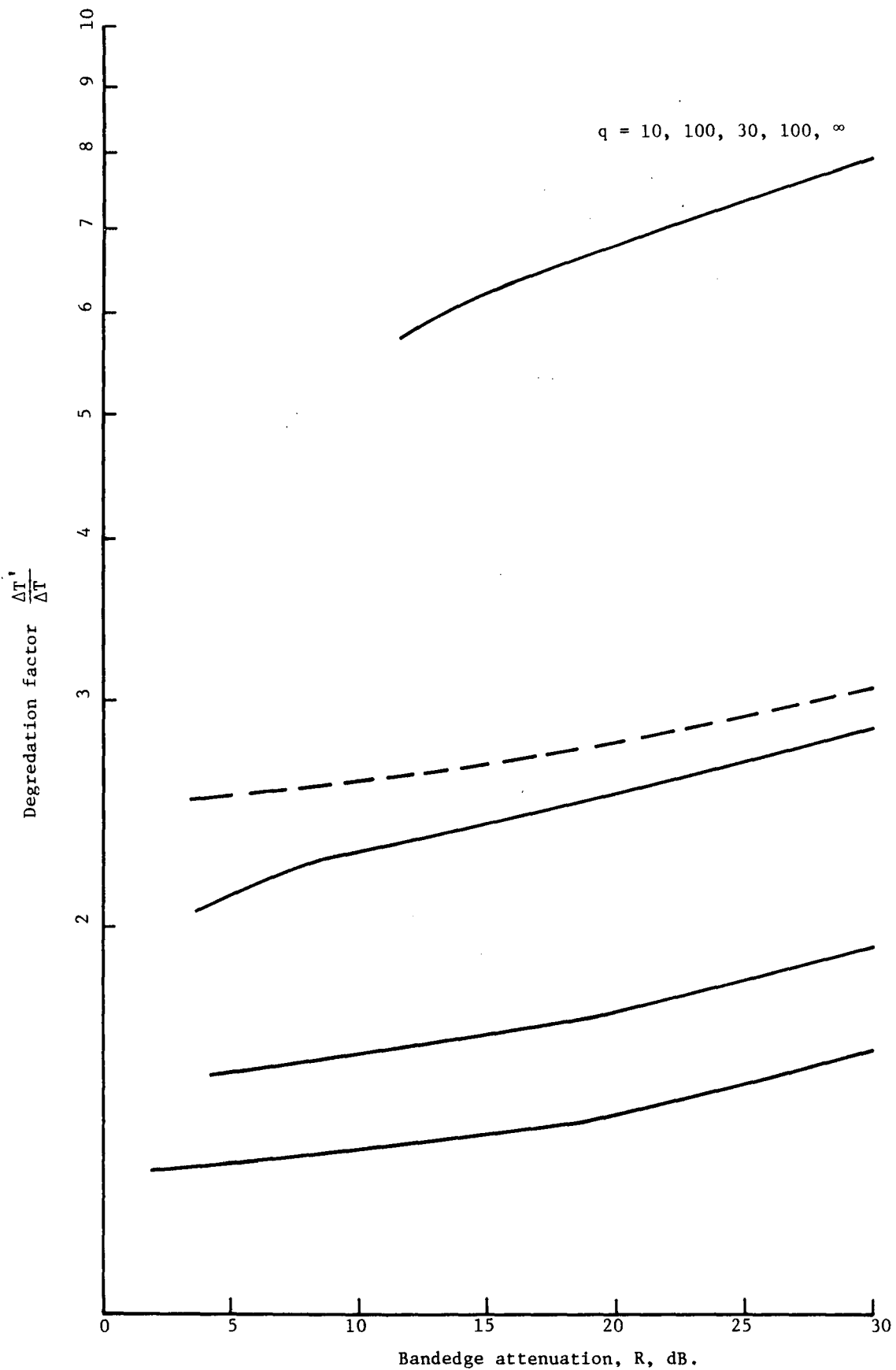
Degredation factor $\frac{\Delta T'}{\Delta T}$
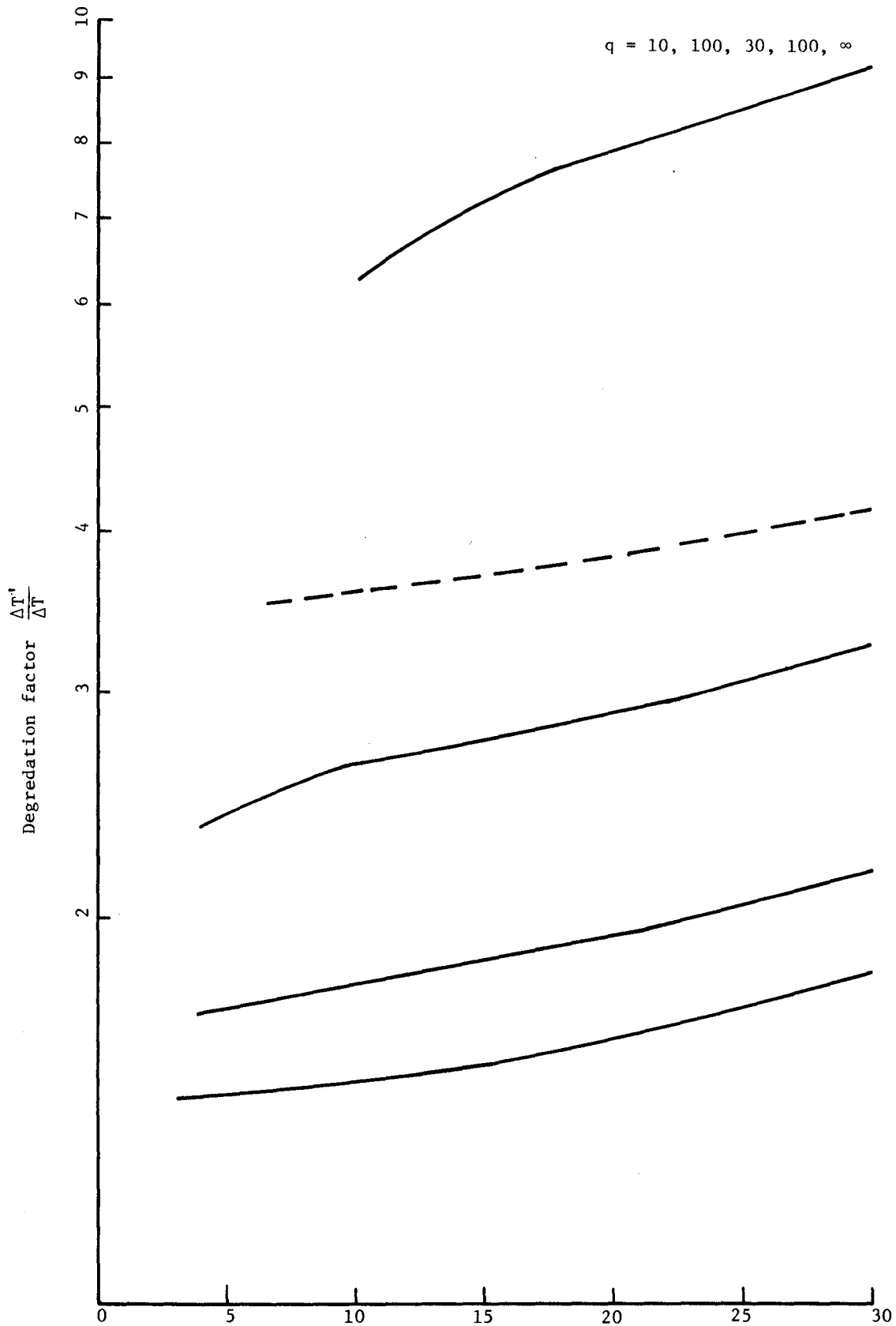
Bandedge attenuation, R, dB.

Fig. E36. r = 3 dB, 7 poles.

CURVES OF DEGRADATION FACTOR VS q WITH RIPPLE AS A PARAMETER

All curves contained in Appendix F are plots of the degradation factor vs low-pass reference q for two specific values of band-edge attenuation: 10 dB and 20 dB. To simplify the presentation, each caption provides only the attenuation and the number of poles for the particular set of curves.

The poles were adjusted by the computer program so that the q values obtained in the data represent the actual low-pass q at the frequency at which the attenuation is the specific level (i.e., 10 dB or 20 dB).

NOTE: In all cases, solid curves represent standard designs, and broken lines represent predistorted designs.
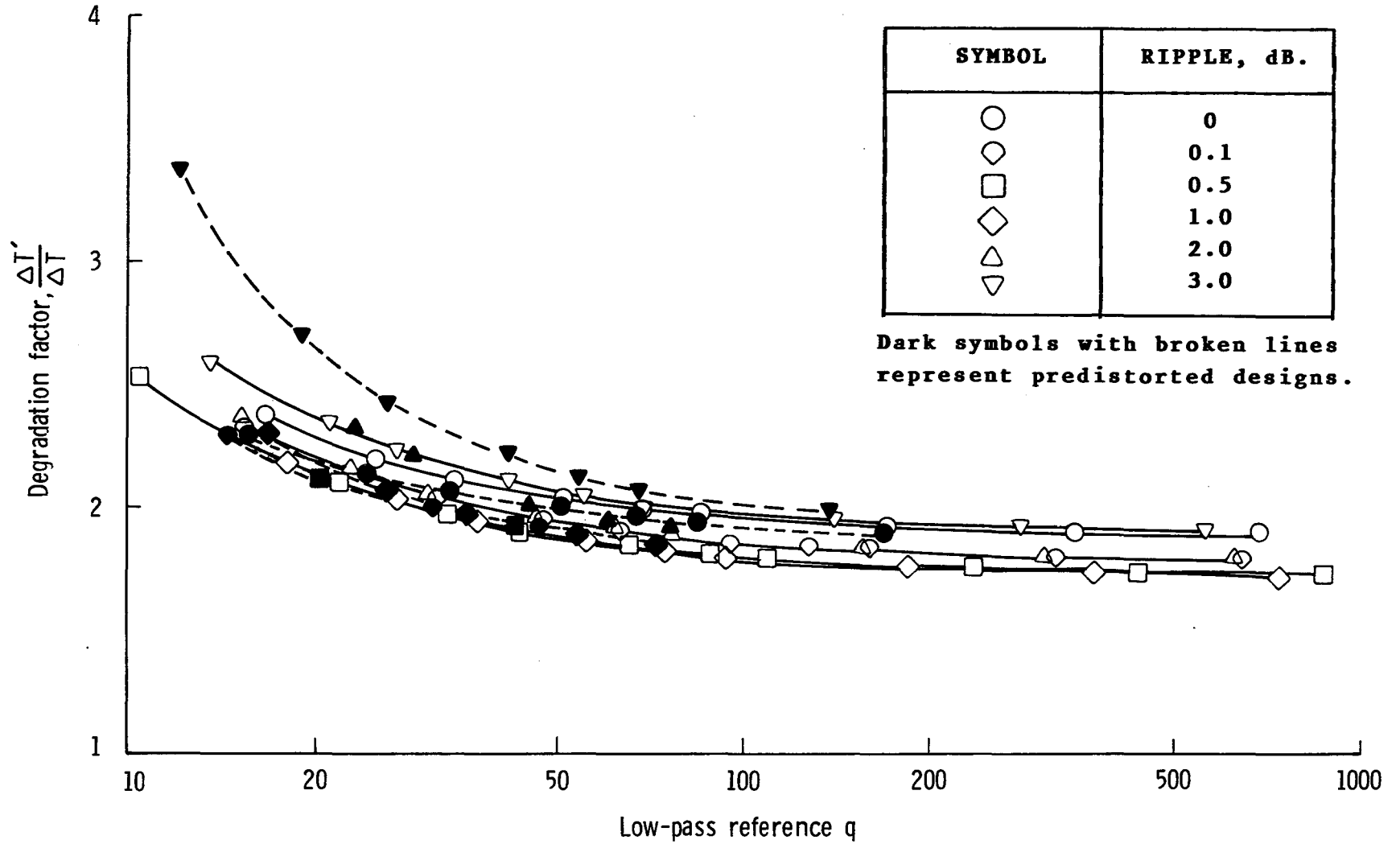
Fig. F1. Band-edge attenuation = 10 dB, 2 poles.

The chart shows Degradation factor, $\frac{\Delta T'}{\Delta T}$ on the vertical axis (ranging from 1 to 5) versus Low-pass reference q on the horizontal axis (logarithmic, ranging from 10 to 1000).

SYMBOL	RIPPLE, dB.
○	0
◇	0.1
□	0.5
◇	1.0
△	2.0
▽	3.0

Dark symbols with broken lines represent predistorted designs.
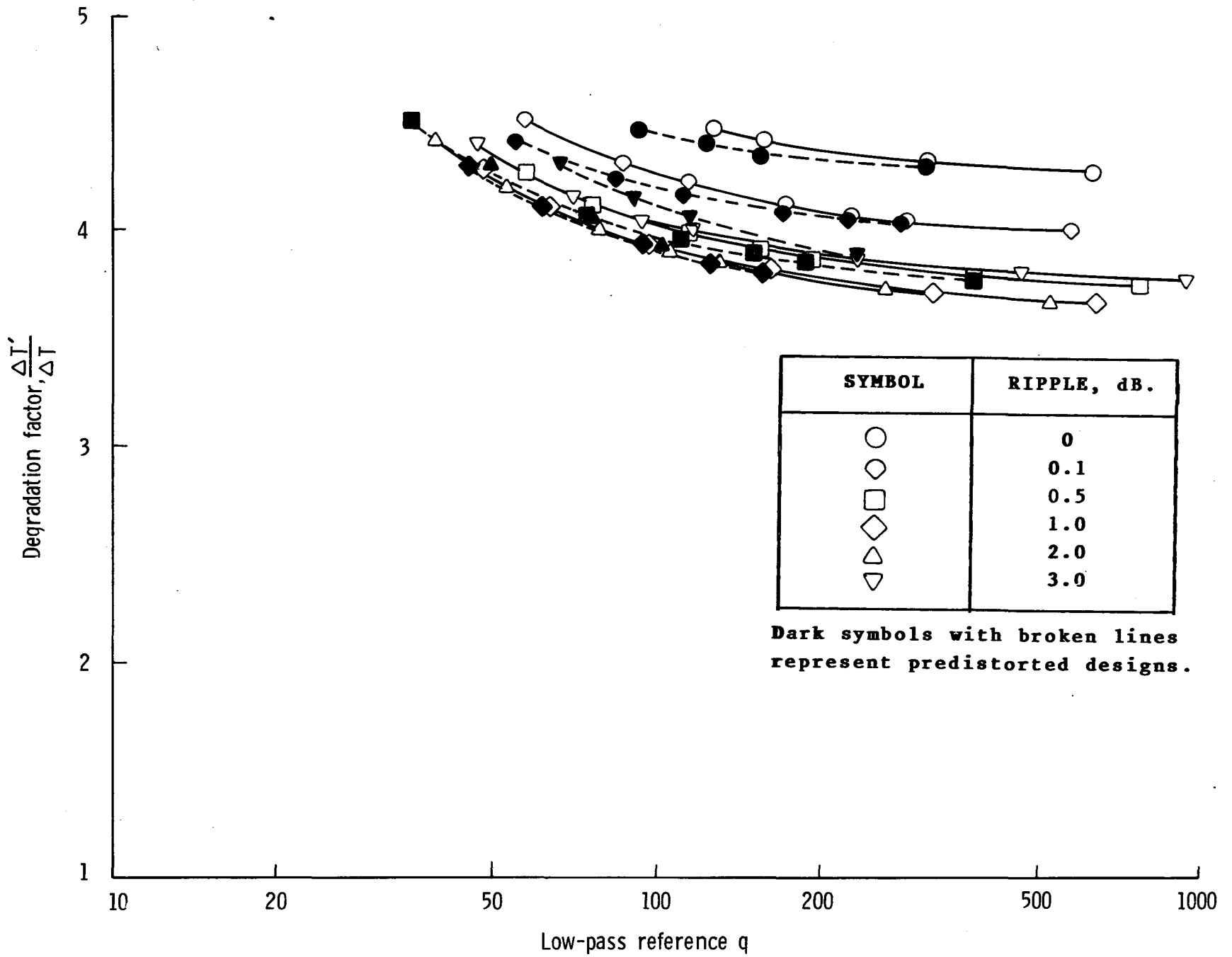
Fig. F2. Band-edge attenuation = 20 dB, 2 poles.

SYMBOL	RIPPLE, dB.
◯	0
◯	0.1
▢	0.5
◇	1.0
△	2.0
▽	3.0

Dark symbols with broken lines represent predistorted designs.
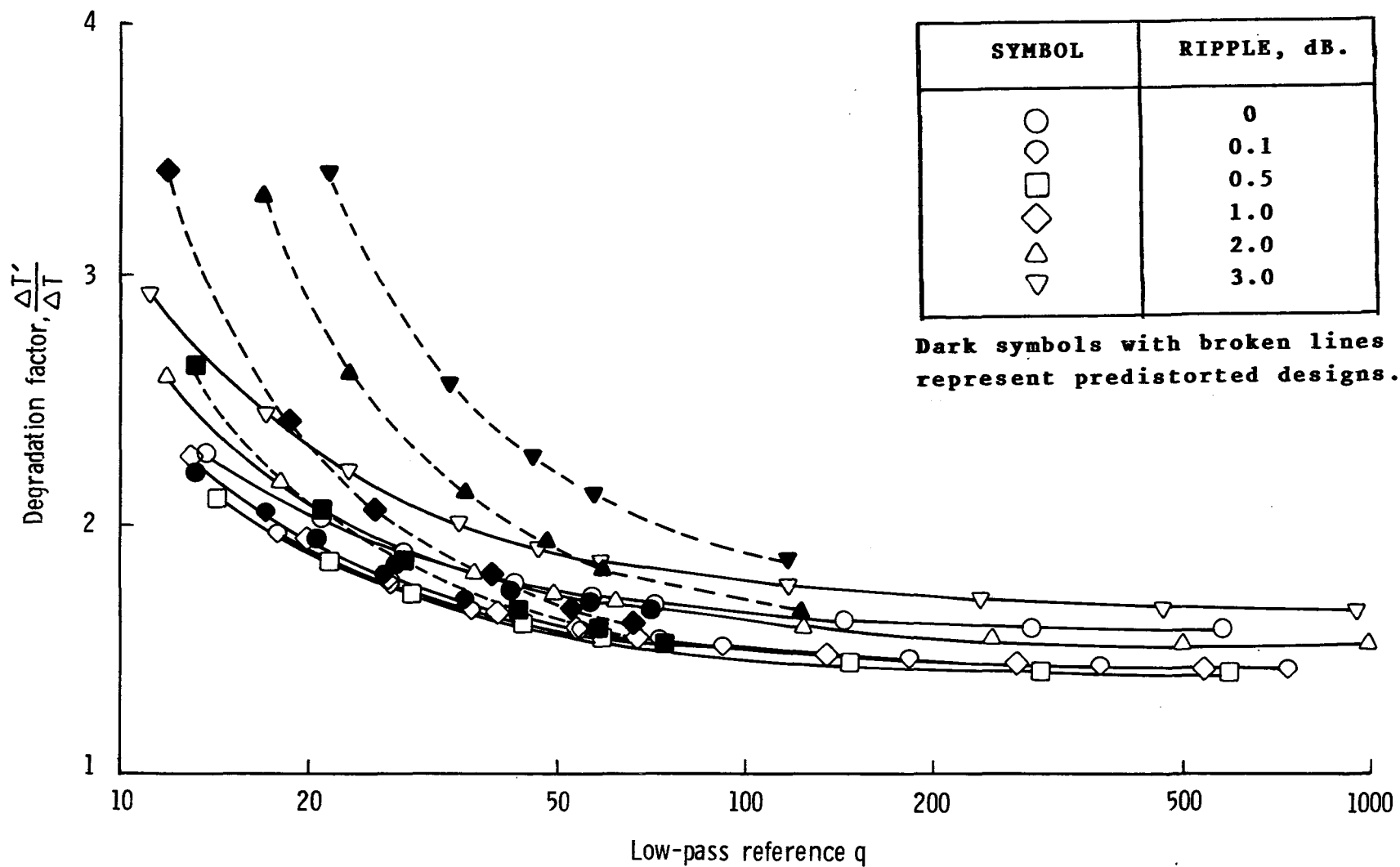
Fig. F3. Band-edge attenuation = 10 dB, 3 poles.

SYMBOL	RIPPLE, dB.
○	0
◇	0.1
☐	0.5
◇	1.0
△	2.0
▽	3.0

Dark symbols with broken lines represent predistorted designs.
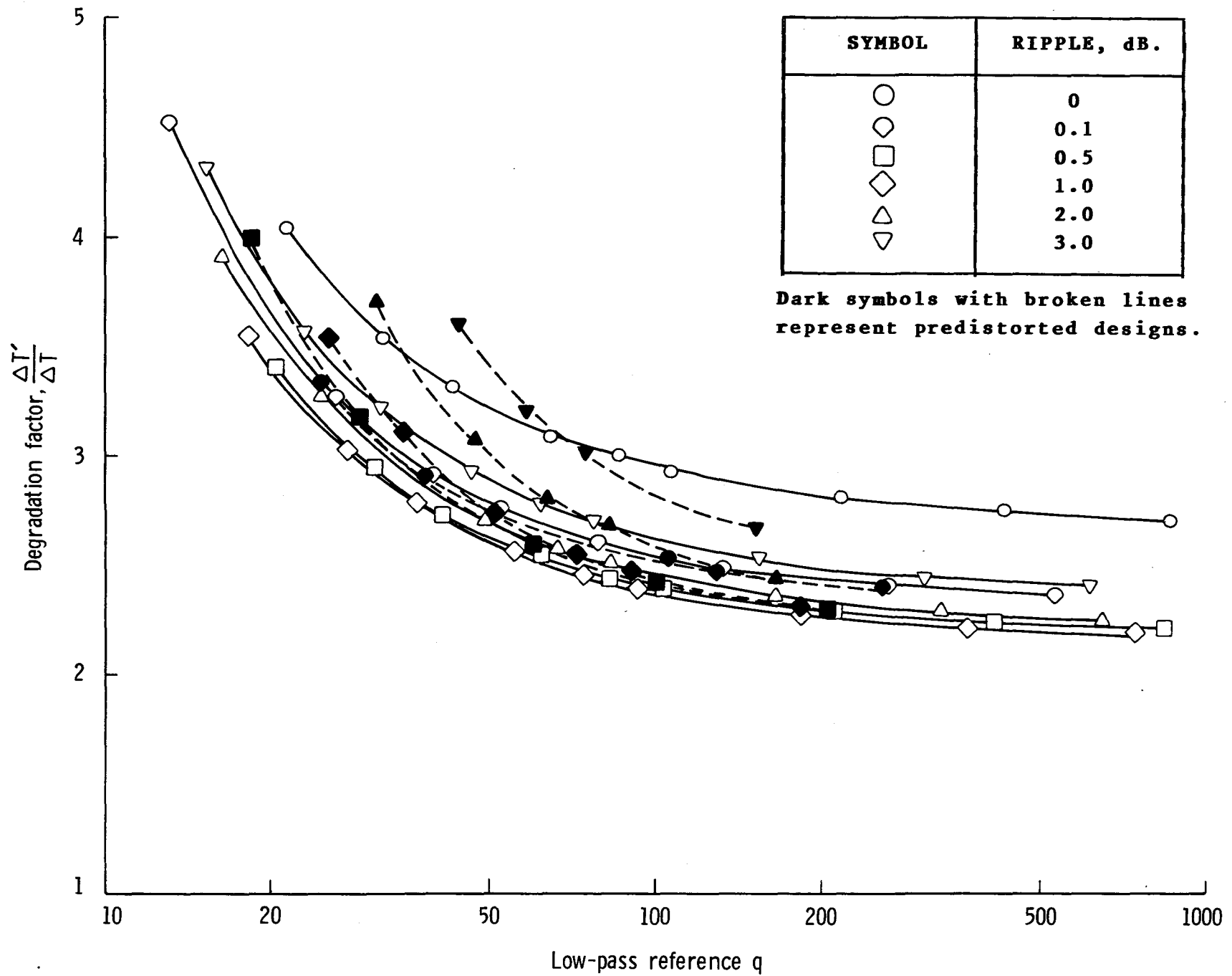
Fig. F4. Band-edge attenuation = 20 dB, 3 poles.

SYMBOL	RIPPLE, dB.
○	0
◇	0.1
□	0.5
◇	1.0
△	2.0
▽	3.0

Dark symbols with broken lines represent predistorted designs
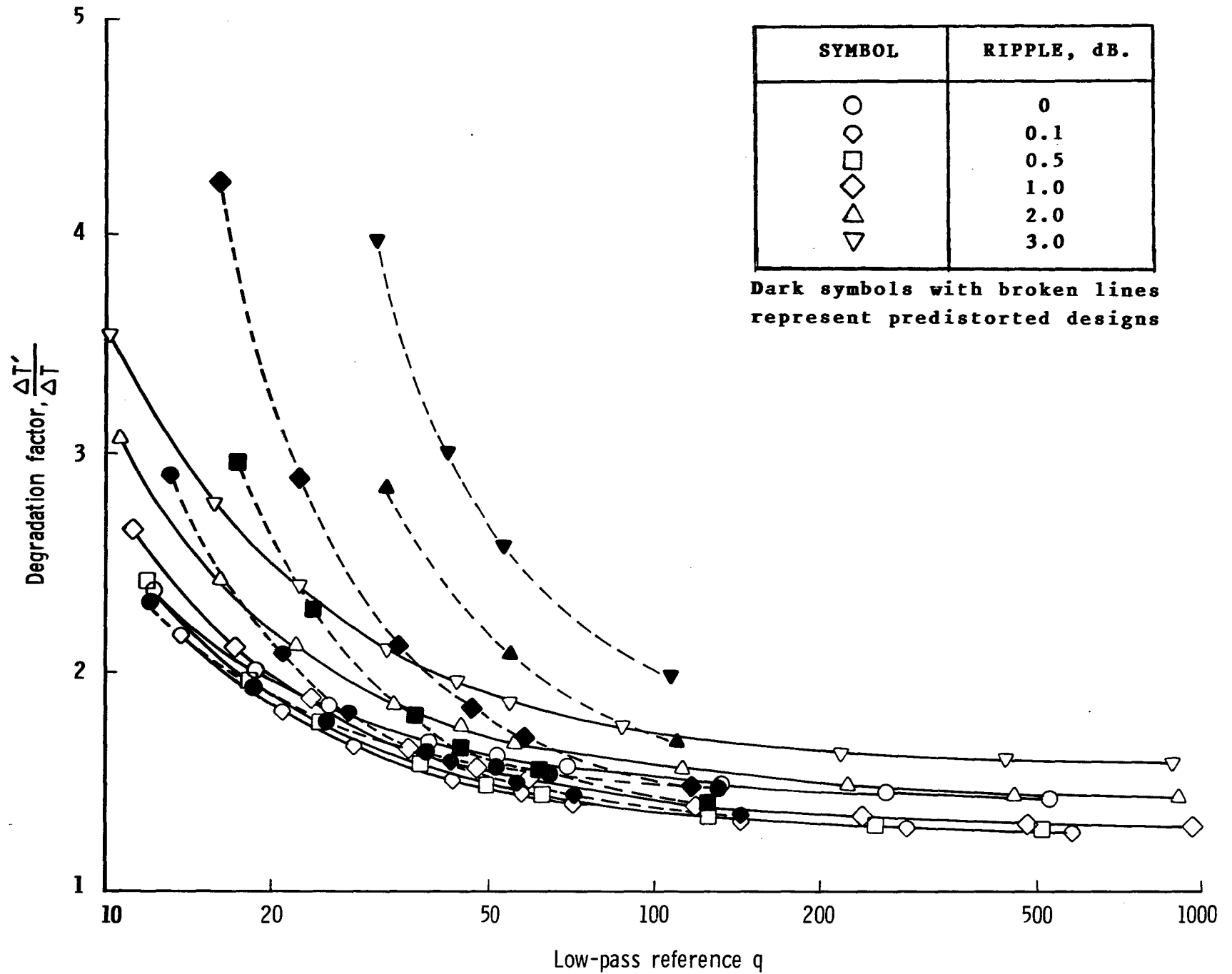
Fig. F5. Band-edge attenuation = 10 dB, 4 poles.

SYMBOL	RIPPLE, dB.
◯	0
◇	0.1
☐	0.5
◇	1.0
△	2.0
▽	3.0

Dark symbols with broken lines represent predistorted designs.
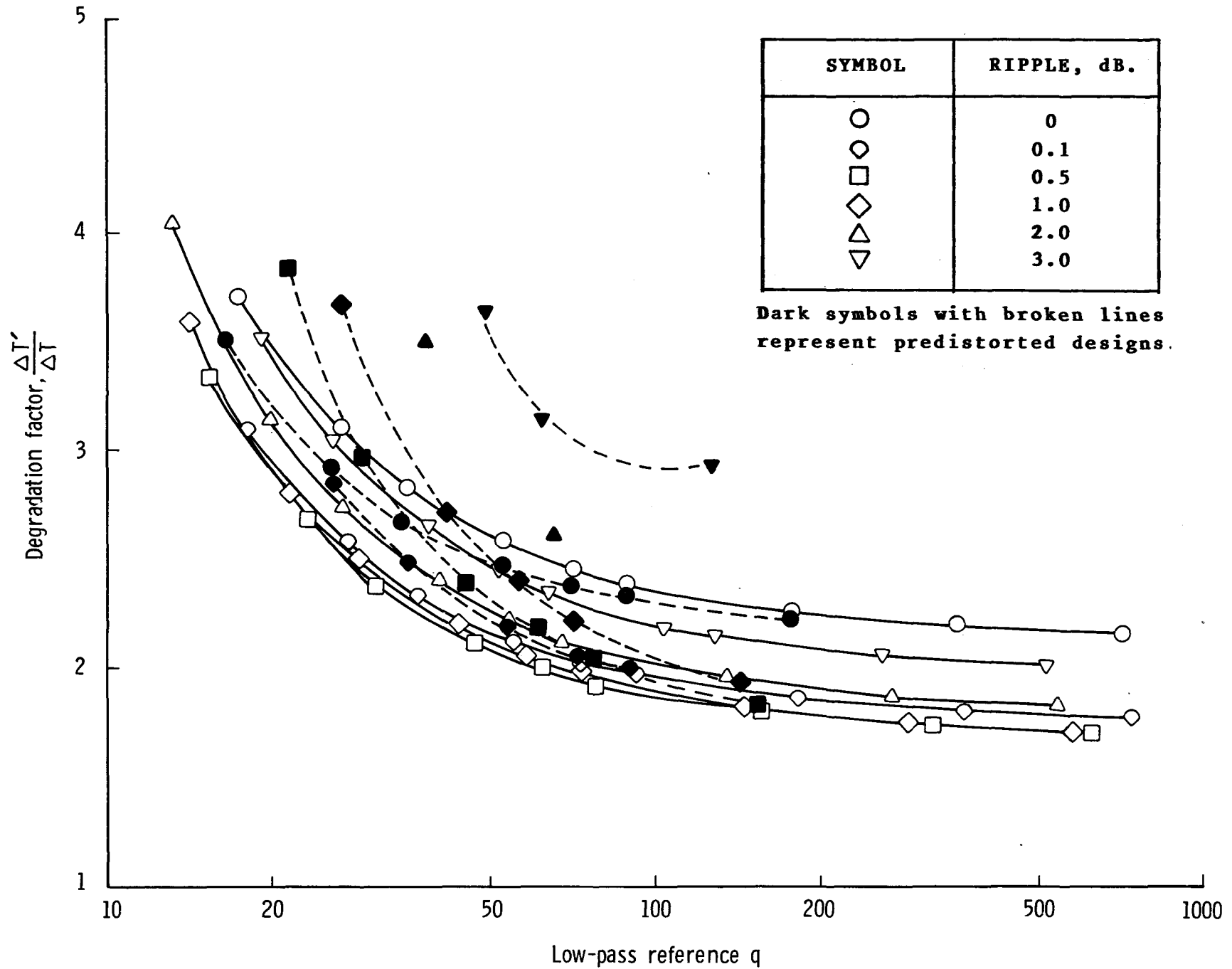
Fig. F6. Band-edge attenuation = 20 dB, 4 poles.

SYMBOL	RIPPLE, dB.
○	0
◇	0.1
☐	0.5
◇	1.0
△	2.0
▽	3.0

Dark symbols with broken lines represent predistorted designs
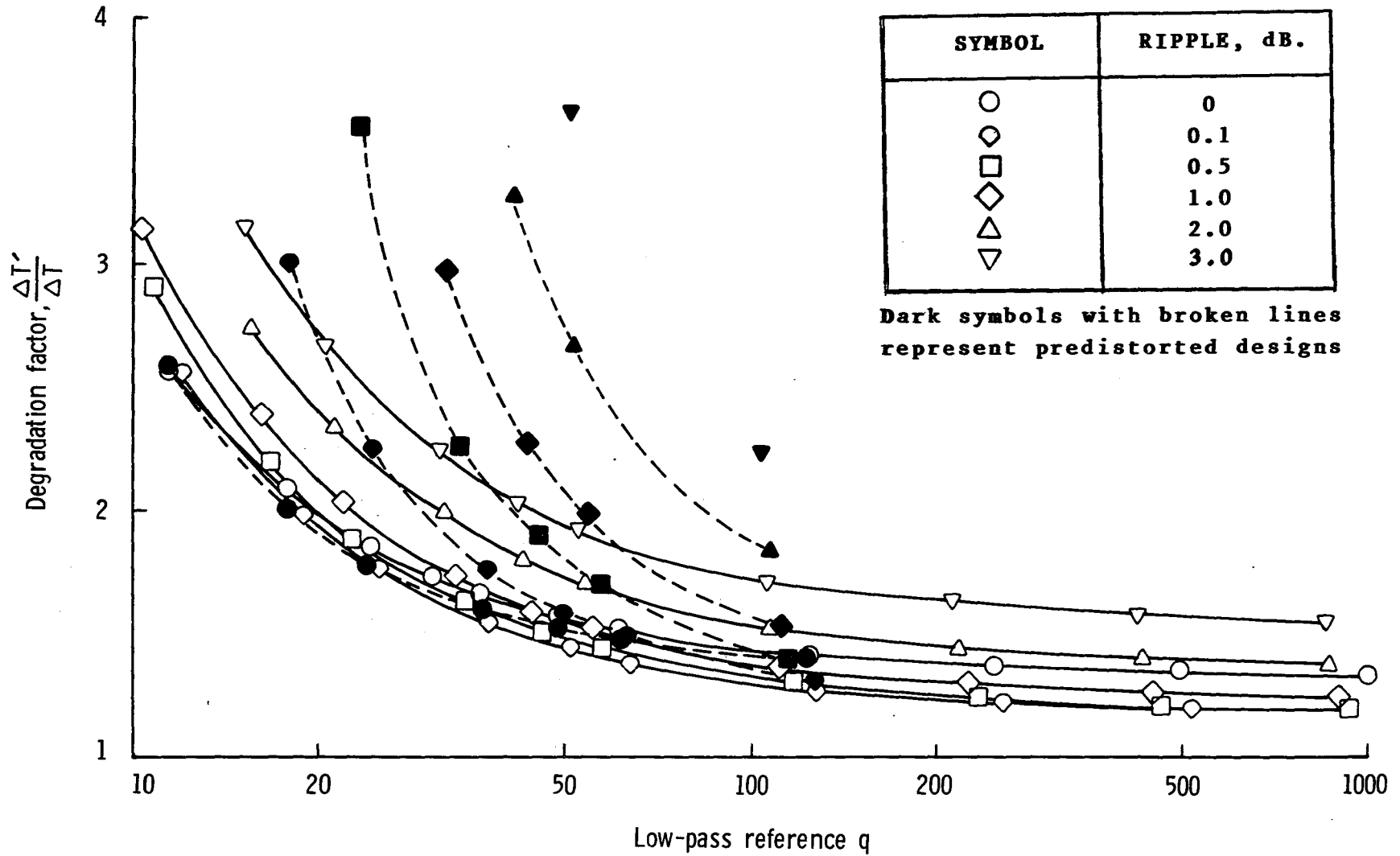
Fig. F7. Band-edge attenuation = 10 dB, 5 poles.

SYMBOL	RIPPLE, dB.
○	0
◇	0.1
□	0.5
◇	1.0
△	2.0
▽	3.0

Dark symbols with broken lines represent predistorted designs
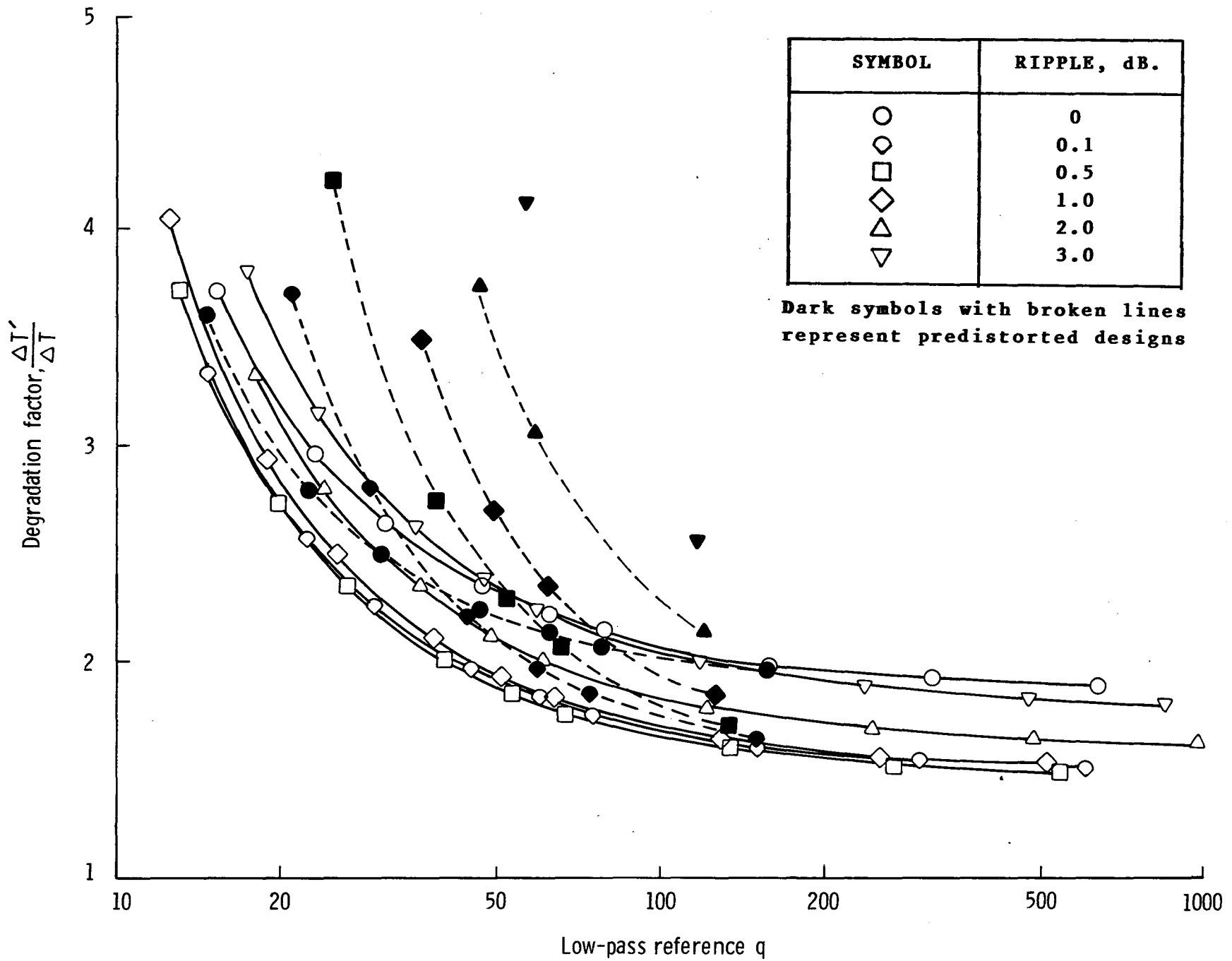
Fig. F8. Band-edge attenuation = 20 dB, 5 poles.

SYMBOL	RIPPLE, dB.
○	0
◇	0.1
□	0.5
◇	1.0
△	2.0
▽	3.0

Dark symbols with broken lines represent predistorted designs.
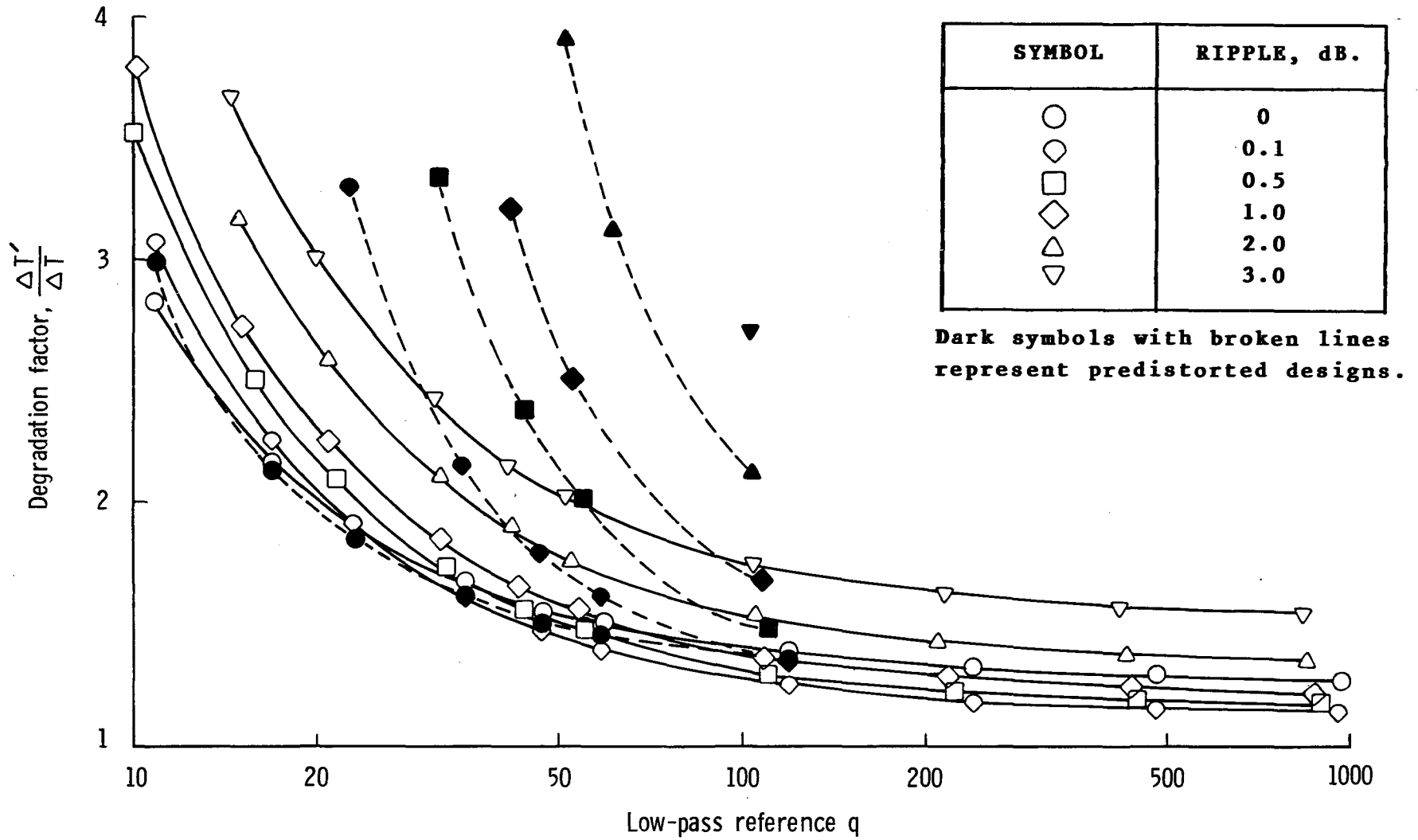
Fig. F9. Band-edge attenuation = 10 dB, 6 poles.

SYMBOL	RIPPLE, dB.
○	0
⬠	0.1
□	0.5
◇	1.0
△	2.0
▽	3.0

Dark symbols with broken lines represent predistorted designs.
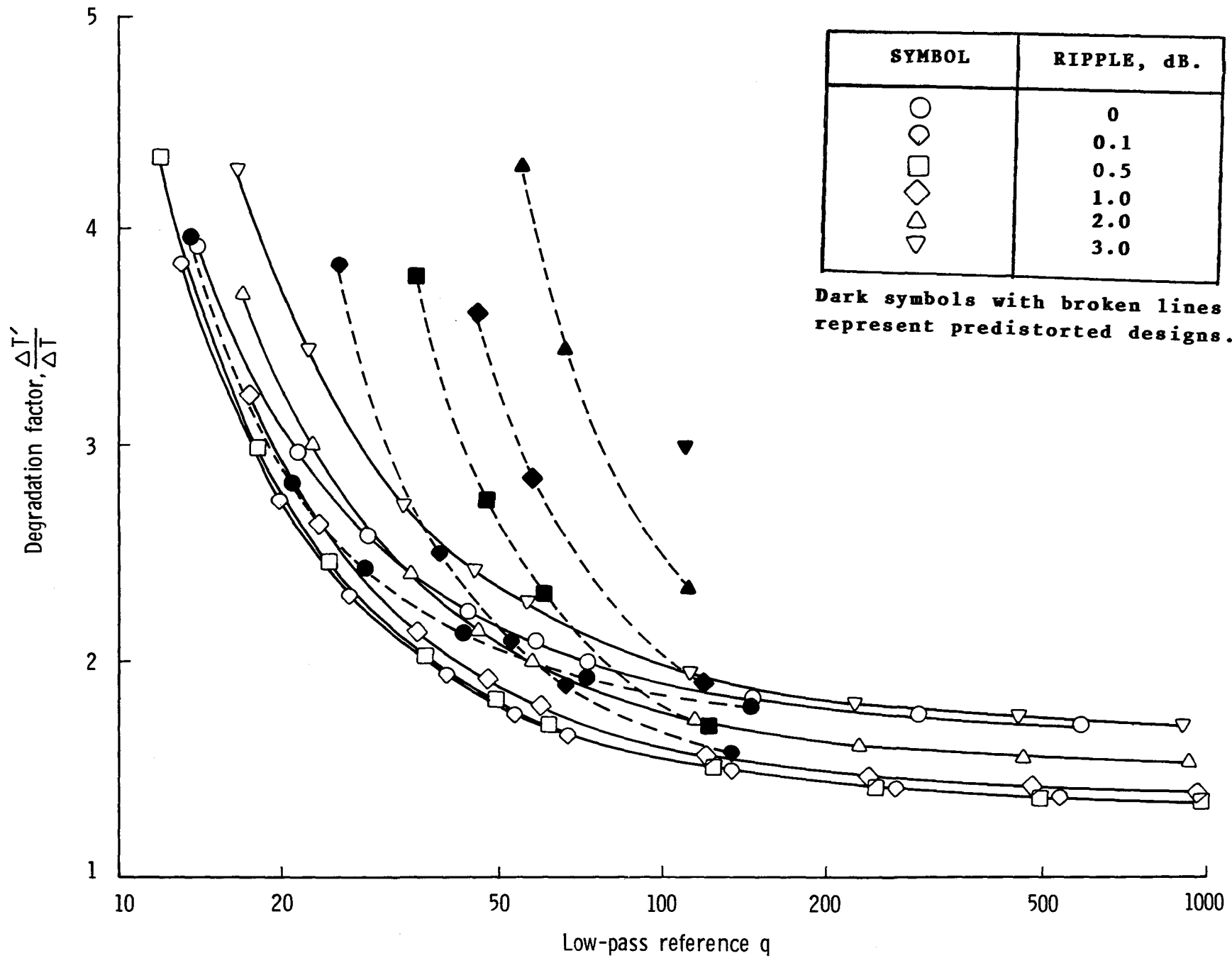
Fig. F10. Band-edge attenuation = 20 dB, 6 poles.

SYMBOL	RIPPLE, dB.
○	0
◊	0.1
□	0.5
◇	1.0
△	2.0
▽	3.0

Dark symbols with broken lines represent predistorted designs

Degradation factor, $\frac{\Delta T'}{\Delta T}$

Low-pass reference q
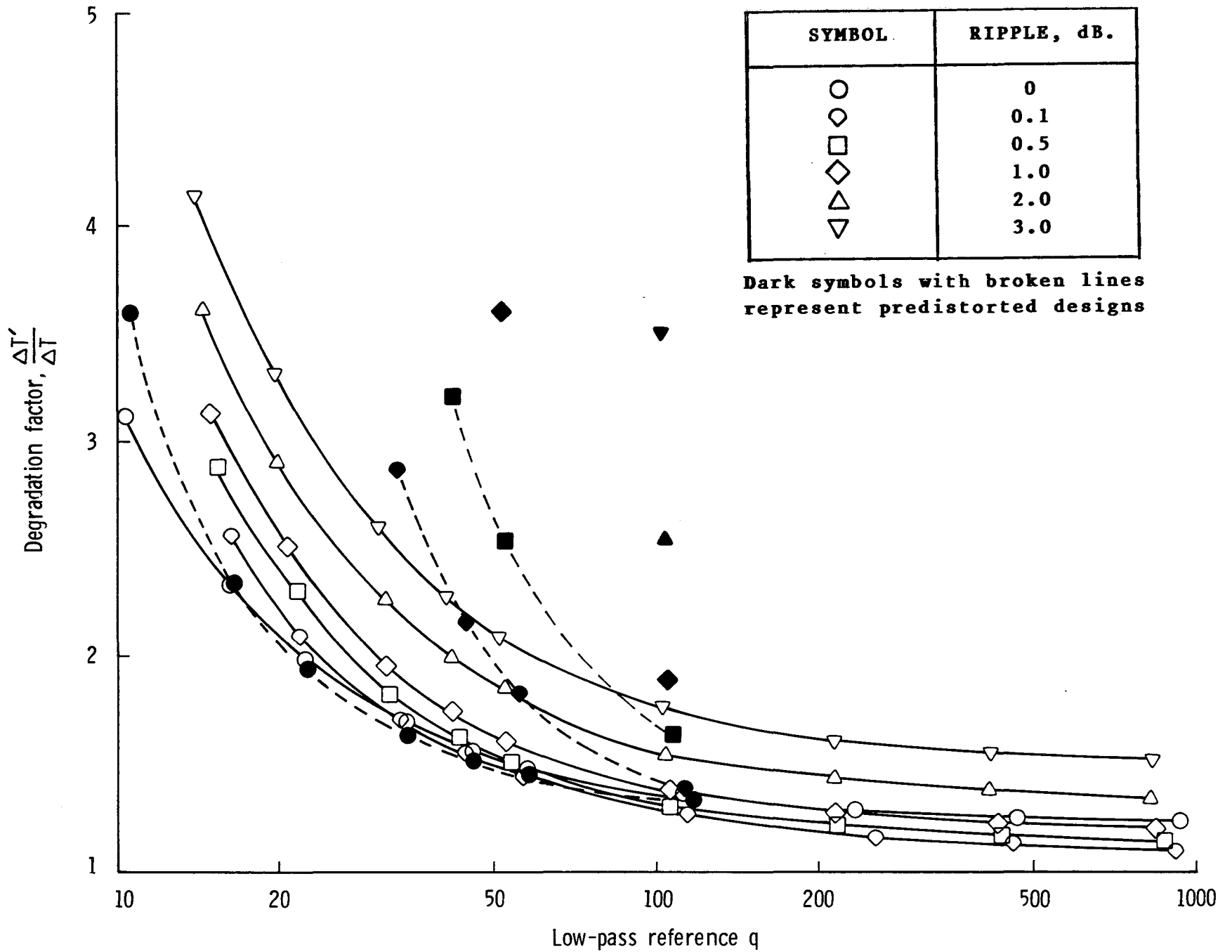
Fig. F11. Band-edge attenuation – 10 dB, 7 poles.

SYMBOL	RIPPLE, dB.
○	0
⬠	0.1
□	0.5
◇	1.0
△	2.0
▽	3.0

Dark symbols with broken lines represent predistorted designs.

Degradation factor, $\frac{\Delta T'}{\Delta T}$

Low-pass reference q
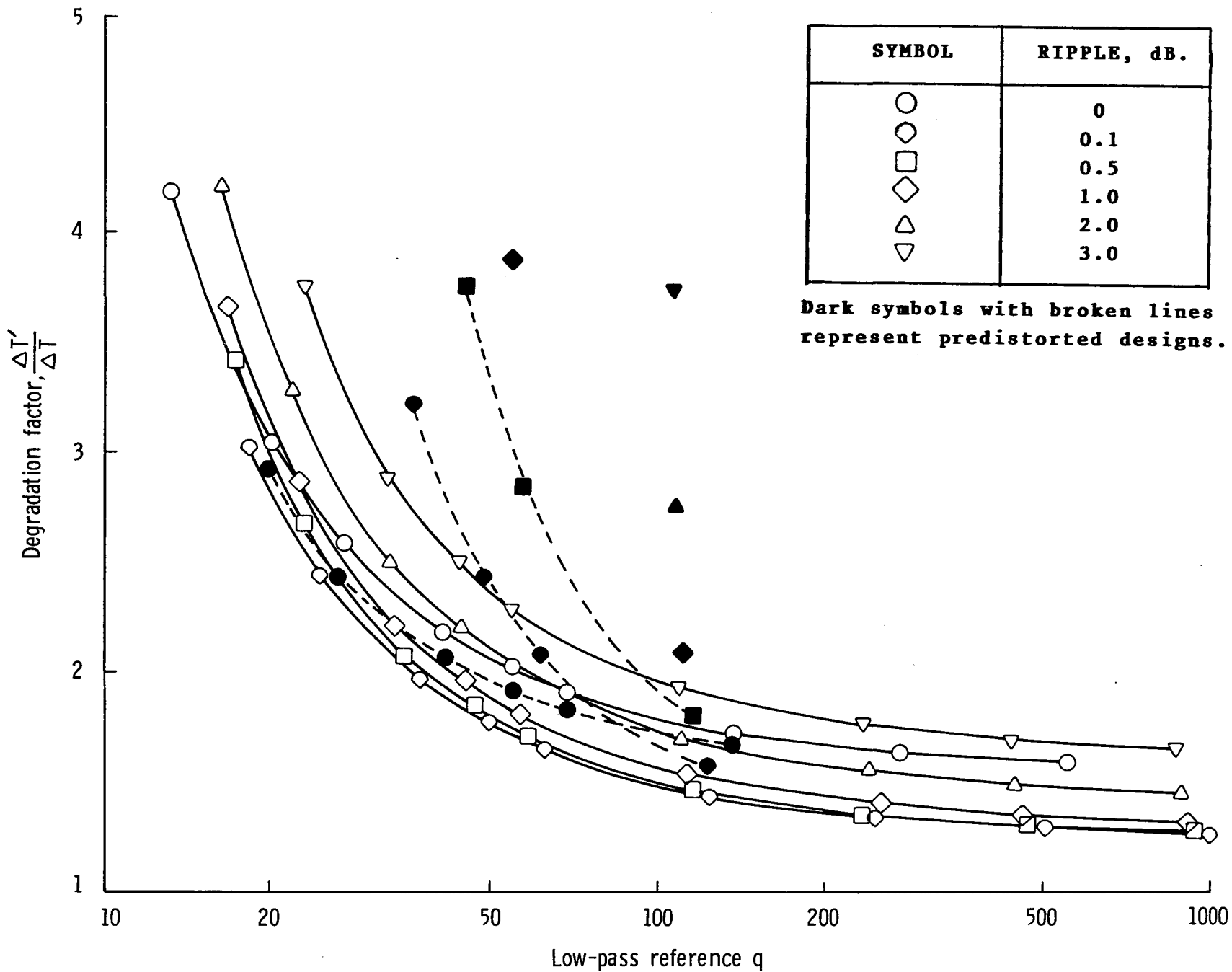
Fig. F12. Band-edge attenuation = 20 dB, 7 poles.

APPENDIX G

SUMMARY CURVES

A summary of the minimum degradation factor that can be obtained (with the filter types investigated) as a function of the number of poles for 10 dB specified bandedge attenuation is provided in figure G1. A similar summary for 20 dB specified bandedge attenuation is provided in figure G2.

The range of minimum degradation factor based on the bounds of three resonators and seven resonators is provided in figure G3.
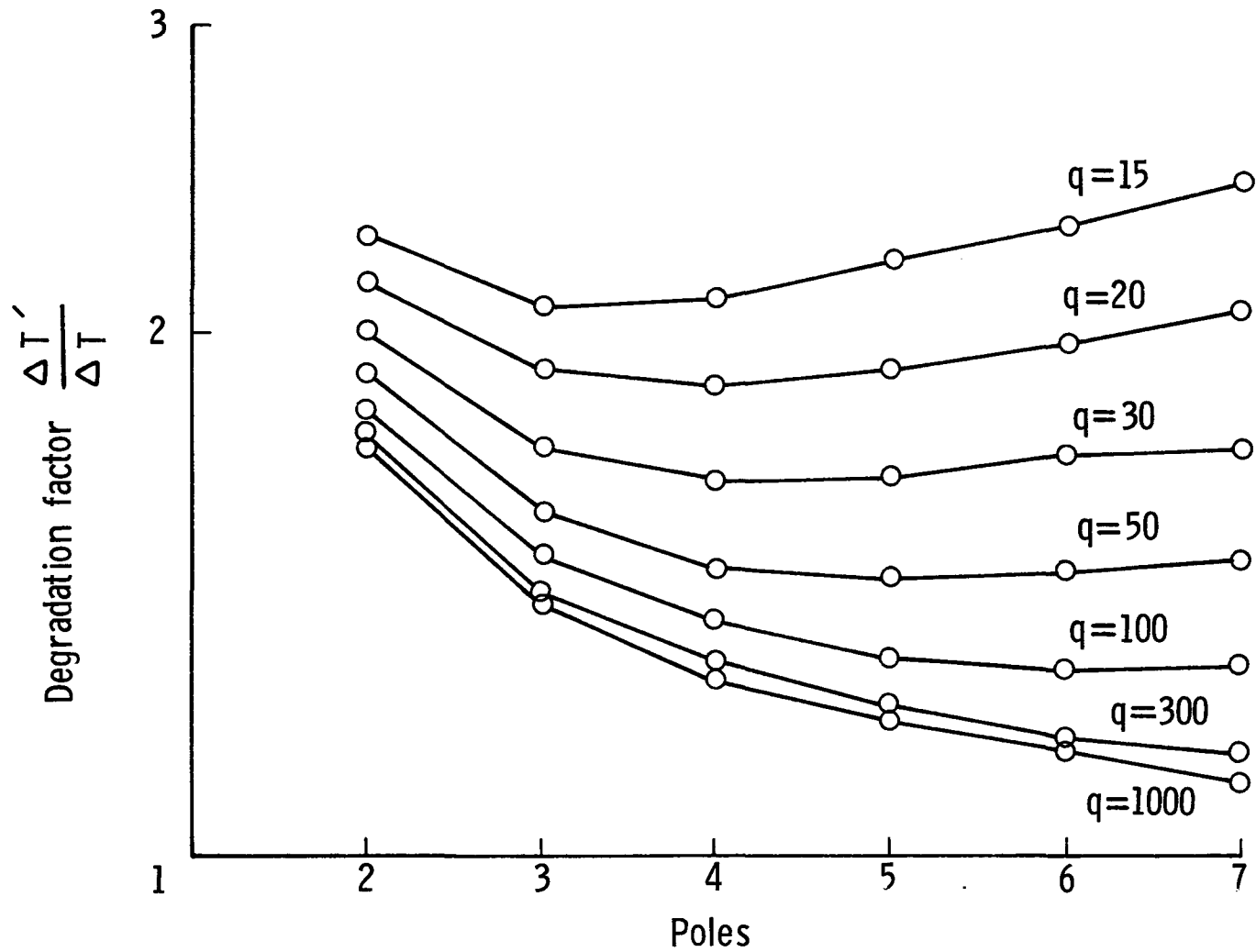
Figure G1.   Minimum degradation factor for 10 dB. specified bandedge attenvation.
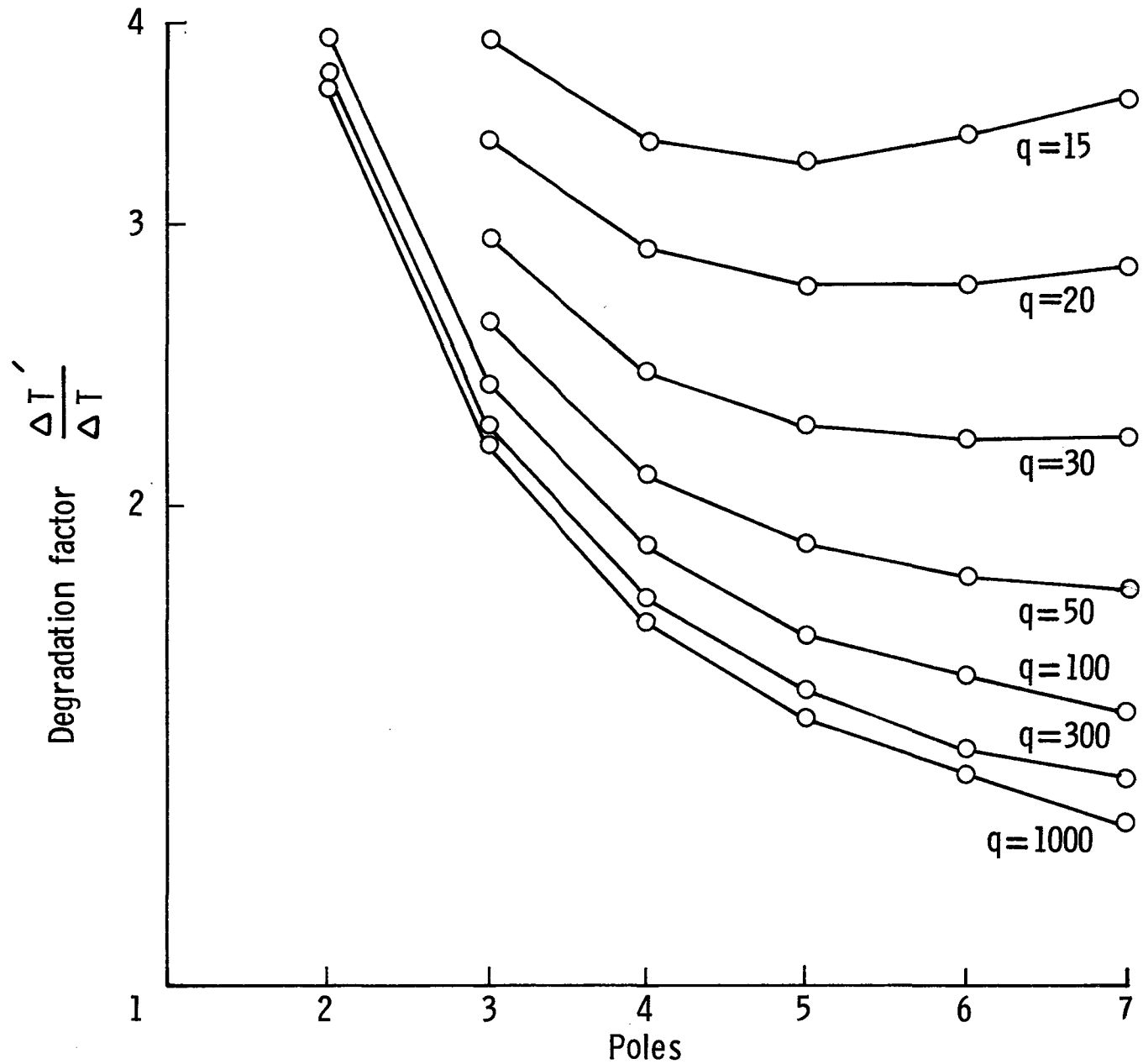
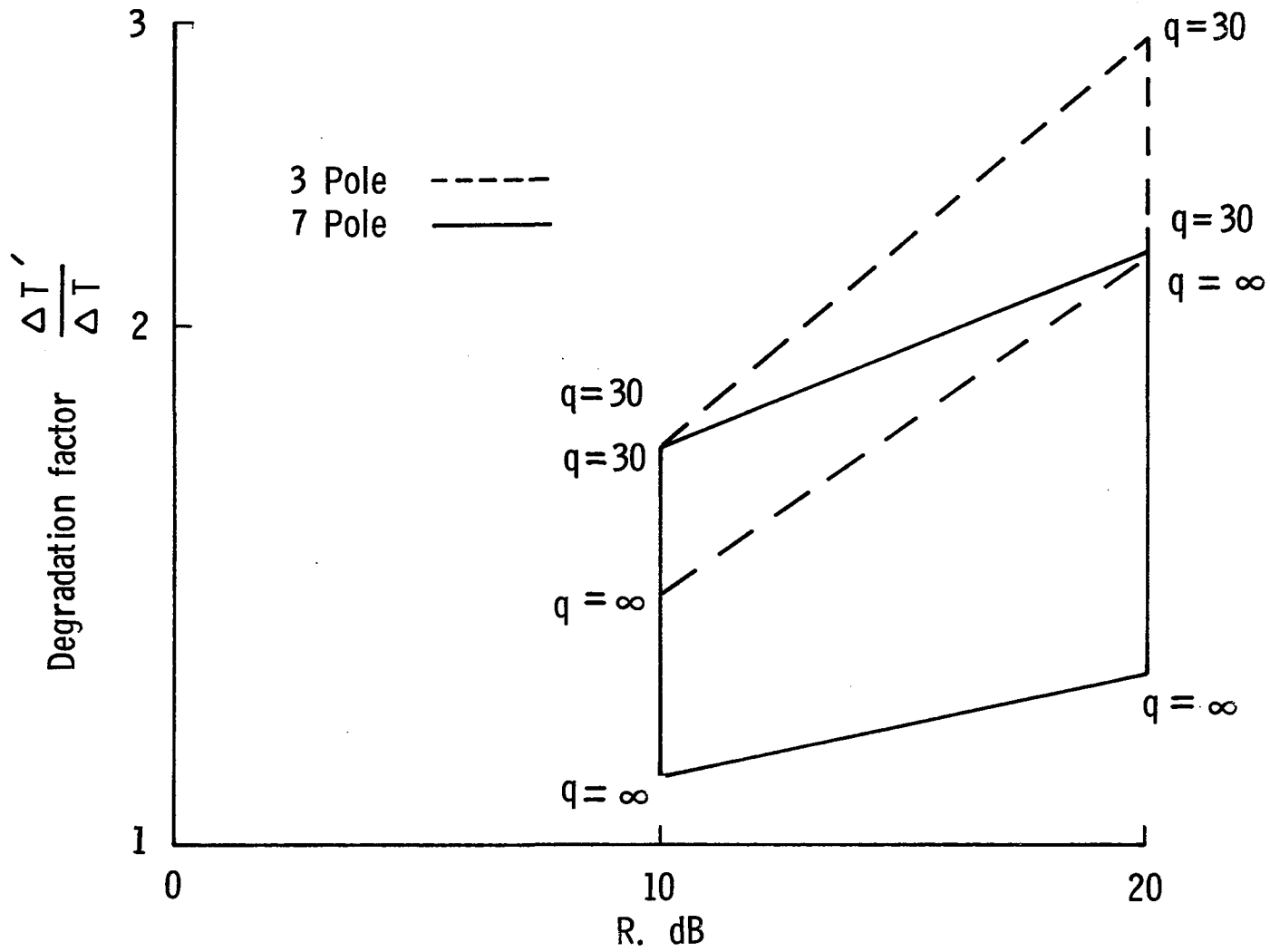Figure G2.   Minimum degradation factor for 20 dB specified bandedge attenvation

Figure G3. Minimum degradation factor for three and seven pole filters.

Standard Bibliographic Page

1. Report No. NASA TM-87651	2. Government Accession No.	3. Recipient's Catalog No.
4. Title and Subtitle A Study of the Effects of Interference-Rejection Filters on Feedback Radiometer Sensitivity		5. Report Date December 1985
		6. Performing Organization Code · 506-58-23-01
7. Author(s) William D. Stanley Chase P. Hearn		8. Performing Organization Report No.
9. Performing Organization Name and Address NASA Langley Research Center Hampton, Virginia 23665-5525		10. Work Unit No.
		11. Contract or Grant No.
12. Sponsoring Agency Name and Address National Aeronautics and Space Administration Washington, D. C. 20546		13. Type of Report and Period Covered Technical Memorandum
		14. Sponsoring Agency Code

15. Supplementary Notes

William D. Stanley, Old Dominion University, Norfolk, Virginia.
Chase P. Hearn, NASA Langley Research Center, Hampton, Virginia.

16. Abstract

The trade-offs between sensitivity and interference immunity resulting from input band-pass filter losses in a noise-injection feedback radiometer are examined. Data are provided to permit the selection of an "optimum" filter configuration based on the independent variables of percentage bandwidth, q-factors, and desired band-edge rejection.

17. Key Words (Suggested by Authors(s)) Radiometer Interference Radiometer Sensitivity	18. Distribution Statement Unclassified – Unlimited Subject Category 32	
19. Security Classif.(of this report) Unclassified	20. Security Classif.(of this page) Unclassified	21. No. of Pages 94	22. Price A05

NASA Langley Form 63 (June 1985)